

EFFECT OF MICROWAVE SINTERING ON THE
DENSIFICATION AND PROPERTIES OF COPPER OXIDE
DOPED Y-TZP CERAMICS

SARA LEE KIT YEE

FACULTY OF ENGINEERING
UNIVERSITY OF MALAYA
KUALA LUMPUR

2019

**EFFECT OF MICROWAVE SINTERING ON THE
DENSIFICATION AND PROPERTIES OF COPPER
OXIDE DOPED Y-TZP CERAMICS**

SARA LEE KIT YEE

**THESIS SUBMITTED IN FULFILMENT OF THE
REQUIREMENTS FOR THE DEGREE OF DOCTOR OF
PHILOSOPHY**

**FACULTY OF ENGINEERING
UNIVERSITY OF MALAYA
KUALA LUMPUR**

2019

UNIVERSITY OF MALAYA
ORIGINAL LITERARY WORK DECLARATION

Name of Candidate: Sara Lee Kit Yee

Matric No: KHA 160001

Name of Degree: Doctor of Philosophy

Title of Project Paper/Research Report/Dissertation/Thesis (“this Work”):

Effect of microwave sintering on the densification and properties of copper oxide doped Y-TZP ceramics

Field of Study: Advanced Materials (Materials Engineering)

I do solemnly and sincerely declare that:

- (1) I am the sole author/writer of this Work;
- (2) This Work is original;
- (3) Any use of any work in which copyright exists was done by way of fair dealing and for permitted purposes and any excerpt or extract from, or reference to or reproduction of any copyright work has been disclosed expressly and sufficiently and the title of the Work and its authorship have been acknowledged in this Work;
- (4) I do not have any actual knowledge nor do I ought reasonably to know that the making of this work constitutes an infringement of any copyright work;
- (5) I hereby assign all and every rights in the copyright to this Work to the University of Malaya (“UM”), who henceforth shall be owner of the copyright in this Work and that any reproduction or use in any form or by any means whatsoever is prohibited without the written consent of UM having been first had and obtained;
- (6) I am fully aware that if in the course of making this Work I have infringed any copyright whether intentionally or otherwise, I may be subject to legal action or any other action as may be determined by UM.

Candidate’s Signature

Date:

Subscribed and solemnly declared before,

Witness’s Signature

Date:

Name:

Designation:

EFFECT OF MICROWAVE SINTERING ON THE DENSIFICATION AND PROPERTIES OF COPPER OXIDE DOPED Y-TZP CERAMICS

ABSTRACT

Yttria-tetragonal zirconia polycrystal (Y-TZP) exhibited good physical and mechanical properties which are advantageous in various engineering and dental applications. In the present work, the effect of microwave sintering on the properties of copper oxide (CuO) doped 3 mol% Y-TZP was studied. The results showed that the pre-sintered green samples flanked with two susceptors in an enclosed alumina fiberboard housing subjected to microwave sintering (heating rate of 30 °C/min with a holding time of 5 min) had successfully produced crack-free sintered samples. Various amount of CuO ranging from 0.05 wt% to 1 wt % was incorporated in Y-TZP to study the effect of microwave sintering on phase analysis, microstructure, density, Vickers hardness and fracture toughness at different sintering temperatures (between 1100 °C and 1400 °C). It was found that the addition of up to 0.5 wt% CuO was beneficial in aiding densification of zirconia without inducing grain coarsening. In particular, 0.2 wt % CuO-doped Y-TZP achieved relative density $\geq 99\%$, Vickers hardness of 14.4 GPa, fracture toughness of 7.8 MPa.m^{1/2} and exhibited fine equiaxed tetragonal grain size of less than 0.25 μm when microwave sintered between 1250°C and 1300 °C. In contrast, the addition of 1 wt% CuO was detrimental and resulted in the formation of about 50% monoclinic phase upon sintering. This research also showed that the microwave effect was significant to enhance densification at low temperatures (< 1300 °C) for undoped Y-TZPs. On the other hand, the addition of 0.2 wt% CuO-doped Y-TZPs was found to be effective as a sintering aid for conventional sintering at temperatures ≥ 1200 °C as the resulting samples exhibited similar properties when using microwave sintering. Grain size was found to have played a role in suppressing the hydrothermal ageing of Y-TZP. It was found that all the samples

with grain size of below 0.28 μm did not undergo the ageing induced phase transformation after 180 °C/10 bar for 200 h.

Keywords: microwave sintering, zirconia, copper oxide, mechanical properties

University of Malaya

KESAN MICROWAVE SINTERING PADA DENSIFICATION DAN SIFAT TEMBAGA OKSIDA DOPEDED Y-TZP SERAMIK

ABSTRAK

Yttria-tetragonal zirconia polycrystal (Y-TZP) mempamerkan sifat fizikal dan mekanikal yang baik dalam pelbagai aplikasi kejuruteraan dan pergigian. Dalam kerja ini, kesan pancaran gelombang mikro terhadap sifat-sifat tembaga oksida (CuO) doped 3 mol% Y-TZP telah dikaji. Hasil kajian menunjukkan bahawa sampel hijau yang diintegrasikan diapit dengan dua susceptor dalam perumahan fiberboard alumina tertutup tertakluk kepada sintering gelombang mikro (kadar pemanasan 30 °C /min dengan masa pegangan 5 minit) telah berjaya menghasilkan sampel sintered bebas retak. Pelbagai jumlah CuO dari 0.05 wt% hingga 1 wt% digabungkan dengan Y-TZP untuk mengkaji kesan pancaran gelombang mikro pada analisis fasa, struktur mikro, ketumpatan, kekerasan Vickers dan keliatan patah pada suhu sintering yang berlainan (antara 1100 °C dan 1400 °C). Telah didapati bahawa penambahan sehingga 0.5% CuO berkhasiat dalam membantu penggabungan zirkonia tanpa menyebabkan gandum kasar. Secara khususnya, 0.2% wt% CuO-doped Y-TZP mencapai ketumpatan relatif $\geq 99\%$, kekerasan Vickers daripada 14.4 GPa, ketumpatan fraktur 7.8 MPa.m^{1/2} dan mempamerkan saiz butiran tetragonal yang bersamaan dengan kurang daripada 0.25 μm apabila gelombang mikro sinter antara 1250 °C dan 1300 °C. Sebaliknya, penambahan 1 wt% CuO adalah merosakkan dan menghasilkan pembentukan kira-kira 50% fasa monoklinik apabila sintering. Kajian ini juga menunjukkan bahawa kesan ketuhar gelombang mikro adalah penting untuk meningkatkan ketumpatan pada suhu rendah (< 1300 °C) untuk Y-TZPs. Sebaliknya, penambahan Y-TZP 0.2% CuO-doped Y-TZPs didapati berkesan sebagai bantuan sintering untuk sintering konvensional pada suhu ≥ 1200 °C kerana sampel yang dihasilkan mempamerkan sifat adalah sama dengan penggunaan sintering gelombang mikro. Saiz bijian didapati telah memainkan peranan dalam menekan penuaan

hidrotermal Y-TZP. Telah didapati bahawa semua sampel dengan saiz butiran di bawah $0.28 \mu\text{m}$ tidak mengalami transformasi fasa induksi yang disebabkan oleh ageing selepas $180 \text{ }^\circ\text{C}/10 \text{ bar}$ sepanjang 200 h.

Kata kunci: sintering gelombang mikro, zirkonia, oksida tembaga, sifat mekanik

University of Malaya

ACKNOWLEDGEMENTS

First, I would like to thank my research supervisor, Professor Ir. Dr. Ramesh Singh. His supervision throughout the experimental process is crucial for the success of this research. I am extremely fortunate to have a responsible supervisor who placed high emphasis on my research. I would also like to express my sincerest gratitude to my co-supervisor, Associate Prof. Ir. Dr. Tan Chou Yong who had been supporting and encouraging me throughout this research.

I am also grateful to my beloved family, who had supported me spiritually throughout my life. Finally, to those who directly or indirectly contributed to this research, your help is greatly appreciated. Thank you very much.

University of Malaya

TABLE OF CONTENTS

Abstract	iii
Abstrak	v
Acknowledgements	vii
Table of Contents	viii
List of Figures	xii
List of Tables.....	xvi
List of Symbols and Abbreviations.....	xvii
CHAPTER 1: INTRODUCTION.....	1
1.1 General Introduction.....	1
1.2 Problem Statement.....	2
1.3 Scope of Research.....	4
1.4 Research Objectives.....	5
1.5 Structure of Thesis.....	5
CHAPTER 2: LITERATURE REVIEW.....	7
2.1 Introduction of Zirconia.....	7
2.2 Low Temperature Degradation.....	8
2.3 Factors Governing LTD.....	9
2.3.1 Ageing Temperature.....	10
2.3.2 Ageing Medium.....	12
2.3.3 Ageing Pressure.....	14
2.3.4 Grain Size.....	14
2.3.5 Sintering Techniques.....	17
2.3.5.1 Two-Step Sintering.....	18

2.3.5.2	Electric Field-assisted Sintering	19
2.3.5.3	Microwave Processing	20
2.3.6	Starting powder	21
2.3.7	Yttria Content	23
2.3.8	Presence of Dopants	24
2.3.8.1	Alumina	24
2.3.8.2	Silica	26
2.3.8.3	Copper oxide	27
2.3.8.4	Other Dopants	28
2.4	Microwave Sintering	29
2.4.1	Introduction of Microwave Heating	29
2.4.2	Microwave Furnace	31
2.4.3	Dielectric Properties	32
2.4.4	Issues in Microwave Heating	33
2.4.5	Design and Configuration for Microwave Processing	35
2.4.6	The Effect of Microwave Heating	36
2.5	Summary	40
 CHAPTER 3: METHODOLOGY		43
3.1	Introduction	43
3.2	Fabrication of Insulation Housing	45
3.3	Preliminary Study: Microwave Processing Parameters	47
3.3.1	The Influence of Susceptors	47
3.3.2	The Influence of Heating Rates	48
3.3.3	The Influence of Pre-sintering	49
3.4	Preparation of Samples	50
3.4.1	Preparation of CuO-doped Y-TZP powders	50

3.4.2	Powder Compaction	50
3.4.3	Sintering	51
3.4.4	Grinding and Polishing.....	52
3.4.5	Thermal Etching	52
3.5	Characterization of Samples	53
3.5.1	Phase Identification	53
3.5.2	Density Determination	54
3.5.3	Vickers Hardness and Fracture Toughness Evaluation.....	54
3.5.4	Microstructure Evaluation.....	56
3.5.5	Low Temperature Degradation Study	57
3.6	Summary.....	58
CHAPTER 4: RESULTS AND DISCUSSIONS		59
4.1	Introduction.....	59
4.2	Preliminary Study: Microwave Processing Parameters.....	59
4.2.1	The Influence of Susceptors	59
4.2.2	The Influence of Heating Rates	61
4.2.3	The Influence of Pre-sintering.....	65
4.3	Effect of Microwave Sintering	67
4.3.1	Tetragonal Phase Stability.....	67
4.3.2	Densification Behaviour.....	70
4.3.3	Microstructure Development and Grain Size	72
4.3.4	Vickers Hardness and Fracture Toughness	77
4.4	Comparison between Conventional Sintering and Microwave Sintering.....	83
4.4.1	Densification Behaviour.....	83
4.4.2	Vickers Hardness and Fracture Toughness	85
4.4.3	Microstructure and Grain Size.....	88

4.4.4	Low Temperature Degradation.....	94
CHAPTER 5: CONCLUSIONS AND FUTURE WORK		99
5.1	Conclusions	99
5.2	Future Work.....	100
	References	101
	List of Publications and Papers Presented	114

University of Malaya

LIST OF FIGURES

Figure 2.1: Monoclinic phase development and flexural strength of commercial zirconia (Vita In-Ceram YZ) exposed at different ageing temperatures (Kim et al., 2009).....	11
Figure 2.2: Monoclinic phase content of 3Y-TZP with respect to different sintering temperatures and holding time after hydrothermal ageing at 134 °C/2 bar for different duration (Chevalier et al., 2004).	16
Figure 2.3: Surface monoclinic phase content as a function of hydrothermal degradation at 134 °C under 2 bar pressures for 3Y-TZP sintering at different temperatures and holding time (Zhang et al., 2014).....	16
Figure 2.4: Monoclinic phase content for microwave (MW) and conventional (CS) sintered 3Y-TZP at different LTD exposure time (Presenda et al., 2017).....	21
Figure 2.5: Heating mechanism for conventional and microwave heating (Bhattacharya & Basak, 2016).	30
Figure 2.6: Example of thermocouple which inserted into a sample (cutaway view) and a pyrometer (Evan et al., 2001).....	32
Figure 2.7: Fractional density of conventional sintering (5 °C/min) and microwave sintering of HMS (50 °C/min) and LMS (5 °C/min) at different temperatures (Mazaheri et al., 2008).....	39
Figure 3.1: Flow chart of the methodology.....	44
Figure 3.2: Top view of insulators of (a) base block, (b) U-shaped block and small block, (c) top block with a diameter of hole 5 mm.	46
Figure 3.3: Side view of stacked insulators before insulator was enclosed with the rectangular middle small block, x = 38.1 mm.....	46
Figure 3.4: Top view and side view of heat shield for susceptor: (a) heat shield, (b) heat shield with susceptor.	49
Figure 3.5: Orientation of samples during grinding	52
Figure 3.6: Schematic diagram of an indentation (a) side view of indentation, (b) top view of indentation.	55
Figure 3.7: Schematic diagram of the number of intercepts at a test line.....	57
Figure 4.1: Hot spot on insulation base after microwave sintering without susceptors..	60
Figure 4.2: Three samples configuration surrounded by four susceptors.	61

Figure 4.3: Example of samples crack after microwave sintering with (a) four susceptors, (b) three susceptors.	61
Figure 4.4: Six samples configuration surrounded by four susceptors.	62
Figure 4.5: Example of samples crack after microwave sintering at 50 °C/min with four susceptors.	62
Figure 4.6: Temperature profile for samples during microwave sintering at a heating rate of 50 °C/min.	63
Figure 4.7: Six samples configuration surrounded by two heat shields with susceptors.	64
Figure 4.8: Temperature profile for samples during microwave sintering at a heating rate of 30 °C/min.	64
Figure 4.9: Temperature profile for pre-sintered samples during microwave sintering at a heating rate of 30 °C/min.	65
Figure 4.10: Comparison of the XRD traces for undoped Y-TZP when microwave sintered at 1100 °C (a) with pre-sintering and (b) without pre-sintering. Key: t - tetragonal phase.	66
Figure 4.11: XRD traces of microwave sintered samples at different temperatures (a) 0.5 wt% and (b) 1 wt% CuO-doped Y-TZPs. Key: m - monoclinic phase and t - tetragonal phase.	68
Figure 4.12: Comparison of the XRD traces for 0.5 wt % CuO-doped Y-TZP when sintered at 1100 °C by (a) microwave method and (b) conventional method. Key: m – monoclinic phase and t - tetragonal phase.	69
Figure 4.13: The effect of CuO and microwave sintering temperature on the relative density of Y-TZPs.	70
Figure 4.14: FE-SEM micrographs of different content of CuO-doped Y-TZPs (a) 0.05 wt% and (b) 0.1 wt% microwave sintered at (i) 1100 °C and (ii) 1200 °C respectively.	71
Figure 4.15: FE-SEM micrographs of 1 wt% CuO-doped Y-TZPs microwave sintered at (a) 1100 °C, (b) 1200 °C, (c) 1250 °C, (d) 1300 °C and (e) 1400 °C. Figure (ii) in each case represents the microstructure taken at higher magnification.	73
Figure 4.16: FE-SEM micrographs of Y-TZPs containing low amounts of CuO that microwave sintered at 1100 °C (a) undoped, (b) 0.05 wt%, (c) 0.1 wt% and (d) 0.2 wt%.	74

Figure 4.17: The effect of microwave sintering and CuO doping on the average grain size of Y-TZPs.	74
Figure 4.18: FE-SEM micrographs of 0.2 wt% CuO-doped Y-TZPs at different microwave sintering temperatures (a) 1100 °C, (b) 1200 °C, (c) 1250 °C, (d) 1300 °C and (e) 1400 °C	75
Figure 4.19: FE-SEM micrographs of microwave sintered samples of different amounts of CuO that microwave sintered at 1400 °C (a) undoped, (b) 0.05 wt%, (c) 0.1 wt%, (d) 0.2 wt%, (e) 0.5 wt% and (f) 1 wt%.....	76
Figure 4.20: The effect of CuO addition on the Vickers hardness of Y-TZPs microwave sintered at different temperatures.....	77
Figure 4.21: The effect of CuO addition on the fracture toughness of Y-TZPs microwave sintered at different temperatures.....	79
Figure 4.22: Schematic diagram on the stabilization and yttria content of CuO-doped Y-TZPs (a) with content \leq 0.5 wt% (b) 1.0 wt%.	80
Figure 4.23: EDS Spectrum of microwave sintered Y-TZPs of different amounts of CuO that microwave sintered at 1100 °C (a) undoped, (b) 0.05 wt%, (d) 0.1 wt%, (d) 0.2 wt%, (e) 0.5 wt% and (f) 1 wt%.....	82
Figure 4.24: The effect of conventional sintering (CS) and microwave sintering (MW) on the relative density of the undoped and 0.2 wt% CuO-doped Y-TZPs.....	84
Figure 4.25: The effect of conventional sintering (CS) and microwave sintering (MW) on the Vickers hardness of the undoped and 0.2 wt% CuO-doped Y-TZPs.....	86
Figure 4.26: The effect of conventional sintering (CS) and microwave sintering (MW) on the Fracture toughness of the undoped and 0.2 wt% CuO-doped Y-TZPs.....	88
Figure 4.27: FE-SEM micrographs of undoped Y-TZPs sintered via: microwave sintering (a) 1100 °C, (a) 1200 °C, (c) 1250 °C, (d) 1300 °C, (e) 1400 °C and conventional sintering (f) 1100 °C, (g) 1200 °C, (h) 1250 °C, (i) 1300 °C, (j) 1400 °C.....	89
Figure 4.28: FE-SEM micrographs of 0.2 wt% CuO-doped Y-TZPs sintered via: microwave sintering (a) 1100 °C, (a) 1200 °C, (c) 1250 °C, (d) 1300 °C, (e) 1400 °C and conventional sintering (f) 1100 °C, (g) 1200 °C, (h) 1250 °C, (i) 1300 °C, (j) 1400 °C.	90
Figure 4.29: Effect of conventional and microwave sintering on the grain size of undoped and 0.2 wt% CuO-doped Y-TZPs at different sintering temperatures.....	92
Figure 4.30: Effect of conventional and microwave sintering on the grain size and density of undoped and 0.2 wt% CuO-doped Y-TZPs.	93

Figure 4.31: XRD traces of undoped Y-TZPs sintered at 1400 °C via (a) conventional sintering, (b) microwave sintering, after exposure in superheated steam at 180 °C/10 bar up to 200 h. Key: t-tetragonal phase. 96

Figure 4.32: XRD traces of 0.2 wt% CuO-doped Y-TZPs sintered at 1400 °C via (a) conventional sintering, (b) microwave sintering, after exposure in superheated steam at 180 °C/10 bar up to 200 h. Key: t-tetragonal phase. 97

Figure 4.33: Surface observation of several samples (a) before ageing and (b) after ageing for 200 h, where the white samples are undoped Y-TZPs and dark grey samples are 0.2 wt% CuO-doped Y-TZPs. 98

University of Malaya

LIST OF TABLES

Table 2.1: Dielectric properties of materials.....	33
Table 3.1: Parameters in microwave control panel for heating rate 30 °C/min.....	48
Table 3.2: Parameters in microwave control panel for heating rate 50 °C/min.....	48
Table 4.1: Tetragonal and monoclinic phase determined from XRD analysis of microwave sintered samples. The monoclinic phase is given in parenthesis if present.	67
Table 4.2: Summary of Vickers hardness of Y-TZP ceramics sintered at different temperatures.....	87
Table 4.3: Summary of grain size for conventional and microwave sintered Y-TZPs at different sintering temperatures and heating rate.....	92

University of Malaysia

LIST OF SYMBOLS AND ABBREVIATIONS

ASTM	:	American Society of Testing and Materials
Al ₂ O ₃	:	Alumina
C	:	Carbon
CS	:	Conventional sintering
Cu	:	Copper
CuO	:	Copper oxide
EDS	:	Energy dispersive X-Ray
FA	:	Flyash
FE-SEM	:	Field emission scanning electron microscope
Fe ₂ O ₃	:	Iron oxide
GO	:	Graphene oxide
HMS	:	High microwave heating rate
Hv	:	Vickers hardness
ISO	:	International organization for standardization
K _{Ic}	:	Fracture toughness
LMS	:	Low microwave heating rate
LTD	:	Low temperature degradation
MnO ₂	:	Manganese oxide
<i>m</i> -phase	:	Monoclinic phase
MW	:	Microwave
O	:	Oxygen
SiC	:	Silicon carbide
SiO ₂	:	Silica
SPS	:	Spark plasma sintering

<i>t</i> -phase	:	Tetragonal phase
<i>t-m</i>	:	Tetragonal to monoclinic
TSS	:	Two-step sintering
XRD	:	X-ray diffraction
Y	:	Yttrium
Y ₂ O ₃	:	Ytria
Y-TZP	:	Ytria tetragonal zirconia polycrystal
Zr	:	Zirconia
ϵ'	:	Dielectric constant
ϵ''	:	Dielectric loss
$\tan \delta$:	Loss tangent or permittivity
ρ	:	density
wt%	:	Weight percentage

University of Malaya

CHAPTER 1: INTRODUCTION

1.1 General Introduction

Ceramics were introduced for orthopaedics application for total hip and knee arthroplasty since the 1970s, owing to the excellent mechanical properties and biocompatibility. Zirconia has been proposed as one of the bioceramics used for orthopaedics application since 1985, where its biocompatibility was studied *in vitro* and *in vivo* with no adverse responses reported (Manicone et al., 2007; Murugan & Ramakrishna, 2005). In the 1990s, yttria tetragonal zirconia polycrystal (Y-TZP) became popular and there is more than 600,000 units of zirconia femoral heads have been used as implant globally (Gremillard et al., 2013).

Nowadays, Y-TZP has been utilized in various application, ranging from wear and bearing applications, engine components, cutting tools, catalyst, oxygen sensors, thermal barrier coatings, solid oxide fuel cell devices, medical devices to dental restoration (Ai et al., 2015; Denry & Kelly, 2008; Shukla & Seal, 2005). Stabilizing zirconia with 3 mol % of yttria and sintering at a range of temperatures ranging from 1300 °C to 1500 °C resulted in a Y-TZP body composed of a tetragonal structure that possesses high fracture toughness of 4-10 MPa.m^{1/2}, Young's modulus of 210 GPa, Vickers hardness of 12-13 GPa and fracture strength of 900-1200 MPa (Chevalier & Gremillard, 2009; Piconi & Maccauro, 1999; Presenda et al., 2015). Other distinctive properties of Y-TZP include low wear resistance, low coefficient of friction, chemical inertness, low thermal conductivity and high melting point (Ai & Kang, 2004; Lorenzo et al., 2002; Shukla & Seal, 2005).

To date, Y-TZP has been commonly used as dental restoration and prosthodontics due to the biocompatibility and aesthetic value of zirconia (Soon et al., 2016; Yang & Ji, 2016). This led to substantial properties evaluation done on commercial Y-TZP dental

ceramics. For instance, manufacturers such as Vita Zahnfabrik, Ivoclar Vivadent and 3M ESPE has produced commercial Y-TZP dental crowns with the code name of In-Ceram YZ and Lava, which exhibit bending strength above 900 MPa and fracture toughness above 5 MPa.m^{1/2} (Yang & Ji, 2016). In summary, zirconia possesses high biocompatibility, good in mechanical properties and aesthetic value which is suitable in dental restoration and prosthodontics applications as crowns, root post, bridges and implant abutments (Khaskhoussi et al., 2017).

1.2 Problem Statement

Between 1999 to 2001, hundreds of total hip prostheses failed and were eventually withdrawn from the market, which has attracted considerable attention (Inokoshi et al., 2014). Also, Food and Drug Administration USA warned that steam sterilization of zirconia femoral heads for total hip prostheses could result in phase transformation and roughening of the surface of the ceramic, leading to increased wear on the acetabular component (Kelly & Denry, 2008). Although Y-TZP have excellent mechanical properties, clinical failures occurred for Y-TZP dental crowns under intraoral environment attributed to the low temperature degradation (LTD) of Y-TZPs (Yang & Ji, 2016).

It is well documented that ageing or LTD is usually accompanied by tetragonal-to-monoclinic (*t-m*) phase transformation at the surface, followed by microcracking and loss of strength (Kelly & Denry, 2008; Zhang et al., 2014). Therefore for the past few decades, many researchers focused on different factors which could influence the hydrothermal ageing behavior of Y-TZPs such as grain size, sintering temperature, sintering technique and starting powder, stabilizer content, and presence of dopant (Kanellopoulos & Gill, 2002; Masaki, 1986; Presenda et al., 2015; Tredici et al., 2016). Among various transition metal oxides doped in Y-TZP, copper oxide had effectively delayed phase transformation

during ageing. The samples doped with 0.05 wt% copper oxide exhibited less than 5% of monoclinic phase as compared with undoped samples after ageing in superheated steam at 180 °C/10 bar up to 3000 h. Besides, shorter sintering holding time and low temperatures doped samples were found to contribute to better hydrothermal ageing resistance (Kanellopoulos & Gill, 2002). On the other hand, densification of ceramics is hard to achieve due to the agglomeration and grain growth by conventional sintering, where high temperatures are required to achieve densification but promote grain growth and hydrothermal degradation (Binner et al., 2008; Borrell et al., 2013). Therefore, different sintering techniques have been proposed to reach densification at lower sintering temperatures and shorter sintering time. This includes microwave sintering, spark plasma sintering, hot isostatic pressing and two step sintering (Binner et al., 2008; Langer et al., 2011; Presenda et al., 2017; Sutharsini et al., 2014).

Among all the sintering methods, microwave sintering has been widely used to improve the densification and mechanical properties of ceramic especially at low temperatures with short sintering holding times (Mazaheri et al., 2008; Pian et al., 2014). In the past few decades, microwave processing on zirconia focused on its densification, mechanical properties, dielectric loss, influence of susceptors and comparison with different sintering techniques (Bhattacharya & Basak, 2016; Oghbaei & Mirzaee, 2010). A group of researchers studies the effect of hydrothermal ageing of microwave and conventional sintered commercial dental zirconia and as-received Tosoh Y-TZP. The latter samples did not degrade after hydrothermal ageing at 125 °C/1.6 bar for 140 h while maintaining the mechanical properties (Presenda et al., 2015).

Owing to the hydrothermal degradation resistance of microwave sintered undoped samples, microwave sintered copper oxide doped Y-TZPs were suggested which could enhance mechanical properties of zirconia at low sintering temperature. In microwave

sintering, the material absorbs microwave energy depending on its dielectric properties and transform it into heat within the body (Bhattacharya & Basak, 2016). Since zirconia is a microwave transparent material at low temperature, doping a microwave absorber such as copper oxide could enhance the dielectric properties of the whole body especially during the preheating stage of sintering. Although microwave sintering could provide higher heating rates at lower sintering temperatures as compared with conventional sintering method, crack-free samples are difficult to be obtained due to different microwave sintering configuration and nonuniform heating. Thus, there is a need in determining the microwave sintering configuration and parameters to achieve uniform heating with crack-free samples. Besides, the effect of microwave sintered copper oxide doped zirconia worth to be explored to achieve better mechanical properties without compromising on the degradation behaviour.

1.3 Scope of Research

The study will provide an optimum microwave sintering parameter which covers the influence of susceptors, microwave heating rates and the necessities of pre-sintering during microwave sintering. Microwave sintering will be performed in a 2.45 GHz multimode microwave furnace (6 kW). Pyrometer was used to record the temperature of the samples. Undoped and copper oxide doped samples which vary from 0.05 wt% to 1 wt% were selected and microwave sintered at the temperatures ranging from 1100 °C to 1400 °C, accompanied with a short holding time of 5 min.

The microwave sintered samples were then evaluated in terms of phase stability, relative density, Vickers hardness, fracture toughness, microstructure and grain size. In addition, conventional sintering was performed at 10 °C/min at the same designated sintering temperatures and holding time on selected samples for further comparison purpose. Ultimately, the selected samples will be subjected to hydrothermal degradation

in an autoclave filled with superheated steam at 180 °C/10 bar up to 200 h. The phase analysis will be performed on the as-sintered and aged samples at selected ageing intervals up to 200 h.

1.4 Research Objectives

The main objective of this study is to enhance the mechanical properties and suppress low temperature degradation behaviour of copper oxide doped zirconia via microwave sintering methods. The following are the sub-objectives of this project:

1. To determine the optimum microwave sintering parameters to produce crack-free samples.
2. To investigate the effects of copper oxide addition and microwave sintering on the densification, mechanical properties and microstructure evolution of the Y-TZP ceramic.
3. To compare the densification behaviour of Y-TZP subjected to microwave and conventional sintering.
4. To evaluate the low temperature degradation of copper oxide doped and undoped zirconia through exposure in the superheated steam environment.

1.5 Structure of Thesis

The thesis is composed of five chapters. Chapter 1 consists of an introduction, which introduces the general background, problem statement, scope of research, research objectives and outlines the structure of thesis.

Chapter 2 elaborates on the literature review of zirconia and low temperature degradation. Section 2.3 highlights the factors governing low temperature degradation, which includes ageing temperature, medium, pressure, grain size, sintering techniques, starting powders and presence of dopants. The last section, Section 2.4 presents the

microwave sintering in terms of introduction, main components, dielectric properties, issues in microwave heating, design and configuration and the effect of microwave heating.

In Chapter 3 discusses the methodology of the current research. The first section covers the preliminary study on the microwave processing parameters and setup prior to sintering. This is followed by the bulk samples preparation of copper oxide doped Y-TZPs. The different characterization methods in terms of phase stability, density, Vickers hardness, fracture toughness, microstructure, grain size and LTD behaviour would be discussed.

Chapter 4 presents all the results obtained from the characterization methods. The effect of addition of copper oxide up to 1 wt% in Y-TZP matrix are discussed in this chapter. This chapter also deals with the comparison between microwave sintering and conventional sintering. Finally, Chapter 5 concludes all the results and recommends works that could be done for further investigations.

CHAPTER 2: LITERATURE REVIEW

2.1 Introduction of Zirconia

Zirconium, Zr is an element of transition metal with atomic number 40, atomic weight of 91.22 and density of 6.49 g/cm³. Zirconium oxide/Zirconia is a metal oxide with the chemical formula ZrO₂, which was discovered by Martin Heinrich Klaproth in 1789 and could be found in the minerals baddeleyite and zircon (Abd El-Ghany & Sherief, 2016; Piconi & Maccauro, 1999). Pure zirconia exists in three allotropes namely monoclinic (*m*), tetragonal (*t*) and cubic (*c*) phase. Pure zirconia exists in the monoclinic structure at room temperature. When the temperature increases to 1170 °C, the structure transforms to tetragonal and subsequently to the cubic phase when the temperature reaches 2370 °C (Zhang & Zhang, 2014). Monoclinic phase is the weakest phase among all three allotropes which exhibit low strength and toughness (Chevalier et al., 2009). Although tetragonal is desirable, the phase transformation from tetragonal to monoclinic (*t-m*) is diffusionless and usually associated with a volume increase up to 5% especially during cooling. Therefore, stabilizers such as calcia (CaO), yttria (Y₂O₃), magnesia (MgO) and ceria (CeO₂) were added to obtain tetragonal phase in metastable form at room temperature (Lughi & Sergio, 2010).

Among all the stabilizers, Y₂O₃ is commonly used as a stabilizer as tetragonal zirconia ranging from structural to biomedical applications due to the outstanding mechanical properties (Piconi et al., 1998). The addition of 3 mol % yttria in Y-TZP possessed high bending strength above 1000 MPa and fracture toughness of about 6 MPa.m^{1/2}, owing to its strengthening mechanism named as transformation toughening. The stress induced *t-m* phase transformation occurred at the tip of the crack, where the expansion results in compressive stresses which inhibit crack propagation, leads to the increase of toughness and strength to the ceramics (Ćorić et al., 2017; Piyapanna et al., 2009). To date, tetragonal zirconia with 3 mol% Y₂O₃ (3Y-TZP) has been commonly used in dental

applications such as crowns, bridges, implant abutments and root post (Khaskhoussi et al., 2017). For instance, zirconia implant abutment has shown excellent survival rates after crown insertion for five years (Zembic et al., 2013). Recently, translucent Y-TZPs were reported by several researchers to achieve good mechanical properties and esthetic appearance for dental restoration (Tong et al., 2016; Zhang et al., 2015; Zhang, 2014).

2.2 Low Temperature Degradation

The major limitation of zirconia is ageing or low temperature degradation (LTD), which induced *t-m* transformation at low temperatures between 150 °C and 400 °C (Lange et al., 1986). Severe degradation occurred between 180 °C and 300 °C, where high *m*-phase was formed and accompanied by deterioration in bending strength and fracture toughness (Lawson, 1995). Besides, ageing was often associated with surface degradation, such as surface roughening, grain pull out, surface uplift, microcracking and leads to deterioration of mechanical properties (Flinn et al., 2014; Harada et al., 2016). This issue has attracted substantial attention when a number of Prozyr ceramic balls failed prematurely with the increase of *m*-phase (Lughi & Sergio, 2010). Apart from orthopaedic implants, LTD was also arise in oral environments due to oral bacteria, pH changes, fluctuating temperatures and constant exposure to heavy mastication loads, which could be deleterious for the dental application (Harada et al., 2016). In general, *t-m* phase transformation occurs with the presence of moisture or local stress is generated, known as LTD or hydrothermal degradation (Pereira et al., 2016). There are many factors that governs the LTD behaviour of Y-TZP and this will be deliberated in the subsequent sections.

2.3 Factors Governing LTD

The kinetics of degradation is greatly affected by the ageing environment such as ageing temperature, pressure, medium and exposure duration. To envisage the ageing in shorter duration, the accelerated ageing test was then introduced to resemble the actual condition of ageing *in vivo*. Based on ISO 13356, accelerated ageing in water is recommended at 134 °C, 0.2 MPa for 5 h, which resemble the ageing condition of 15–20 years of implants (in water at 37 °C) in the orthopaedic industry (Harada et al., 2016). It was also predicted that 1 h ageing in autoclave at 134 °C could represent the ageing condition for three to four years *in vivo* at 37 °C (Deville et al., 2005). According to the requirement for clinical application by ISO 13356, *m*-phase content should not exceed 25% after subjected to ageing in an autoclave at 134°C /0.2 MPa for a duration of 5 h (Pereira et al., 2016). In the case of industrial ceramics, the ageing test conditions were in accordance to ISO standard for medical zirconia and the Japanese industrial standard, which is at 180 °C in water, 1 MPa for 1 h. This condition has become a reference for the dentistry industry (Harada et al., 2016). The recommended ageing temperature for Y-TZP ceramics for dental and industrial applications is harsher because ageing at higher temperature provides an aggressive environment to gauge the vulnerability of the zirconia to undergo the phase transformation (Flinn et al., 2014).

There are also other important factors governing the LTD behaviour of Y-TZP ceramics, which are grain sizes and the presence of dopants. According to thermodynamics approach, the factors that affect LTD is controlled by the change of total free energy of phase transformation (ΔG_{t-m}). ΔG_{t-m} is the summation of the change of chemical free energy (ΔG_{CHEM}), change of surface free energy (ΔG_{SURF}) and change of strain free energy (ΔG_{STRAIN}) (Lughi & Sergio, 2010). To maintain in the tetragonal phase, ΔG_{t-m} must be positive to prevent phase transformation to occur. ΔG_{CHEM} is the chemical free energy difference between the monoclinic and tetragonal phase. It is reliant on

composition and temperature, thus could be increased by adding stabilizer or addition of dopant contents. ΔG_{STRAIN} is dependent on the modulus surrounding matrix and the change of shape. This could be increased by introducing higher modulus dopants into zirconia such as alumina, to stabilize the tetragonal phase. ΔG_{SURF} is dependent on the critical size of the particle, where this could be increased by reducing grain size (below critical grain size) (Chevalier et al., 2009; Lange, 1982; Lughì & Sergo, 2010; Singh, 1999). In general, $\Delta G_{\text{t-m}}$ could be increased by reducing grain size and adding sintering additives (Lawson, 1995). Due to the limitation of conventional sintering and chemical composition of Y-TZP, different sintering methods and sintering dopants were introduced to reduce sintering temperatures, without compromising on the densification and reduce grain size. The next section will elaborate on the influence of grain size, which affected by the sintering temperatures. Also, other sintering techniques will be introduced to achieve high density and small grain size to suppress LTD. The LTD behaviour of different starting powder, stabilizer (yttria) content and selective dopants will also be discussed.

2.3.1 Ageing Temperature

Several researchers revealed that severe phase transformation occurs between 180 °C and 300 °C. At these temperatures, higher monoclinic phase was formed and accompanied by deterioration in the mechanical properties (Kim et al., 2009; Lawson, 1995). Kim et al. (2009) studied the effect of ageing on the flexural strength of commercial zirconia (Vita In-Ceram YZ) exposed at different temperatures (20 °C, 75 °C, 100 °C, 125 °C, 150 °C, 175 °C, 200 °C and 225 °C) in distilled water for 10 h. The results showed that flexural strength increased when exposed between 20 °C and 125 °C but starts to decline when the monoclinic phase content reached about 54% at 150 °C, as illustrated in Figure 2.1. When the Y-TZP was aged at high temperatures above 175 °C,

the monoclinic phase content reached saturation at 75%, while the flexural strength continues to fall.

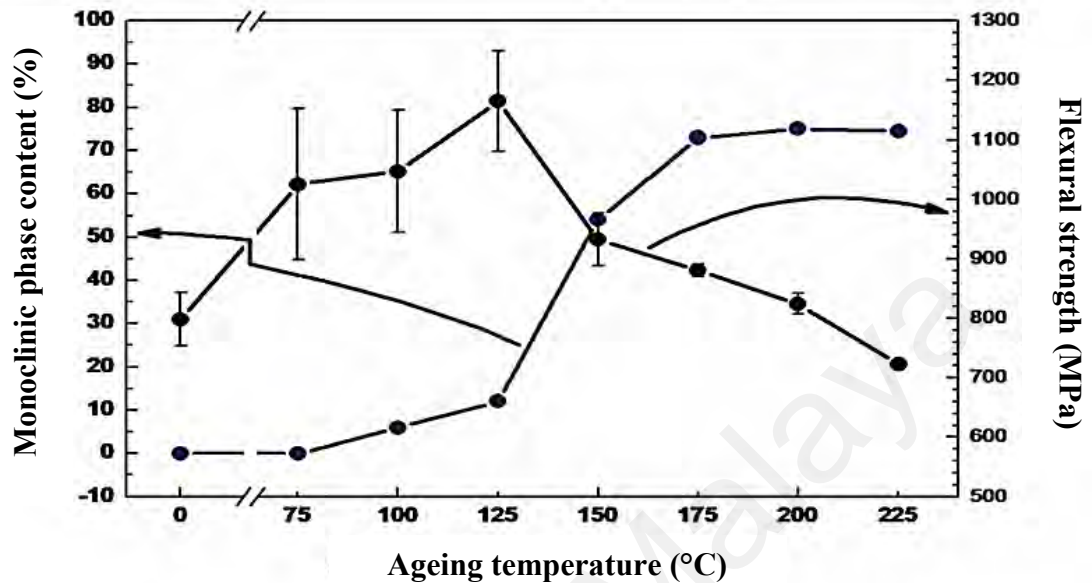


Figure 2.1: Monoclinic phase development and flexural strength of commercial zirconia (Vita In-Ceram YZ) exposed at different ageing temperatures (Kim et al., 2009).

Borchers et al. (2010) who exposed commercial (Lava) Y-TZP in water at 134 °C/3bar for 8 h, 80 °C for 64 days and 36 °C for 200 days, found that regardless of ageing condition, there was an increased in the monoclinic content but did not significantly affected the flexural strength. On the other hand, another research showed that hydrothermal ageing of (Lava) Y-TZP in steam at 140 °C for 7 days resulted in a 30% reduction in Young's modulus and hardness (Cattani-Lorente et al., 2011). This outcome is consistent with the results reported by Chowdhury et al. (2007), who observed a 30% reduction in Young's modulus and 40% reduction in hardness. The authors observed a development of about 78% monoclinic phase in the zirconia femoral head when aged in saturated water vapour at 121 °C. Binner et al. (2011) found that 3 mol% Y-TZP developed about 73.5% monoclinic content after 168 h of ageing at 140 °C/4bar and disintegrated after prolong exposure for 336 h in an autoclave filled with deionized water. However, when the ageing temperature increased to 245 °C/7bar, the Y-TZP

disintegrated after 1 h of exposure. Keuper et al. (2014) found that a few hours of ageing commercial (Vita In-Ceram) Y-TZP in water vapour at 134 °C/3 bar produced a monoclinic layer which was similar to that observed after four years kept under body temperature condition at 37 °C.

In recent years, most ageing studies have focused either at 134 °C or 180 °C in accordance with the ISO standards. According to standard autoclave sterilization conditions, the Y-TZP should be exposed at 134 °C/2 bar. On the other hand, based on the industrial ceramic standard, ageing is normally performed under autoclave steam condition at 180 °C/10 bar to examine the vulnerability of the Y-TZP to undergo the *t-m* phase transformation (Flinn et al., 2012; Flinn et al., 2014).

2.3.2 Ageing Medium

Kawai et al. (2011) aged commercial Y-TZP manufactured by Daiichi Japan in three different solutions i.e. distilled water, Hank's solution, and lactic acid at 140 °C for 7 days. A similar monoclinic phase content of about 60% was measured in the Y-TZPs regardless of medium type. The outcome prompted the authors to believe that the solutions have negligible effect on the ageing behaviour of Y-TZP. In an oral environment, constant exposure to heavy loads of mastication, fluctuating temperatures, pH changes, and oral bacteria could amplify the effect of ageing compared to when used for orthopaedic implants in the body (Harada et al., 2016; Lughì & Sergo, 2010). In another study, Kosmač et al. (2008) performed an experiment on commercial Tosoh biomedical-grade Y-TZP (TZ-3YB-E) by exposing the samples in artificial saliva at 37 °C. The authors discovered that flexural strength reduced from 1000 MPa (as-sintered samples) to about 900 MPa after 24 h of exposure. This result is consistent with that reported by Miragaya et al. (2017) who observed a decreased in the flexural strength from 1322.9 MPa to 843.7 MPa for commercial dental Y-TZP (Lava Frame) after exposure in

human oral cavity using intra-oral appliances for 60 days. Similar degradation in terms of flexural strength occurred with the commercial dental Y-TZP (Lava Plus), where the strength decreased from 955.9 MPa to 603.2 MPa. The decrease of flexural strength is accompanied with the formation of monoclinic phase of Y-TZP (Lava Frame) (7.7%) and Lava Plus (4.7%). The authors explained that the decreased of flexural strength was due to the presence of ions and humidity in the human saliva.

Ban et al. (2008) further aged TZ-3YB-E samples in physiological saline (0.88% NaCl) at 80 °C for 30 days, 4% acetic acid at 80 °C for 30 days and in an autoclave containing steam at 121 °C/1 bar for 10 days. After the ageing experiment in the different mediums, all the Y-TZP samples developed monoclinic phase accompanied by a declined in the biaxial flexural strength. According to the authors, ageing in an autoclave for 10 days was most severe as the samples yielded a monoclinic content of 50% and suffered a 15% reduction in flexural strength. In contrast, Y-TZP samples aged in saline and acetic acid recorded a monoclinic phase of about 2 %. Cotes et al. (2014) explored different ageing conditions and found that autoclave ageing commercial Y-TZP (Vita In-Ceram) samples at 134 °C/2 bar for 12 h induced accelerated ageing with the formation of 30% monoclinic phase, as compared to 12.2% obtained for samples aged in distilled water at 37 °C for 400 days. Another study demonstrated that the monoclinic phase content measured for a commercial Y-TZP (Kobe) in an autoclave at 121 °C/1.5 bar for 190 h was almost equivalent to the ageing effect in physiological saline at 62 °C for 18 months. Both mediums resulted in the development of about 80% monoclinic phase in Y-TZP after ageing (Tanaka et al., 2003).

2.3.3 Ageing Pressure

Accelerated ageing methods were necessary to save time in determining the ageing behaviour of Y-TZP. According to ISO 13356, for a zirconia to be accepted for biomedical application, the monoclinic phase content must be less than 25% after autoclave in steam at 134 °C, 2 bar pressure for 5 h (Lucas et al., 2015; Lughì & Sergo, 2010). A general consensus is that 1 h of autoclave ageing is equivalent to 3 to 4 years *in vivo*; hence 5 h of accelerated ageing would typically represents more than 15 years of actual exposure (Deville et al., 2005; Roy et al., 2007). According to Lucas et al. (2015), ageing Y-TZP in steam at 134 °C/2 bar for 5 h would produce a similar ageing effect (i.e. monoclinic phase content of about 20%) with the same sample that exposed in hot water (100 °C) for 3.5 days. Likewise, ageing Y-TZP at 134 °C/2 bar for 3 h would also yielded similar monoclinic phase content of about 13% as the samples that exposed in hot water (100 °C) for 40 h.

The results implied that applied pressure for a short time (3-5 h) could accelerate the ageing condition of Y-TZP; resulting in an outcome that is equivalent to the normal ageing condition at a prolonged duration. A lower pressure of 1 bar (at 121°C) produced 9.27% monoclinic phase content after ageing for 5 h but 3 h of ageing at 2 bar pressure (at 134°C) resulted in the development of 12.6% monoclinic content (Lucas et al., 2015). Therefore, the higher the steam pressure applied during ageing, the more aggressive would be the test environment and hence accelerating the monoclinic phase development within a shorter period of time.

2.3.4 Grain Size

Grain size has been frequently been associated with the stability of the tetragonal grains as this has an effect on the ageing behaviour of Y-TZPs. Many researchers have proposed that a critical grain size limit existed, above which resulted in the *t-m* phase

transformation. Masaki (1986) who studied the ageing behaviour of Y-TZP by exposing the samples in hot air at 200 °C for 2000 h, found that the *t-m* phase transformation was suppressed in samples that have grain sizes below 0.5 µm. Chen and Lu (1989) proposed an ageing map to describe the LTD behaviour of Y-TZP in air and water. They varied the ageing temperatures from 100 °C to 500 °C for different periods (30 h in air and 1 week in water) and found that the critical grain size for air was 0.52 µm and for water was 0.37 µm. This result clearly indicates that the hydrothermal ageing becomes more severe when exposed in hot water or steam condition than in air. Thus, most of the studies on LTD focuses on exposing the zirconia samples under hydrothermal conditions, particularly in superheated steam conditions (Lawson et al., 1995; Li & Watanabe, 1998).

Dental implants made from 3 mol% Y-TZP have been studied extensively since 1999, especially after the failure of the Prozyr femoral head between 2001 and 2002. Following the recommendation of Chevalier (2006), ISO 13356 was revised in 2008, where the critical grain size was reduced from 0.6 µm to 0.4 µm. Lucas et al. (2015) investigated the degradation of commercial Y-TZPs having different grain sizes according to the revised ISO 13356:2008 standard by exposing the samples in water vapour at 134°C/2 bar for 5 h. They found that after ageing for 5 h, the samples with a grain size of 0.428 µm yielded 4.03% of *m*-phase, whereas sample with a larger grain size of 0.574 µm yielded a high *m*-phase of 6.64%. However, no significant changes were observed in the Young's modulus and hardness.

Y-TZPs sintered at high sintering temperature have been reported to influence the kinetics of phase transformation during ageing. As typically shown in Figure 2.2, high sintering temperature and long holding time led to high *m* phase transformation rates. In this experiment, the tetragonal grain size was found to increase from 0.4 µm to 0.9 µm when the sintering temperatures increased from 1450 °C (2 h) to

1550 °C (5 h) (Chevalier et al., 2004). Similarly, Zhang et al. (2014) found that the rate of phase transformation for 3 mol% Y-TZP samples sintered at high sintering temperatures (≥ 1500 °C) and a combination of long holding time e.g. 1450 °C (4h) during ageing in steam at 134 °C/2 bar for 40 h was rapid as illustrated in Figure 2.3. A sigmoidal-shape curve representing the *m* phase development of up to 80% was observed for these samples.

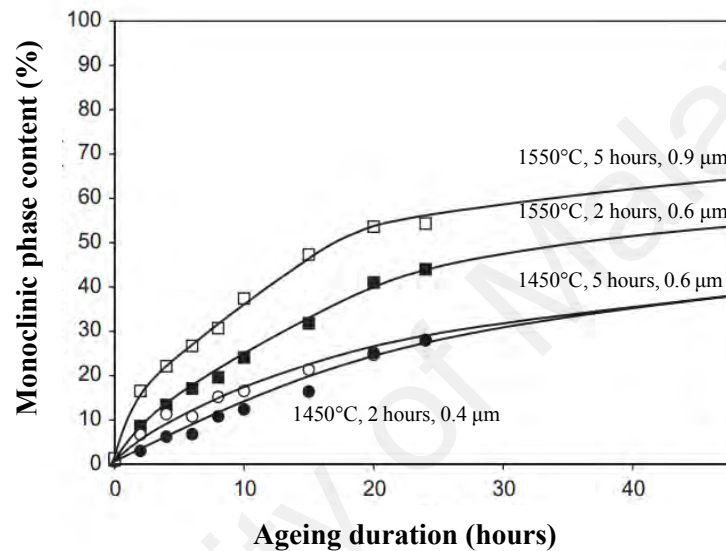


Figure 2.2: Monoclinic phase content of 3Y-TZP with respect to different sintering temperatures and holding time after hydrothermal ageing at 134 °C/2 bar for different duration (Chevalier et al., 2004).

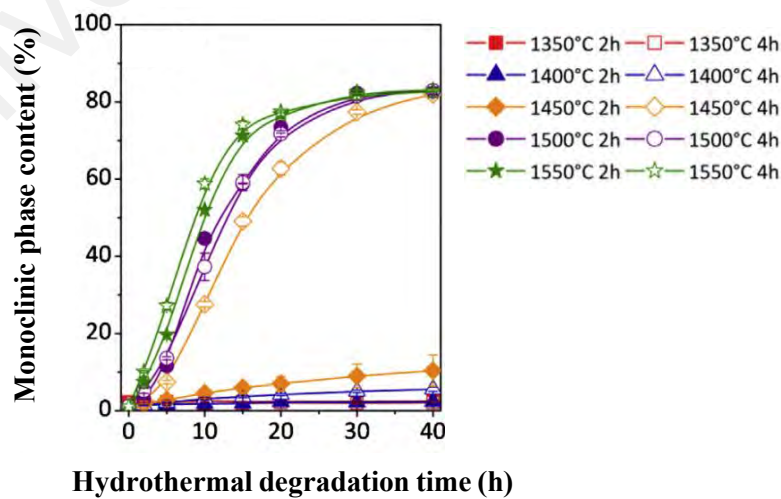


Figure 2.3: Surface monoclinic phase content as a function of hydrothermal degradation at 134 °C under 2 bar pressures for 3Y-TZP sintering at different temperatures and holding time (Zhang et al., 2014).

In another study, Palmeira et al. (2016) found that the nano-sized 3 mol% Y-TZP powders could attained high densification of 97% with a grain size of 0.20 μm when sintered at 1350 $^{\circ}\text{C}$. For micro-sized powders, a similar densification could only be achieved when the sintering is conducted at 1530 $^{\circ}\text{C}$ but at the expense of having a larger grain size i.e. 0.40 μm . The degradation behaviour of Y-TZP, however, was not reported by the authors. Paul et al. (2011) reported similar observation and they showed that nano-sized starting Y-TZP powder could suppress degradation with no *m*-phase content detected after exposure in steam at 245 $^{\circ}\text{C}$ /4 bar for 168 h. However, submicron-sized zirconia experienced LTD and recorded a *m*-phase content of 73.6% after ageing in steam at 140 $^{\circ}\text{C}$ /4 bar for 168 h.

A small grain size is therefore beneficial in suppressing ageing-induced phase transformation in Y-TZPs. However, conventional sintering temperatures above 1400 $^{\circ}\text{C}$ are generally required to achieve better densification and mechanical properties but this would lead to an increase in grain size and hence making the zirconia susceptible to ageing. Since 2000, many researchers have explored the use of different sintering techniques including two-step sintering, electric field-assisted sintering and microwave sintering in the quest to maximize densification while preventing grain coarsening.

2.3.5 Sintering Techniques

Some of the most prevailing non-conventional sintering methods used to sinter Y-TZP that have been reported by various researchers and their ageing behaviour will be discussed in this section which includes two-step sintering (TSS), electric field-assisted and microwave (MW) processing. Besides, advantages and drawbacks of each technique will be explained in the subsequent sections.

2.3.5.1 Two-Step Sintering

TSS is a technique where the sample is first sintered to a high temperature T_1 to achieve an intermediate density, followed by cooling down to a lower temperature T_2 and hold at this temperature for specific period until full densification is achieved. For TSS, the intermediate density should be above 70%–75% theoretical density before proceeding to T_2 . These researchers have shown that densification proceeded without grain growth during the second step of sintering (Chen & Wang, 2000). Mazaheri et al. (2008) performed several sintering cycles on 3 mol% Y-TZP and found that the effect of TSS would be diminished if the selected T_1 and T_2 temperatures are too close to each other, e.g. 1300 °C and 1250 °C, respectively. The researchers suggested that the optimum intermediate density should be at least 83% of theoretical value for densification to proceed without grain growth.

In a study for 3 mol% Y-TZP to determine the LTD behaviour in superheated steam at 180 °C/10 bar, two sintering profiles were selected. In this experiment, the T_1 temperature was set at 1400 °C and T_2 at 1150 °C or 1250 °C, and hold for 1 min and 2 h, respectively. After hydrothermal ageing for 50 h, samples sintered by TSS effectively prevented the phase transformation. For sintering at the higher temperature T_2 , i.e. 1250 °C, Young's modulus increased to 201 GPa along with the increased in bulk density (Sivakumar et al., 2011). This finding was also supported by the work of Sutharsini et al. (2014), who revealed that smaller grain size of 0.29 μm produced by TSS could suppress LTD in superheated steam at 180 °C/10 bar for period up to 24 h with minimal *m*-phase content detected, i.e. 0.3%. The sintering profile used by them was T_1 at 1500 °C and T_2 at 1200 °C, held for 1 min and 3 h, respectively. The researchers also reported that Vickers hardness (12–14 GPa) was not significantly affected by the sintering holding time and TSS sintering temperatures. They continued the research on TSS with a lower T_1 at 1400 °C (held for 1 min) and the same T_2 at 1200 °C which held at different holding time. They

found that sintered samples at T_2 for 20 and 30 h could suppress LTD without surface spalling or crack formation when exposed to the same ageing profile with a longer duration up to 100 h. However, samples which sintered at T_2 with the holding time ≤ 4 h fully disintegrated into powder form (Sutharsini et al., 2017). More recently, Wei and Gremillard (2018) modified the TSS method by adding post sintering thermal treatment on 3 mol% Y-TZP. They also found that a small grain size of 0.29 μm could delay the ageing-induced monoclinic formation when compared to conventional sintered samples, which had a grain size of 0.41 μm . In short, TSS could suppress LTD with controlled grain growth, but accompanied with a long processing time.

2.3.5.2 Electric Field-assisted Sintering

Another established sintering technique capable of enhancing the densification of Y-TZP is electric field-assisted sintering. This technique includes spark plasma sintering (SPS), field assisted sintering technique (FAST) or pulsed electric current sintering (PECS) (Langer et al., 2011). These methods are well known for rapidly consolidating ceramics in a short period of time. The advantages of these methods are the high heating rates (600-1000 $^{\circ}\text{C}/\text{min}$) and short holding time (3-5 min), which are capable of reducing the grain size of the sintered bodies (Basu et al., 2004; Langer et al., 2011). For instance, it has been reported that SPS with a heating rate of 600 $^{\circ}\text{C}/\text{min}$ could achieve high density ($> 99\%$) and high hardness, about 14.5 GPa. In addition, it was found that the SPS-sintered Y-TZP at 1200 $^{\circ}\text{C}$, 1250 $^{\circ}\text{C}$, and 1300 $^{\circ}\text{C}$ experienced less wear compared to Y-TZP hot isostatic pressed at 1450 $^{\circ}\text{C}$ (Basu et al., 2004). Ageing studies conducted by Smirnov et al. (2015) revealed that SPS-sintered Y-TZP in a vacuum at 1300 $^{\circ}\text{C}$ with a heating rate of 600 $^{\circ}\text{C}/\text{min}$ yielded *m*-phase content around 20% after hydrothermal ageing in steam at 134 $^{\circ}\text{C}/2$ bar for 30 h. The authors also reported that SPS-sintered zirconia could attain a high density of 99%, Vickers hardness of 11.3 GPa, fracture toughness of 5 $\text{MPa}\cdot\text{m}^{1/2}$ and Young's modulus of 197 GPa. Although SPS could sinter

ceramics in a short period, various parameters such as temperature, heating rate, holding time, pulse sequence and pressure are required to be determined.

2.3.5.3 Microwave Processing

Microwave processing and heating has been extensively used to enhance the densification of zirconia especially at low temperatures with short sintering holding times. Aside from producing fine grain microstructure, microwave sintering was also found to be effective in enhancing the density and Vickers hardness of ceramics when compared with that produced via the conventional sintering method. Microwave sintering of Y-TZP could achieve density above 98%, with shorter time of 40 min instead of 350 min typically employed for conventional sintering. In addition, exceptional Vickers hardness (16 GPa) could be achieved by microwave sintering compared with that by conventional sintering (13.7 GPa) at the same sintering temperature due to the positive effects of microwaves on densification (Borrell et al., 2013).

Recently, Presenda et al. (2017) reported that microwave sintered Y-TZP was resistant to hydrothermal degradation in steam at 125 °C/1.6 bar for 200 h, as compared with conventional sintered samples. The Y-TZP which was microwave sintered at 1200 °C at a rate of 100 °C/min for 10 min did not degrade after ageing for 200 h, as shown in Figure 2.4. However, the Y-TZP which conventional sintered at 1400 °C reached about 70% *m*-phase after ageing. They also revealed that microwave sintering provides higher fretting wear resistance as compared to conventional sintering, owing to the smaller grain size produced by microwave sintering (Presenda et al., 2017). In a study, Ai et al. (2015) prepared Y-TZP with two step microwave sintering method, where the samples were first heated to 900 °C with a heating rate of 25 °C/min for 30 min. This was proceeded to sinter at the designated temperature (1350 °C) at a heating rate of 20 °C/min for another 30 min. It was found that the improvement of density and

mechanical properties of the Y-TZP is statistically insignificant, if compared to microwave sintered at 1350 °C with the rate of 20 °C/min for 30 min. However, the degradation behaviour of Y-TZPs was not reported by the authors.

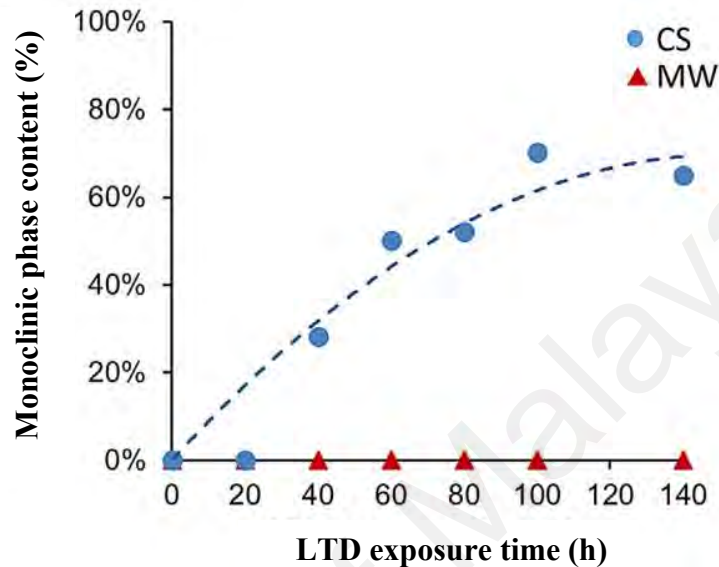


Figure 2.4: Monoclinic phase content for microwave (MW) and conventional (CS) sintered 3Y-TZP at different LTD exposure time (Presenda et al., 2017).

There are also other techniques which have been reported to suppress LTD of Y-TZPs. For example, Muñoz-Saldaña et al. (2003) discovered that the combination of conventional sintered at 1400 °C and hot isostatic pressed (HIP) at 1400 °C for Y-TZP had successfully resisted degradation in hot air (300 °C for 2000 h) and hot water (200 °C for 8 h). In another study, the combination of SPS followed by HIP for transparent Y-TZP resulted in a small grain size of 87 nm. Besides, there is no *t-m* phase transformation occurred after ageing in water vapour at 134°C/2 bar up to 100 h compared to conventional sintered samples (Yan et al., 2014).

2.3.6 Starting powder

It was discovered in 1991 that the degradation behaviour of Y-TZP was not only depended on the sintering method and grain size but also on the starting powder used (Swab, 1991). The author studied the ageing behaviour of two different 3 mol% Y-TZP

powders manufactured by different companies i.e. Koransha 1986 and NGK Locke Z-191. The results indicated that NGK Locke was resistant to ageing after exposure in water vapour for 50 h between 200 °C and 400 °C, while Koransha 1986 sample suffered phase transformation after ageing at 200 °C. A similar observation was reported by Lawson et al. (1995) who found that 3 mol% Y-TZP manufactured by Tosoh (TZ-3Y) degraded 10 times faster than Dai-ichi (HSY-3SD) after hydrothermal ageing in superheated water at 180 °C/10 bar up to 200 h. They attributed the different powder synthesis method for the reason for the different ageing behaviour observed for the two commercial powders.

It was found that colloidal processing method was useful in producing a fine and homogeneous microstructure without the presence of aggregates compared with conventional powder mixing method (Deville et al., 2003). Paul et al. (2011) prepared nano-sized 3 mol% Y-TZP using slip casting and compared the ageing behaviour with submicron Tosoh Y-TZP (3YSB-C) having a grain size of 0.52 µm. They found that the sample yielded about 73.6% *m*-phase content and developed about 25 µm thick *m*-layer after ageing in steam at 140 °C/4 bar for 168 h. In contrast, the slip-cast Y-TZP, having a grain size of 90 nm, showed no degradation and no loss in hardness after hydrothermal ageing at 140 °C and 245 °C/ 4 bar for 180 h. The authors attributed the excellent ageing resistance of the slip-cast zirconia to the uniform distribution of yttria across the grains and grain boundaries. For submicron samples that sintered at 1500 °C, yttria content was heterogeneously distributed at grain boundaries and triple points, generating several cubic grains.

There is also a huge difference in the ageing induced monoclinic phase development for 2 mol% Y-TZP prepared by different synthesis methods i.e. CO₂ laser vaporization (LAVA) and wet mixing method (Smirnov et al., 2015). They found that (LAVA) Y-TZP exhibited high toughness of 13 MPa.m^{1/2} and was resistant to hydrothermal ageing when

exposed to steam at 134°C/2 bar for 30. In contrast, wet mixing of 2 mol% Y-TZP yielded a *m*-phase content of 85% after exposure for 30 h. Therefore, the synthesis method could play a significant role in determining the LTD behaviour of Y-TZP.

2.3.7 Yttria Content

It has been postulated by many researchers that water or hydroxyls preferentially attacks low yttria regions in the tetragonal structure, causing *t-m* phase transformation. Yttria content has also been identified as a key factor influencing LTD. The general consensus is that increasing yttria content could suppress hydrothermal ageing (Paul et al., 2011; Zhang et al., 2015). It was reported that nano-size 3 mol% Y-TZP was resistant to hydrothermal ageing up to 168 h, however nano-sized 1.5 mol% Y-TZP developed monoclinic content of above 99% within 4 h of exposure and disintegrated into powder form after 16 h exposure at 140 °C. It was also found that 2 mol% Y-TZP yielded 20% *m*-phase when subjected to ageing at 140 °C for 120 h (Paul et al., 2011). Similarly, observation was reported by Tredici et al. (2016) who found that the *t-m* phase transformation proceeded in Y-TZP having 0.5 mol% and 1.5 mol% yttria when exposed to steam at 134 °C/2-3 bar for 25 h, whereas 3 mol% Y-TZP did not experience phase transformation at the same condition. Zhang et al. (2015) also confirmed that 3 mol% Y-TZP exhibited better LTD resistance as compared with 2 mol% and 2.5 mol% Y-TZPs when subjected to ageing in superheated steam at 134 °C/2 bar up to 40 h. The higher the yttria content, the better the degradation resistance of Y-TZP when exposed in superheated steam, varying from 0.5 mol% to 3 mol% of yttria content.

One of the common observations as the yttria content increased to 4-5 mol% is the development of a microstructure comprised of abnormal large cubic grains within the tetragonal matrix. A microstructure comprised of fully cubic grains would result when the yttria content increased to 6-8 mol%. Although the ageing seemed to be suppressed

with increasing yttria content, the presence of the cubic phase resulted in lower strength and toughness (Cutler et al., 1992; Ghatee & Irvine, 2010). In a recent study on translucency of commercial Y-TZP material, higher cubic phase content (~6 mol% Y_2O_3) contributed in better translucency and suppressed hydrothermal degradation in steam at 134 °C/2 bar up to 54 h. However, these samples experienced a decrease in mechanical properties, i.e. toughness and strength (Camposilvan et al., 2018). In short, chemical-free energy for *t-m* phase transformation increases linearly with yttria content, where positive chemical-free energy inhibits phase transformation of zirconia (Bravo-Leon et al., 2002).

2.3.8 Presence of Dopants

Numerous researchers have reported that the ageing-induced phase transformation of Y-TZP could be suppressed by adding a small amount of dopants or sintering additives. In particular, dopants including copper oxide (CuO), iron oxide (Fe_2O_3), manganese oxide (MnO_2), alumina (Al_2O_3), cerium oxide (CeO_2), silica (SiO_2), titania (TiO_2), tantalum oxide (Ta_2O_5), zinc oxide (ZnO_2) and magnesium oxide (MgO) have been studied (Bowen et al., 1998; Nogiwa-Valdez et al., 2013; Ran et al., 2006; Zhang et al., 2014). The subsequent section will discuss the influence of selective dopants on the hydrothermal degradation behaviour of Y-TZP.

2.3.8.1 Alumina

Alumina (Al_2O_3), is one of the popular dopants to be added in Y-TZP. Vasylykiv et al. (2003) reported that a small amount of Al_2O_3 (2.5 wt%) was sufficient in aiding densification compared to the undoped, 1.25 wt% and 5 wt% Al_2O_3 . The authors showed that high hardness of 16.23 GPa and fracture toughness of 7.86 $MPa \cdot m^{1/2}$ could be achieved for 2.5 wt% Al_2O_3 -doped Y-TZP. Al_2O_3 had a high elastic modulus of 380 GPa as compared with 210 GPa for Y-TZP, which increases the elastic strain energy for

transformation. This condition will amplify the change of total free energy and prevent the ageing-induced phase transformation (Chevalier et al., 2009; Piconi & Maccauro, 1999).

Matsui et al. (2016) investigated the degradation behaviour of various Al₂O₃-doped (0.12, 0.54, and 1.1 mol%) 3 mol% Y-TZP when exposed in hot water at 140 °C/0.4 MPa up to 60 h. They found that the rate of monoclinic phase development increased slightly with increasing amount of Al₂O₃ from 0.12 mol% to 1.1 mol%. The authors inferred that further addition of Al₂O₃ has the tendency to deplete the Y₂O₃ concentration in the tetragonal grains, thus making the grains more vulnerable to hydroxyl attack. In another study, Wu et al. (2013) doped 0.5-5.0 wt% of Al₂O₃ into 3 mol% Y-TZP and found that the ageing-induced phase transformation when exposed in water vapour at 140°C/3.6 bar up to 48 h could be delayed. The authors explained at high sintering temperatures (> 1300 °C), tetragonal grains partitioned into Y³⁺ ion-rich regions and Y³⁺ ion-depleted regions. The Y³⁺ ion-depleted regions would act as nucleation sites for monoclinic formation.

Zhang et al. (2015) studied the effect of doping varying amount of Al₂O₃ content (0.25, 2, and 5 wt%) into coated 2 mol% Y-TZP, 2.5 mol% Y-TZP, and 3 mol% Y-TZP. They found that the addition of 0.25 wt% Al₂O₃ when sintered at 1450 °C and 1550 °C was most effective in retarding monoclinic formation during exposure in an autoclave containing steam at 134 °C/2 bar for 40 h. In general, several researchers found that alumina addition between 0.15 wt% and 0.30 wt% were beneficial in enhancing the ageing resistance of several commercial dental Y-TZPs such as Lava 3 M ESPE (0.2 wt% Al₂O₃) (Harada et al., 2016), Zlock3-411 YTZP A-BIO HIP (0.25 wt% Al₂O₃) (Sevilla et al., 2010), Zirprime, Kuraray Noritake Dental Inc. (0.22 wt% Al₂O₃) (Flinn et al., 2014), Vita In-Ceram (< 0.3 wt% Al₂O₃) (Keuper et al., 2014) and Everest Zirconium Soft, Kavo (0.3 wt% Al₂O₃) (Harada et al., 2016).

2.3.8.2 Silica

Silica (SiO_2) is a controversial dopant as there is no general consensus in the literature with regards to its role in suppressing hydrothermal ageing. For example, popular selection as a dopant for Y-TZP owing to its silica glass phase which improves the degradation resistance towards LTD. For example, in one research it was reported that 0.2 or 0.5 wt% SiO_2 -doped 2.5 mol% Y-TZO yielded the same monoclinic phase content as the undoped samples, which was 70% after exposure in superheated steam at 180 °C/10 bar for 200 h (Tan et al., 1996). However, in another research, it was found that doping 0.1 mol% SiO_2 in Y-TZP could reduce the monoclinic content from 80% for the undoped to 70% for the SiO_2 -doped Y-TZP after ageing in hot water at 130 °C/2-4 bar for 48 h (Takigawa et al., 2009). Samodurova et al. (2015) also reported a similar effect for their 0.25 wt% SiO_2 -doped 3 mol% Y-TZP, i.e. the monoclinic content decreased from 80% for the undoped to 58% for the SiO_2 -doped samples after ageing in distilled water at 134 °C for 48 h.

Gremillard et al. (2002) found that doping 0.5 wt% SiO_2 in 3 mol% Y-TZP could introduce a glassy phase at triple junctions, which serves to reduce internal stresses in the zirconia matrix. They found that the monoclinic content of the aged samples reduced from 70% (undoped) to 30% (SiO_2 -doped) after ageing in steam at 134 °C, 2 bars for 15 h. Nakamura et al. (2011) sintered SiO_2 -doped and undoped 3 mol% Y-TZPs at different temperatures from 1400 °C to 1500 °C and the sintered samples were subjected to ageing in water at 200 °C/2 bar for 50 h. Both the SiO_2 -doped and undoped samples sintered at 1400 °C yielded about the same monoclinic content of 82% after ageing. At higher sintering temperatures of 1450 °C and 1500 °C, the 0.2 mol% SiO_2 -doped samples exhibited a reduction in the monoclinic content after ageing to about 48% and 56%, respectively. Hence, the actual role of silica in the LTD of Y-TZP is still unclear.

2.3.8.3 Copper oxide

Copper oxide (CuO) is low in melting point and a small addition of CuO had great effects on microwave dielectric properties, sintering temperature and microstructure. (Zhang & Li, 2017). Besides, CuO has good thermal conductivity, high stability, photovoltaic properties and antimicrobial activity (Tran & Nguyen, 2014). In recent studies, it was found that adding 100 ppm of CuO into 8 mol % yttria stabilized zirconia show better performance for solid oxide fuel cell electrolyte application (Lee et al., 2015).

The addition of 0.5 wt% of CuO-doped Y-TZP has been reported to be beneficial in promoting densification at low temperatures. This improvement was attributed to the transition liquid phase during sintering owing to the low melting point of CuO (Kanellopoulos & Gill, 2002; Ran et al., 2006). A group of researchers investigated the degradation behaviour of 2.5 mol% Y-TZP containing varying amounts of CuO (0.05, 0.1, 0.2, 0.5, 1 wt%). They observed that hydrothermal ageing (in steam at 180 °C/10 bar up to 200 h) still proceeded but at a lower kinetics for CuO-doped Y-TZP when compared to the undoped sample. The authors found that 0.05 wt% CuO-doped Y-TZP yielded monoclinic content of 40% when compared to 80% measured for the undoped sample after ageing for 200 h (Ramesh & Gill, 2001; Ramesh et al., 2012).

In another research, Kanellopoulos and Gill (2002) reported that the addition of 0.05 wt% CuO was beneficial in enhancing the densification of 3 mol% Y-TZP but resulted in large grain microstructure and lower fracture toughness when sintered at low temperatures between 1300 °C and 1325 °C. This observation has been confirmed by other researchers who added 5 wt% CuO to Y-TZP and sintered at a higher temperature of 1400 °C and 1500 °C (Ran et al., 2007). Hydrothermal ageing experiment conducted in steam at 180 °C/10 revealed that the 0.05 wt% CuO-doped Y-TZP sintered at 1315 °C

with a short holding time of 12 min exhibited excellent ageing resistant (m content $< 5\%$) even after prolonged exposure for 3000 h.

2.3.8.4 Other Dopants

Aside from copper oxide, there are also other dopants which was reported to delay LTD for Y-TZP. For examples, low amounts of iron oxide (Fe_2O_3) (< 0.15 wt%) facilitated the densification of 3 mol% Y-TZP and did not show detrimental effect under hydrothermal ageing in water vapour at 134 °C, 2.3 bar for 2 h (Hallmann et al., 2012). Recently, a small amount of Fe_2O_3 (0.1, 0.2 and 0.4 wt%) was doped in Y-TZP to obtain desired colour for jewellery and watchmaking. It was found that addition of Fe_2O_3 positively changed the material colour and did not affect the mechanical properties significantly (Holz et al., 2018). Also, Zhu et al. (2018) revealed that the presence of cobalt chrome stained in Y-TZP could retard the t - m phase transformation after subjected to hydrothermal ageing in water vapour at 121 °C for 72 h, as compared with the non-stained Y-TZP samples.

Ramesh et al. (2016) reported that the addition of graphene oxide (GO) in 3 mol% Y-TZP resulted in a large-grain size of about 0.4 μm but the tetragonal phase was not disrupted even after prolonged ageing in an autoclave containing superheated steam at 180 °C/10 bar pressure for 200 h. The authors found that 0.2 wt% GO-doped 3 mol% Y-TZP achieved a high relative density of 99%, Vickers hardness of 14.3 GPa, and fracture toughness of 4.8 $\text{MPa}\cdot\text{m}^{1/2}$ when sintered at 1400 °C. In another research, the authors investigated the effect of flyash (FA) obtained from coal-fired power stations as a potential dopant for Y-TZP. The main constituents making up the FA was SiO_2 , Al_2O_3 and Fe_2O_3 . The researchers found that the addition of FA (0.05, 0.1, 0.3, 0.5, and 1 wt%) in 3 mol% Y-TZP did not suppress the monoclinic phase formation after exposure in superheated steam at 180 °C/10 bar for 24 hours (Kelvin Chew et al., 2015).

Co-doping two different dopants were found to be beneficial in suppressing LTD. Khan et al. (2014) studied the effect of co-doping two additives together i.e. CuO+MnO₂ into 3 mol% Y-TZP and sintered the samples at low sintering temperatures (≤ 1350 °C). They found that the co-doped Y-TZP exhibited excellent degradation resistance to hydrothermal ageing in superheated steam at 180 °C/10 bar for 200 h. The sintered co-doped Y-TZP also exhibited better fracture toughness and Vickers hardness when compared to the undoped ceramic sintered at the same temperature. In another study, the effect of co-doping 3 mol% Y-TZP with small amount of Al₂O₃ + SiO₂ was studied. The authors found (0.05 wt% Al₂O₃+0.15 wt% SiO₂)-doped Y-TZP and (0.25 wt% Al₂O₃+0.25 wt% SiO₂)-doped Y-TZP exhibited round grains with a glassy phase present at multiple grain junctions. This was found to be beneficial in strengthening the grain boundaries as the samples exhibited a transgranular fracture. They found that both co-doped sintered samples exhibited better ageing resistance in distilled water at 134 °C up to 48 h, as compared to the undoped, Al₂O₃-doped and SiO₂-doped Y-TZPs. In addition, co-doping (0.25 wt% Al₂O₃+0.25 wt% SiO₂) into Y-TZP was found to be more effective in retarding monoclinic formation when exposed under harsh conditions at 200 °C for 240 h. In comparison, the Al₂O₃-doped Y-TZP was found to disintegrate when exposed under the same conditions (Samodurova et al., 2015; Samodurova et al., 2015).

2.4 Microwave Sintering

2.4.1 Introduction of Microwave Heating

Microwaves are electromagnetic waves with the wavelength ranging from 1mm to 1m and the frequencies between 300 MHz and 300 GHz (Oghbaei & Mirzaee, 2010). Frequencies which are commonly employed in domestic and industrial microwave heating are 2.45 GHz and 915 MHz (Chandrasekaran et al., 2012). Microwave heated materials based on the interactions of the molecules via an electromagnetic field. The main variance between conventional and microwave sintering is the heating mechanism

as shown in Figure 2.5. Heat was generated by heat elements for conventional sintering, where heat was transferred from the surface to the samples core via convection, conduction and radiation. In the case of microwave sintering, microwave energy was absorbed by the sample and converted it into heat, where the heat generated from the core of the sample. This led to a volumetric heating, shorter sintering time and lower sintering temperatures (Bhattacharya & Basak, 2016). Also, some authors defined the advantage of microwave processing as ‘microwave effect’, due to the reduced lower sintering temperature with the enhanced of diffusion rate (Mishra & Sharma, 2016; Rybakov et al., 2013; Źymelka et al., 2013). A significant reduction of 50-100 °C temperatures was observed during the intermediate stage of microwave sintering as opposed to conventional sintering (Wang et al., 2006).

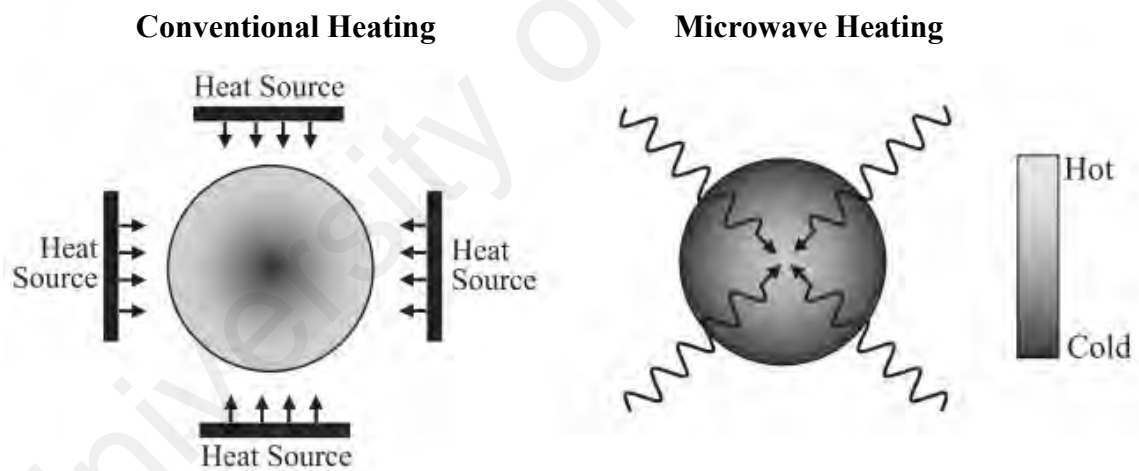


Figure 2.5: Heating mechanism for conventional and microwave heating (Bhattacharya & Basak, 2016).

2.4.2 Microwave Furnace

A microwave furnace composed of three main components which are the microwave generator, applicator and waveguides (transmission lines). The microwave generator is the microwave source such as magnetrons, klystrons and gyrotrons, which could generate microwave ranging from 1 to 40 GHz. Waveguides transmits microwaves from the generators to the main chamber of the furnace. Applicator is the cavity of the chamber with the metallic wall. There are two types of applicators, namely single mode cavity and multimode cavity. Single mode applicator usually consists of small cavities which could process small and simple geometry of samples. In contrast, the multimode applicator has large cavities with about three times the wavelength of the microwave. This cavity is able to produce complex and large samples which usually employed in industrial application (Bhattacharya & Basak, 2016; Das et al., 2008).

In microwave sintering furnace, temperature measurement technique of samples is important. There are two common measurement methods which are thermocouple (contact method) and pyrometer (contactless method) as illustrated in Figure 2.6 (Evan et al., 2001). The thermocouple is inserted into the cavity of applicator and placed directly in contact with the samples for temperature measurements (Monaco et al., 2015). Thermocouple could perturb the local microwave heating environment, which leads to local heating, thermal runaway and errors in temperature measurements. On the other hand, pyrometer measure the temperature of the samples indirectly through the infrared radiation emitted by the samples. Thus, the temperature of the samples could be obtained by boring a hole to the insulation housing without directly in contact with the samples. Besides, pyrometer could provide relatively accurate temperature as oppose to a thermocouple (Evan et al., 2001).

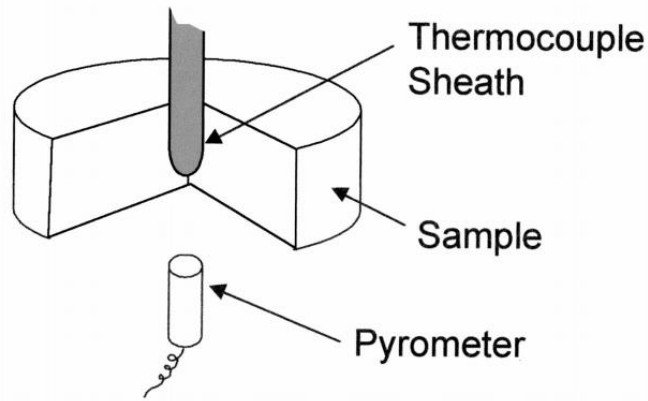


Figure 2.6: Example of thermocouple which inserted into a sample (cutaway view) and a pyrometer (Evan et al., 2001).

2.4.3 Dielectric Properties

The ability of the material to be polarized and convert the microwave energy into heat dependent on the dielectric properties of the material, i.e. dielectric loss, dielectric constant and permittivity. Dielectric constant (ϵ') measures the ability of a material to be polarized, whereas dielectric loss (ϵ'') is the ability of the material to convert microwave energy to heat. Loss tangent or permittivity ($\tan \delta$) is the ability of the material to be polarized and heated, which is the ratio of dielectric loss to dielectric constant. According to the microwave absorption ability, there are three classifications of material, which are reflectors, microwave transparent and microwave absorber. Reflectors completely reflecting microwaves energy while microwave transparent material has $\tan \delta \leq 0.01$, which the microwave able to pass through the material without significant absorption of microwave energy. Microwave absorber material has $\tan \delta \geq 0.1$ and able to absorb microwave energy and convert the energy into heat. At different temperature, the microwave absorption ability of material could be changed attributed to the changes in the dielectric properties (Bhattacharya & Basak, 2016). Dielectric properties for 3 mol% Y-TZP, copper oxide powder and silicon carbide are listed in Table 2.1. 3 mol% Y-TZP is microwave transparent at 200 °C but became microwave absorber after heating to 600 °C and above. For copper oxide powder, it is microwave absorbing from 25 °C

onwards. Silicon carbide remains as a good microwave absorber up to 1350 °C, which is recommended as a good susceptor to assist in microwave sintering.

Table 2.1: Dielectric properties of materials.

Material	Temperature (°C)	Dielectric constant, ϵ'	Dielectric loss, ϵ''	Loss tangent, $\tan \delta$
3 mol% Y-TZP	200	34	0.04	0.0012
	600	40	6.25	0.16
	1200	50	93	1.86
Copper Oxide Powder	25	3.1	0.27	0.09
	500	14.5	17.0	1.172
	800	42.6	31.0	0.73
Silicon Carbide	25	245	95	0.38
	800	433	175	0.40
	1350	456	360	0.79

(Bhattacharya & Basak, 2016)

2.4.4 Issues in Microwave Heating

In microwave heating, the challenge is to produce crack-free zirconia sample as the dielectric loss increased tremendously with the rise in temperature. The main issue of microwave sintering zirconia is thermal runaway or hot spot effect, where microwave heating will result in the uncontrolled sudden rise of temperature (Bhattacharya & Basak, 2016). Due to the poor thermal conductivity of zirconia, hot spot has the tendency to stay localized (Janney et al., 1992). When the local area reached the critical temperature earlier than the remaining area, this local area will be heated rapidly, which results in thermal runaway and fracture of samples (Das et al., 2008). Also, uneven heating and thermal runaway will occur during microwave sintering dielectric materials which the dielectric loss increases with temperature (Chandrasekaran et al., 2012).

Hot spot effect normally occurs during direct microwave heating. Charles et al. (2017) discovered that direct microwave heating Y-TZP developed hot spot at the center of the sample during pre-heating stage of microwave heating. This is in accordance with that

reported by Charmond et al. (2010), who found that direct microwave heating caused heterogeneous microstructure due to the thermal gradients of the samples. In contrast, susceptor assisted microwave heating provided homogeneous samples with improved density. From their observation, susceptor contributed on heating the samples during the pre-heating stage below 600 °C, since Y-TZP has a poor dielectric loss during this stage. Zhao et al. (2000) also found that long warm-up time was required for direct microwave heating before the material starts to couple with microwaves, which also increase the risk of plasma formation in the cavity.

Therefore, susceptors were introduced to assist in the initial microwave heating owing to its high dielectric loss. The susceptor is necessary for microwave transparent samples at the preheating stage of microwave heating to gain two-way heating, which also called hybrid microwave sintering. At low temperatures, susceptors could absorb microwave and reached high temperatures. This is to ensure that the high temperatures of the samples could be reached to possess a high dielectric loss to absorb microwave energy (Oghbaei & Mirzaee, 2010). The common example of susceptors is silicon carbide (SiC) which could be in the form of powders or rods, that placed along with green samples in a crucible or insulation housing (Monaco et al., 2015). Insulation is also important in preventing heat loss and minimize wastage of microwave energy during sintering. The insulation normally made from microwave transparent material such as alumina-based insulating materials (Bhattacharya & Basak, 2016). This is because alumina-based insulating materials such as alumina fiberboard is highly porous, low thermal conductivity and microwave transparent up to high temperature. Also, this ensures that the insulation material would not couple microwaves which potentially leads to interference between insulation and samples during sintering. In short, insulation is designed to prevent heat loss from the samples and achieve uniform heating (Xu et al., 2003).

Another alternative to overcome the issues of the uncontrolled sudden rise in temperature and dielectric properties of the material is by incorporating microwave absorbing material in zirconia (Bhattacharya & Basak, 2016). In the past, Upadhyaya et al. (2001) microwave sintered 3 mol% Y-TZPs which had doped with titania (TiO_2) and manganese oxide (MnO_2) respectively. However, the composition of the dopants was not reported and the microwave doped Y-TZPs yielded lower Vickers hardness and toughness although they have a relatively same density as the undoped Y-TZPs. The authors suggested that the transition metal oxides could be the heat boosters to increase the dielectric loss of zirconia.

2.4.5 Design and Configuration for Microwave Processing

Due to issues arising from microwave heating for zirconia, the design and configuration for microwave processing is crucial to producing crack-free samples. In a review study, a configuration consisted of four to six susceptor rods with picket fence arrangement around the samples in an insulation housing was suggested (Bhattacharya & Basak, 2016). In the past, it was reported that five SiC susceptor rod enclosed in an alumina fiber crucible could produce crack-free samples but with a low heating rate of $2\text{ }^\circ\text{C}/\text{min}$ to $3.5\text{ }^\circ\text{C}/\text{min}$ (Janney et al., 1992). Other researchers reported that a three or two SiC susceptor enclosed in alumina insulating chamber are sufficient in producing crack-free samples for microwave sintering (Almazdi et al., 2012; Sujith et al., 2009). Sujith et al. (2009) elaborated that placing one susceptor at one side of samples will cause sample crack due to initial boost of heating from susceptor and low thermal conductivity of zirconia, which created uneven coupling within the sample. However, Charmond et al. (2010) claimed that a cylindrical SiC susceptor is sufficient in producing crack-free samples when placed around the alumina fiberboard insulating material. Over the years, most of the group claimed that SiC susceptor is necessary to be used in the microwave

sintering but the detailed setup information was not reported (Borrell et al., 2013; Mazaheri et al., 2008; Nath et al., 2008; Presenda et al., 2015).

Apart from the role of susceptors, the necessity for pre-sintering prior to microwave sintering remains ambiguous. In a few studies, the green samples were heated at 600 °C with a ramp rate of 5 °C/min for 3 h prior to microwave heating to obtain crack-free samples (Borrell et al., 2013; Charmond et al., 2010; Travitzky et al., 2000). Borrell et al. (2013) explained that the pre-sintering stage is essential to avoid development of cracks in samples due to heterogeneous temperature distribution. Besides, the initial heating of zirconia is sluggish as the dielectric loss is relatively low below 600 °C, accompanied by its low thermal conductivity and high thermal expansion ($10 \times 10^{-6} \text{ K}^{-1}$). Therefore, when the samples were microwave sintered at a high heating rate, thermal stress will result in warpage or sample crack (Goldstein et al., 1999). Since the dielectric loss of zirconia changes with temperature, there is the possibility of uneven heating, hot spot or thermal runaway to occur during microwave sintering (Chandrasekaran et al., 2012). In summary, the assistance of susceptors and pre-sintering deemed to be beneficial in producing crack-free samples.

2.4.6 The Effect of Microwave Heating

Over the years, conventional sintering method was conducted at low heating rate which is in between 5 °C/min to 10 °C/min with a long holding time (2 h to 4 h) to achieve high density for Y-TZPs as reported by various researchers (Kumar et al., 2010; Mazaheri et al., 2008; Palmeira et al., 2016). The low heating rates were employed in conventional sintering mainly due to the limitation of the heat transfer mechanism, where thermal expansion mismatch could occur within the sample during sintering (Kalousek et al., 2017). This is because zirconia has low thermal conductivity, i.e. $2 \text{ Wm}^{-1}\text{K}^{-1}$, while thermal conductivity of metals could vary from 100 to $300 \text{ Wm}^{-1}\text{K}^{-1}$ (Paula et al., 2015).

Therefore, the heating rates for conventional sintering is restricted to prevent the formation of cracks within samples during sintering (Kalousek et al., 2017).

In the past, microwave sintering of 8 mol% yttria stabilized zirconia was not successfully performed at heating rates of 10 °C/min, 20 °C/min and 30 °C/min, arranged with the picket fence arrangement of five susceptors. However, the researchers found that crack-free samples could be produced by applying lower heating rate of 2 °C/min and or 3.5 °C/min during the initial heating to 500 °C (Janney et al., 1992). According to Reidy et al. (2011), 3 mol% Y-TZP were successfully microwave sintered at 1300 °C, with a heating rate of about 16 °C/min, with one hour holding time. Microwave sintered Y-TZP resulted in a higher density and Vickers hardness if compared to conventional sintered samples at the same heating profile. A density of 96.8% and Vickers hardness of 12.5 GPa was achieved by microwave sintered 3 mol% Y-TZP samples. Nevertheless, both sintering methods possessed similar grain size of about 0.2 µm. In another research, Binner et al. (2008) successfully microwave sintered Y-TZP at a heating rate of 20 °C/min without cracks on the samples. Microwave heating method had resulted in finer average grain size as compared to conventional sintering at a lower heating rate of 7 °C/min. The authors mentioned that the samples could not microwave sintered at higher heating rates as samples was found crack due to the thermal expansion mismatch of the samples.

Borrell et al. (2013) studied the density and mechanical properties of microwave and conventional sintered 3 mol% Y-TZPs. Susceptor assisted microwave sintering was carried out in a 2.45 GHz mono-mode cavity (1 kW), at various sintering temperatures with the same heating rate of 25 °C/min at different holding time (5, 10, 15 min). Conventional sintering was conducted at 1400 °C with a heating rate of 5 °C/min and 1 h holding time. All the microwave sintered samples showed high density and Vickers hardness as compared to conventional sintered samples. At 1400 °C, theoretical density

of 99.9%, Vickers hardness of 16 GPa and a grain size of 0.22 μm were achieved by microwave sintered samples which hold for 10 min. In contrast, conventional samples yielded a lower density of 98.3%, Vickers hardness of 13.7 GPa and grain size of 0.27 μm . The grain size of conventional sintered Y-TZP was slightly higher than microwave sintered samples but possessed higher fracture toughness. The higher fracture toughness was attributed to the heating mechanism of conventional sintering with the lower thermal stress that prevents crack propagation. Borrell et al. (2012) had also explored the microwave effect of 3 mol% Y-TZPs with a higher heating rate of 30 $^{\circ}\text{C}/\text{min}$ which held for 10 min in 800 W, 2.45 GHz mono-mode cavity. The sample was successfully microwave sintered at 1400 $^{\circ}\text{C}$ and achieved a relative density of 99.9% and grain size of 0.23 μm .

Different studies were carried out by comparing two different heating rates (10 times different) between conventional sintering and microwave sintering. In a study, Mazaheri et al. (2008) microwave sintered 8 mol% yttria stabilized zirconia in a 2.45 GHz multimode microwave cavity with 1.1 kW of power, assisted with hollow SiC rods as susceptors. The samples were microwave sintered up to 1500 $^{\circ}\text{C}$ with a low heating rate of 5 $^{\circ}\text{C}/\text{min}$ (LMS) and a high heating rate of 50 $^{\circ}\text{C}/\text{min}$ (HMS). Another set of samples was prepared by conventional sintering with a heating rate of 5 $^{\circ}\text{C}/\text{min}$ (CS). LMS sample exhibited the highest density (~97%) among HMS (~95%) and CS sample (~95%) when sintered at 1400 $^{\circ}\text{C}$ as shown in Figure 2.7. When these samples reached about the density of 98%, HMS samples yielded a smaller grain size of 0.9 μm as compared with LMS (2.35 μm) and CS (2.14 μm). The researchers postulated that high microwave heating rate enhances the microstructural uniformity within the samples and contribute on higher fracture toughness of 3.17 $\text{MPa}\cdot\text{m}^{1/2}$ as opposed to low heating rate (1.9 $\text{MPa}\cdot\text{m}^{1/2}$). Apart from that, HMS samples exhibited a higher Vickers hardness of 13.7 GPa as compared to LMS and CS samples which shared similar hardness of 12.9 GPa.

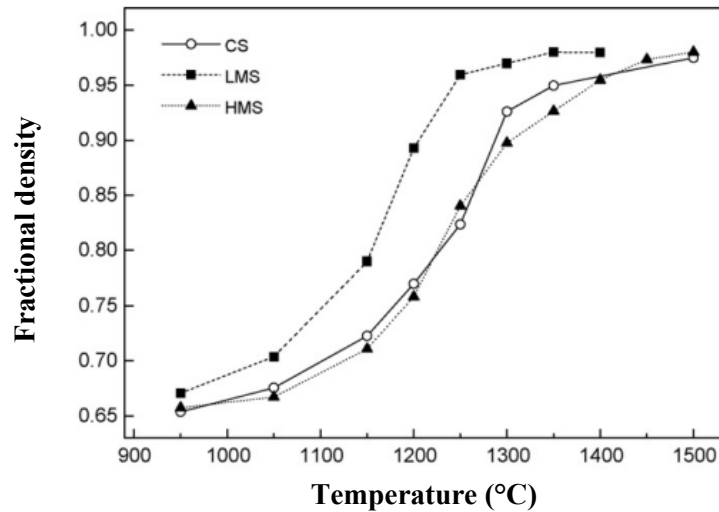


Figure 2.7: Fractional density of conventional sintering (5 °C/min) and microwave sintering of HMS (50 °C/min) and LMS (5 °C/min) at different temperatures (Mazaheri et al., 2008).

In another experiment, Charmond et al. (2010) conducted microwave sintering of 2 mol% yttria doped zirconia in a 2.45 GHz single mode cavity (2 kW), with the assist of the susceptor in an alumina fiberboard box. The selected heating rate for microwave sintering was 25 °C/min (LMS) and 250 °C/min (HMS), while conventional sintering was conducted at 25 °C/min (CS) for comparison purposes. When the samples were microwave sintered at 1225 °C, HMS contributed on the slightly higher density of 86.9% and grain size ranging from 130 nm to 180 nm. At similar temperature, LMS samples yielded a lower density of 80.7% and grain size between 120 nm and 140 nm. When the sintering temperature was rise to about 1340 °C, a higher density of 95.8% was achieved by LMS samples while CS gave a lower density of 91.4%. As predicted, LMS and CS samples led to the similar grain size of 0.2 μm at the similar sintering temperature.

An elevated microwave heating rate was further discussed by different researchers, which is at 100 °C/min. Kumar et al. (2010) microwave sintered 3 mol% Y-TZP at 1400 °C with a heating rate of 100 °C/min and held for 10 min, while conventional sintering was performed at the a of 10 °C/min that held for 2 h. They found that the grain size for microwave sintered samples was smaller (165 nm) as compared with the conventional

sintered sample (205 nm). Once the sintering temperature was increased to 1500 °C, both samples reached a relative density of 99%, accompanied with similar grain size at about 300 nm. In another research, microwave sintering was carried out in a mono mode cavity at 1300 °C with a heating rate of 100 °C/min and held for 10 min. Conventional sintering was conducted at the same temperature, with a heating rate of 10 °C/min and holding time of 2 h. The outcome is in accordance to the previous research, where the density of microwave sintered Y-TZPs was higher (99%) and accompanied with remarkable Vickers hardness of 14.7 GPa and fracture toughness of 5.8 MPa.m^{1/2}. Grain size obtained by both methods were similar, which is at about 2 µm (Presenda et al., 2017; Presenda et al., 2015).

From the above experimental observations, it was postulated that the grain size of the conventional and microwave sintered samples would be similar regardless of heating rate. However, some of the researchers reported that microwave sintered Y-TZP would exhibit slightly smaller grain size than conventional sintered Y-TZP. Nevertheless, microwave sintered Y-TZP usually yield higher mechanical properties and density as compared with conventional sintered samples. Besides, microwave sintering methods could achieve high density and good mechanical properties at low sintering temperatures (about 1200 °C to 1300 °C). Since microwave sintering was conducted at higher heating rates and lower temperatures, there would be a reduction in processing time for microwave sintering as opposed to conventional sintering.

2.5 Summary

In summary, 3 mol% yttria tetragonal zirconia possesses excellent mechanical properties ranging from structural to biomedical applications. However, the major limitation of zirconia is LTD which subsequently led to *t-m* phase transformation and catastrophic failure of the material. The kinetics of degradation was greatly affected by

the ageing condition such as ageing temperature, pressure, medium and exposure time. Accelerated ageing Y-TZP in an autoclave in superheated steam at 180 °C, 1 MPa pressure provides an aggressive environment to gauge the vulnerability of the ceramics after ageing. The prime factors which governed the LTD behaviour of Y-TZP are grain size and presence of dopants. A small grain size was found to be beneficial in suppressing LTD, however, conventional sintering would lead to grain growth at high sintering temperatures. Therefore, other sintering techniques were introduced to consolidate Y-TZPs in lower temperatures or/and to reduce grain size. For example, microwave sintering was reported to achieve better mechanical properties, shorter processing time and better LTD resistance on Y-TZPs. On the other hand, the presence of small amounts of dopants in Y-TZPs could delay the LTD degradation such as alumina and silica. Copper oxide was found to effectively suppressed LTD after hydrothermal ageing in superheated steam at 180 °C/1 MPa up to 3000 h.

Microwave sintering was introduced in the last section of this chapter, which mainly covered the mechanism of heating, dielectric properties and issues in microwave heating. Microwave heat materials based on the interactions of molecules via an electromagnetic field. According to the dielectric properties of the material, samples absorb microwave energy to reach volumetric heating of the entire samples. However, there are some detrimental issues such as thermal runaway, hot spot effect which leads to nonuniform microwave heating. From the literature, the assistance of susceptors and pre-sintering prior to microwave sintering deemed to be beneficial in producing crack-free Y-TZP samples. However, detailed design and configurations of microwave sintering were not reported by most of the researchers. Lastly, the influence of microwave heating profile on density, grain size and mechanical properties as opposed to conventional sintering of Y-TZPs were discussed.

From the literature, it was found that the addition of copper oxide in 3 mol% Y-TZP could suppress LTD after hydrothermal accelerated ageing. Besides, microwave sintering method could enhance density and mechanical properties of Y-TZP as opposed to conventional sintering. In addition, microwave sintering was beneficial in suppressing LTD for Y-TZP samples. Owing to the benefits of microwave sintering and the addition of copper oxide in Y-TZP, it is envisaged that the microwave sintered copper oxide doped Y-TZP could produce high density, good mechanical properties and suppress LTD. Besides, copper oxide has higher dielectric loss as compared to Y-TZP and was expected to increase the dielectric properties of the material during microwave sintering. Although there are issues in microwave sintering, the assistance of susceptors and pre-sintering deemed to be beneficial in producing crack-free samples. Not many researchers had reported in detail about susceptors and pre-sintering during microwave sintering. Besides, microwave sintering Y-TZP with dopants are seldom discussed. Clearly, there is a necessity in exploring the feasibility of microwave sintering copper oxide doped Y-TZP in terms of physical and mechanical properties.

CHAPTER 3: METHODOLOGY

3.1 Introduction

In this chapter, the experimental methods will be discussed in different sections. The first section covers the procedures applied for the fabrication of insulation housing for microwave sintering. This is followed by the development of a preliminary study on microwave processing parameters such as the influence of susceptors, the effect of heating rates and the necessity of pre-sintering.

The experimental procedures include preparation of CuO doped-Y-TZP powder, characterization and LTD study on samples. Sample preparation includes powder mixing, powder compaction (uniaxial pressing and cold isostatic pressing), sintering (conventional sintering and microwave sintering), grinding, polishing and thermal etching. Subsequently, the characterization techniques on sintered samples will be discussed, which covers phase identification, density, Vickers hardness, fracture toughness and microstructure. A general flow chart of the methodology is shown in Figure 3.1.

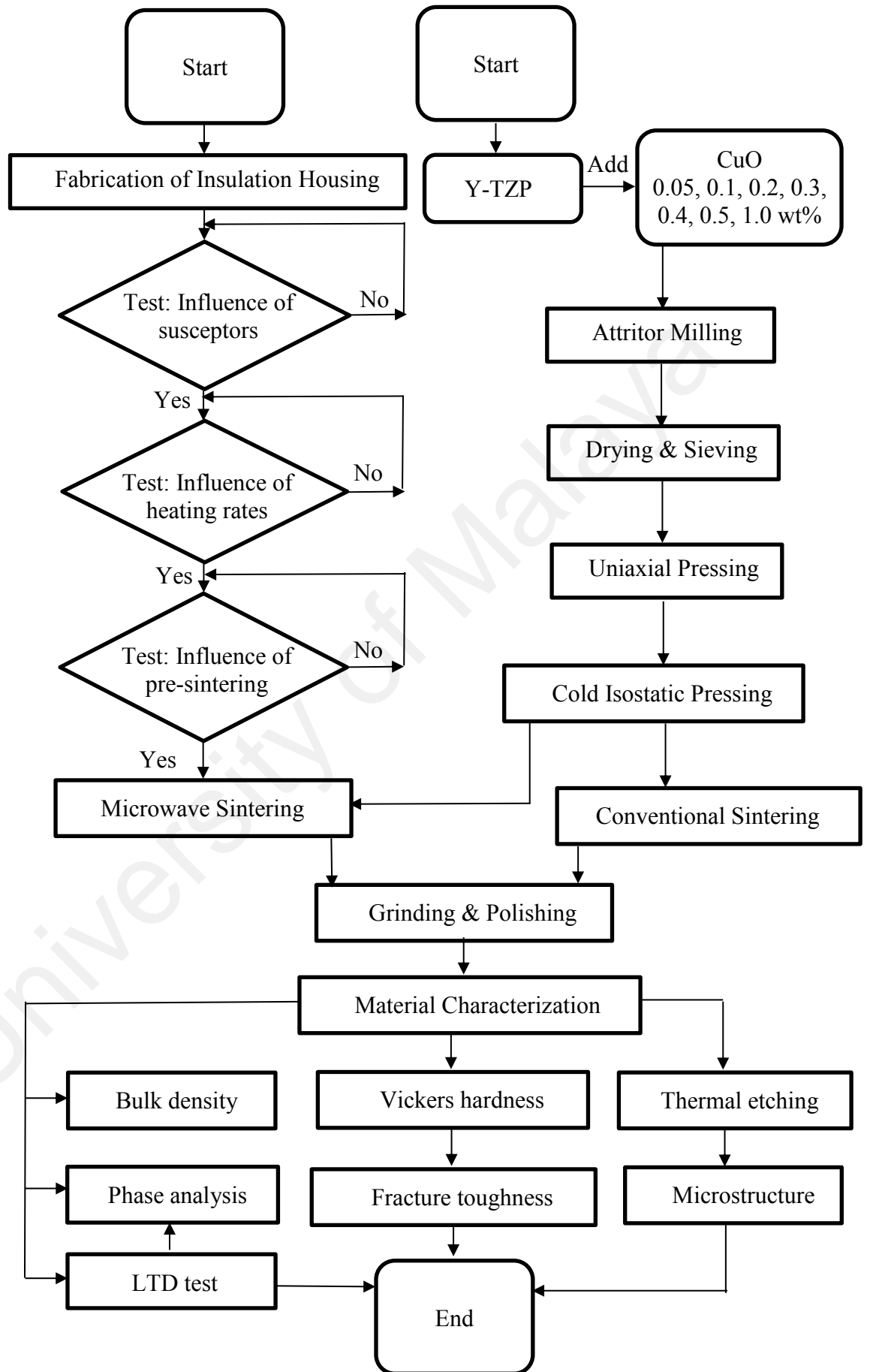


Figure 3.1: Flow chart of the methodology.

3.2 Fabrication of Insulation Housing

According to literature studies, alumina-based insulating materials housing was designed to prevent heat loss from the samples. In this study, a piece of alumina fiberboard (TOMBO No. 5461-17UD, Japan) with the dimension of 40 mm x 600 mm x 900 mm was used. According to specification, the selected alumina fiberboard has a density of 0.70 g/cm³, low thermal conductivity and could withstand a high temperature up to 1700 °C. It is a high temperature insulating board made of Rubiel bulk fiber and special inorganic fillers and binders. Rubiel is a polycrystalline alumina fiber of which Al₂O₃ content up to 95%, and do not become brittle or shrink at high temperature. Therefore, this alumina fiberboard had fulfilled the requirement as microwave transparent insulator which is highly porous and has low thermal conductivity.

The insulator board was cut into different sections by a vertical band saw (Formahero FH-600BS) which consists of base block, U-shaped middle block, small block and top block as illustrated in Figure 3.2. Due to the limitations of the vertical band saw, the cutting for the U-shaped block was done by a bench drilling machine and a jigsaw power tool. In the case for the top block, a 5 mm hole was bored by a high-speed steel (HSS) drill bit manually through the thickness of the block. This hole is necessary for the infrared from the pyrometer to pass through from the top block to measure the sample surface. The overall dimension for each block is 152.4 mm x 152.4 mm, with a thickness of 38.1 mm. These blocks were subsequently stacked into 3 levels to assemble the complete insulation housing for microwave sintering, where green samples were placed on the base block as shown in Figure 3.3. After ensuring the infrared of pyrometer focused on the green samples from the side view, the insulator housing will be enclosed with the rectangular small block (152.4 mm x 38.1 mm).

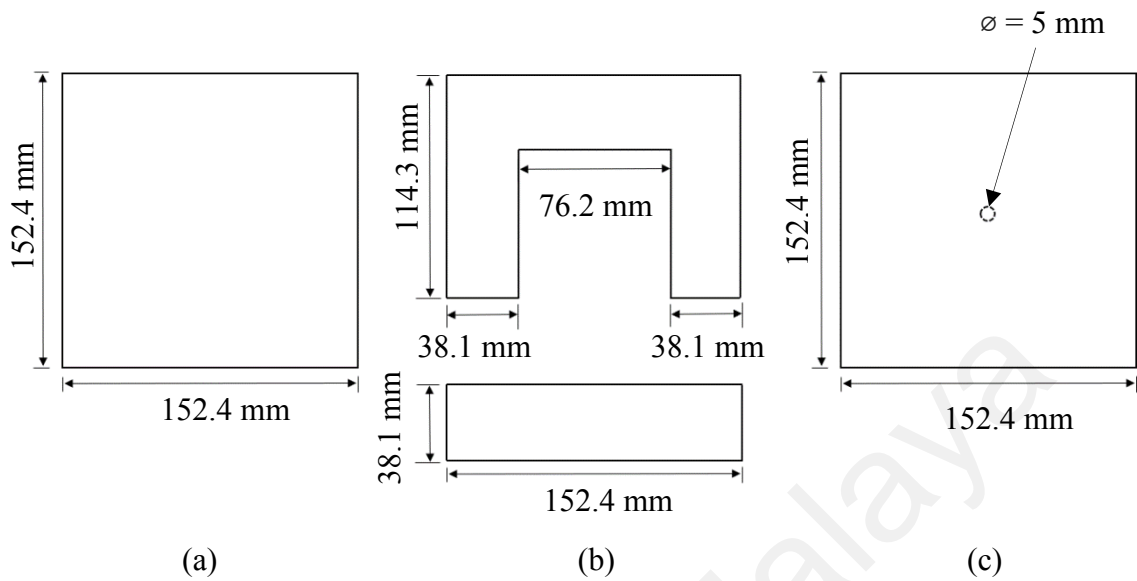


Figure 3.2: Top view of insulators of (a) base block, (b) U-shaped block and small block, (c) top block with a diameter of hole 5 mm.

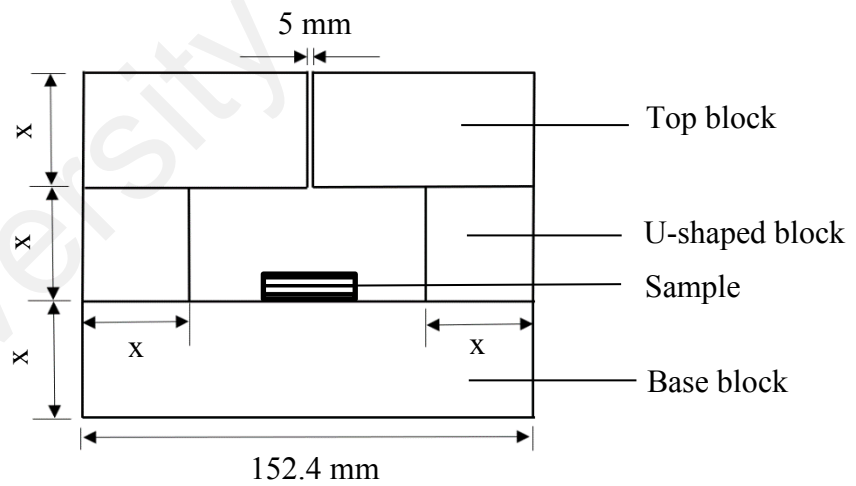


Figure 3.3: Side view of stacked insulators before insulator was enclosed with the rectangular middle small block, $x = 38.1$ mm.

3.3 Preliminary Study: Microwave Processing Parameters

3.3.1 The Influence of Susceptors

The 3 mol % Y-TZP powder (Kyoritsu Corporation, Japan) was employed as the starting powder in this study. The dopants used in the preliminary study were 0.5 wt % and 1 wt % of copper oxide (CuO) (Sigma-Aldrich, USA). Each of the dopants was mixed with the starting powder of Y-TZP by attritor milling (Union Process, USA) at 500 rpm for 30 minutes. Zirconia balls with the diameter of 3 mm were used as the milling media, while ethanol as the mixing medium. The slurries were then oven dried at 60 °C overnight. The dried cake was crushed and sieved to obtain CuO-doped Y-TZP powders. Discs samples (2.5 g) and bar samples (3.0 g) were uniaxially pressed at 3 MPa, followed by cold isostatic pressing (Shanxi Golden Kaiyuan Co. Ltd. China) at 200 MPa for 1 min. Microwave sintering of the green samples was performed with a 2.45 GHz, 6 kW multi-mode microwave furnace.

In the preliminary study, the microwave sintering temperature was selected at 1100 °C with a heating rate of 30 °C/min, holding time of 5 minutes for all the samples. The parameter was set in the microwave control panel as in Table 3.1. These heating rates were controlled by the auto power control loop in the microwave furnace. The power was supplied at 3 kW during the initial heating up to 250 °C. During the initial heating period, the actual temperature was recorded as 250 °C, since pyrometer could only record from 250 °C and above. After the actual temperature reached 250 °C, cycle 1 would be executed with the power up to about 6 kW based on the calculated temperature and time, i.e. heating the samples to 500 °C in 12 minutes. During the initial heating (cycle 1), a low heating rate of 20 °C/min was selected to prevent thermal shock at low temperatures. When the temperature reached at 500 °C, cycle 2 would be performed at a heating rate of 30 °C/min and sinter the samples to 1100 °C, followed by holding time of 5 minutes (cycle 3) at the same temperature. When the microwave heating had completed all the

cycles, the power of the microwave would be turned off for cooling. No susceptors were employed in the first attempt, where three green samples were placed side by side at the center of the insulator base. This was followed by placing a different quantity of silicon carbide (SiC) susceptor rod (diameter of 8 mm and length of 20 mm), surrounding the three green samples.

Table 3.1: Parameters in microwave control panel for heating rate 30 °C/min.

Parameter	Cycle 1	Cycle 2	Cycle 3
Temperature (°C)	500	1100	1100
Time (min)	12	20	5

3.3.2 The Influence of Heating Rates

The CuO-doped samples were used as the second preliminary study on the influence of heating rates. Since multi-mode microwave cavity could sinter a large quantity of samples, six samples which consist of four disc and two rectangular bar samples were attempted in this part. Since the number of samples increased, four susceptors were employed for a heating rate of 50 °C/min as presented in Table 3.2.

Table 3.2: Parameters in microwave control panel for heating rate 50 °C/min.

Parameter	Cycle 1	Cycle 2	Cycle 3
Temperature (°C)	500	1100	1100
Time (min)	12	12	5

In the next attempt, the heating rate was reduced to 30 °C/min and the parameter in Table 3.1 was employed with two susceptors. Besides, alumina fiber heat shield was made to avoid overheating and boost from the susceptors to samples during microwave heating. The heat shield had a dimension of 22 mm x 22 mm with the height of 25 mm. The center of the heat shield was bored with a hole of a diameter of 12 mm throughout the height of the heat shield as shown in Figure 3.4 (a). During microwave sintering, the susceptor was placed at the center of the heat shield, which allowed a gap of 2 mm in between the hole and the susceptor as illustrated in Figure 3.4 (b).

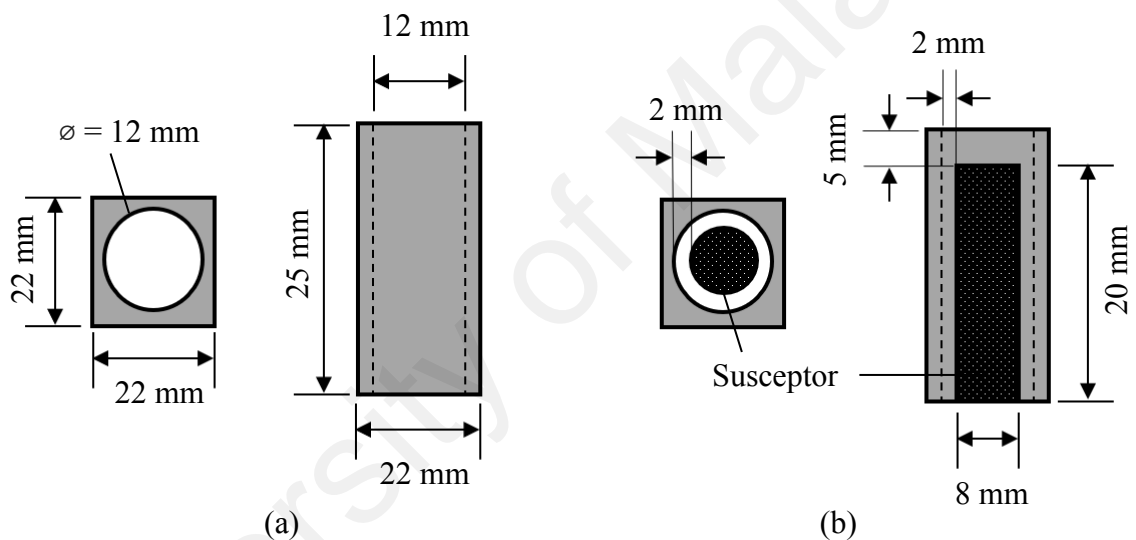


Figure 3.4: Top view and side view of heat shield for susceptor: (a) heat shield, (b) heat shield with susceptor.

3.3.3 The Influence of Pre-sintering

To achieve uniform microwave heating, the green samples were pre-sintered at 600 °C, with a ramp rate of 10 °C/min and held for 2 h in a box furnace. This was followed by the microwave sintering with the parameters set according to Table 3.1. The effect of pre-sintering prior to microwave sintering was studied with the assistance of two susceptors (with heat shield).

3.4 Preparation of Samples

3.4.1 Preparation of CuO-doped Y-TZP powders

In the present work, 3 mol% Y-TZP powder (Kyoritsu Corporation, Japan) was employed as the starting powder in this study. The dopants used were 0.05 wt%, 0.1 wt%, 0.2 wt%, 0.3 wt%, 0.4 wt%, 0.5 wt% and 1 wt% of high purity copper oxide (CuO) manufactured by Sigma-Aldrich, USA. Each of the dopants was mixed with the starting Y-TZP powder in 150 mls of ethanol in a beaker, which immersed in the ultrasonic water bath and subjected to 10 to 15 min ultrasonication to break agglomerates. Mixing was accomplished by attritor milling (Union Process, USA) at 500 rpm up to 30 minutes with 3 mm diameter zirconia balls as the milling media while ethanol as the mixing medium. The slurries were then oven dried at 60 °C for 24 hours. The dried cake was crushed and sieved using a stainless-steel test sieve with a mesh aperture size of 212 μm (Endecotts, England) to obtain CuO-doped Y-TZP powders.

3.4.2 Powder Compaction

Prior to the sintering process, CuO-doped Y-TZP powders were compacted by uniaxial pressing at 3 MPa by hydraulic bench press. Disc (20 mm diameter x 3 mm thickness, each weighing 2.5 g) and rectangular bar (32 mm x 13 mm x 4 mm, each weighing 3 g) were compacted by a hardened steel mould and die set. Before the powder compaction, WD-40 was used to clean the dies and punches to prevent powder lamination and contamination.

Next, the uniaxially pressed green samples were subjected to cold isostatic pressing (CIP) at 200 MPa for 1 min, where the uniform isostatic pressure was applied from all directions. CIP was introduced after uniaxial pressing to produce homogeneous compacted green sample, which prevents thermal cracking during sintering.

3.4.3 Sintering

Sintering is a key processing step to consolidate material without melting them. In general, sintering temperatures were selected at about 0.6 to 0.8 of the melting temperature of the samples. In the present work, after uniaxial pressing and CIP, the green samples were pre-sintered at 600 °C, at a ramp rate of 10 °C/min with a holding time of 2 h in a box furnace. Next, microwave sintering was carried out at 2.45 GHz, multi-mode microwave furnace (6 kW). The samples were placed at the center of the enclosed alumina fiberboard insulator and flanked with two heat shields filled with susceptors. The sample temperature was measured by a pyrometer placed at the center of the insulator base. This was followed by the microwave sintering with a heating rate of 20 °C/min during the initial heating until 500 °C. Next, the samples were sintered to the designated sintering temperatures i.e. 1100 °C, 1200 °C, 1250 °C, 1300 °C and 1400 °C at a heating rate of 30 °C/min. The holding time at each temperature was 5 min. The heating rates were controlled by the auto power control loop in the microwave furnace. The power was supplied at 3 kW during the initial heating up to 250 °C. After the actual temperature reached 250 °C, all cycles would be executed with the power up to about 6 kW based on calculated temperature and time. The microwave would be turned off after the cycle was completed. Besides, selected samples were subjected to conventional sintering, where the temperature selected was 1100 °C, 1200 °C, 1250 °C, 1300 °C and 1400 °C. The ramp rate for heating and cooling for conventional sintering was set at 10 °C/min and held for 5 min.

3.4.4 Grinding and Polishing

The sintered samples were ground and polished to acquire desired surface quality to be revealed under the microscope during characterization testing. The samples were wet ground using silicon carbide papers starting from the grades of 120 (coarse), followed by finer grades of 240, 600, 800 and 1200 (fine). During grinding, water was used as the lubricant, coolant and medium to remove debris. The grinding orientation was changed to 90 ° with the change of each paper grade. This is to ensure that the grinding was done successively for every grade, where the previous ground lines had been removed as in Figure 3.5. The samples were then polished using 6 µm and 1 µm diamond paste to obtain an optical reflective surface.

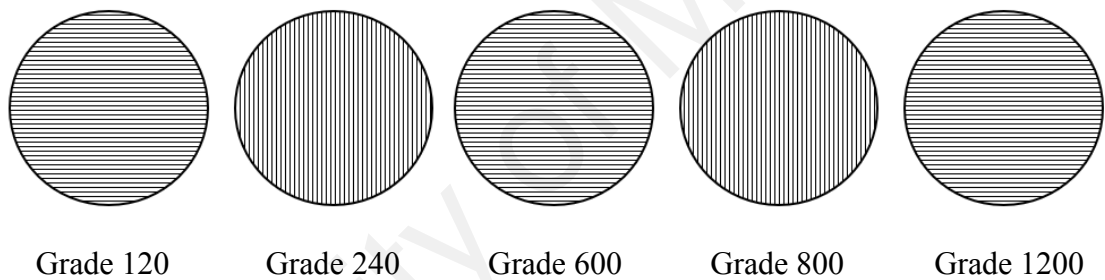


Figure 3.5: Orientation of samples during grinding.

3.4.5 Thermal Etching

Thermal etching is important to delineate grain boundaries and microstructure details, which are not apparent on the polished surface of samples. Prior to microstructure evaluation, the sintered samples were thermally etched in a box furnace at a temperature of 50 °C below the sintering temperature for 30 min with a ramp rate of 10 °C/min.

3.5 Characterization of Samples

3.5.1 Phase Identification

The phase presented in the microwave sintered samples were characterized at room temperature by X-ray diffraction (XRD) (EMPYREAN, PANalytical, Netherlands) using Cu-K α ($\lambda = 0.154$ nm) radiation operated at 40 kV/40 mA. The samples were scanned with a 0.02° 2θ step and a step scan of $0.5^\circ/\text{min}$ over the 2θ range 27° to 32° . These cover the monoclinic (m) and tetragonal phase (t) related $\{111\}$ peaks. The crystalline phases presented in the samples were identified by comparing the reference patterns code in HighScore Plus for tetragonal zirconia (98-009-0884) and monoclinic zirconia (98-006-0900). The peak at $\approx 30.2^\circ$ 2θ correspond to the $(111)_t$, while the peaks at $\approx 28.2^\circ$ and $\approx 31.5^\circ$ 2θ correspond to the $(11\bar{1})_m$ and $(111)_m$ respectively. The volume fraction of monoclinic phase content, V_m in the ceramic was calculated with the method developed by Toraya et al. (1984) as in Eqn. 3.1 and Eqn. 3.2 below:

$$V_m = \frac{1.311X_m}{1 + 0.311X_m} \times 100 \% \dots\dots\dots\text{Eqn. 3.1}$$

$$X_m = \frac{I(11\bar{1})_m + I(111)_m}{I(11\bar{1})_m + I(111)_m + I(111)_t} \dots\dots\dots\text{Eqn. 3.2}$$

where V_m is the volume fraction of monoclinic zirconia, X_m is the monoclinic fraction and I is the peak intensity and subscript of m and t represents the monoclinic and tetragonal related peaks respectively. The volume fraction of tetragonal phase V_t (%) was then calculated by Eqn. 3.3:

$$V_t = 100 \% - V_m \dots\dots\dots\text{Eqn. 3.3}$$

3.5.2 Density Determination

Water immersion technique (Archimedes principle) was used to determine densities of sintered samples using an analytical balance (GR200 analytical balance A&D) mounted with density determination kit according to ASTM-C373. Archimedes principles explained that a body which was partially or wholly submerged in a fluid is buoyed up by a force equal to the weight of the fluids which it had displaced. First, a sample was placed on an upper density pan and the weight of the sample in the air was recorded, Subsequently, the sample was placed on the lower density pan which immersed with distilled water in a beaker, and weight of the samples in water was recorded. Bulk densities of samples were calculated by Eqn. 3.4:

$$\rho_{\text{bulk}} = \frac{W_a}{W_a - W_w} \times \rho_{\text{water}} \dots\dots\dots \text{Eqn. 3.4}$$

where ρ_{bulk} is the bulk density of the sample, W_w is the weight of sample in water, W_a is the weight of sample in air and ρ_{water} is the density of distilled water according to the temperature. The weight obtained is in unit g and the density is in unit g/cm³. The theoretical density of Y-TZP, ρ_{th} is 6.09 g/cm³, therefore the relative density of the sample was calculated by Eqn. 3.5:

$$\rho_{\text{relative}} = \frac{\rho_{\text{bulk}}}{\rho_{\text{th}}} \times 100 \% \dots\dots\dots \text{Eqn. 3.5}$$

3.5.3 Vickers Hardness and Fracture Toughness Evaluation

Hardness is a measure of the resistance of a material to surface indentation. The Vickers hardness (H_v) and fracture toughness (K_{Ic}) of polished samples were measured using the Vickers indentation method (Mitutoyo AVK-C2, USA) according to ASTM C1327. The Vickers hardness indenter is a square-base diamond pyramid with the angle

of 136 ° as shown in Figure 3.6. The indentation load was set constant at 10 kgf with a loading time of 10 s, with six indentations were made on each sample. The Vickers hardness was calculated using Eqn. 3.6:

$$H_v = \frac{2P \sin\left(\frac{\theta}{2}\right)}{D^2} = 1.854 \frac{P}{D^2} \dots\dots\dots \text{Eqn. 3.6}$$

where P is the applied load (N), D is the average diagonal length of D₁ and D₂, θ is the angle of the diamond indenter (136 °) and the obtained value H_v is the Vickers hardness.

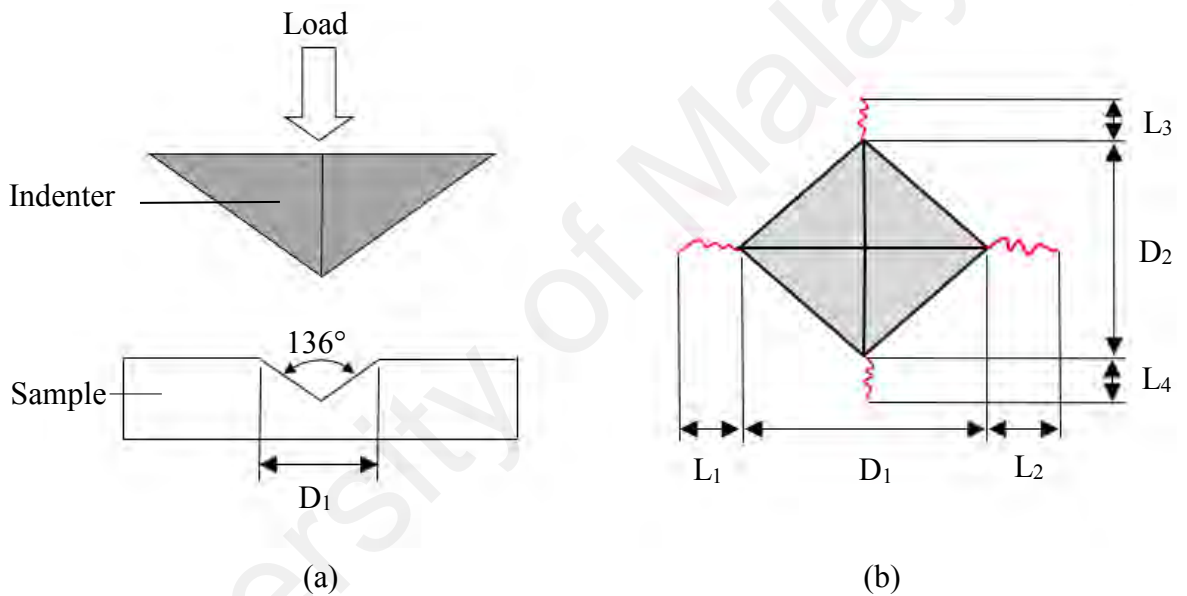


Figure 3.6: Schematic diagram of an indentation (a) side view of indentation, (b) top view of indentation.

It has been possible to calculate the fracture toughness of the samples by the cracks emanated from the vertices of the Vickers indentation. Different crack length (L₁, L₂, L₃, L₄) were measured and fracture toughness (K_{Ic}) was calculated using the Eqn. 3.7 proposed by Shetty and Wright (1986):

$$K_{Ic} = 0.0889 \left(\frac{H_v P}{4L} \right)^{\frac{1}{2}} \dots\dots\dots \text{Eqn. 3.7}$$

where P is the applied load (N), L is the average crack length (m), H_v is the Vickers hardness (GPa) and K_{Ic} is the fracture toughness, in the unit of $\text{MPa}\cdot\text{m}^{1/2}$.

3.5.4 Microstructure Evaluation

Microstructure characterization was carried out using a Field Emission Scanning Electron Microscope (FE-SEM, Philips). FE-SEM offers ultra-high resolution imaging at a low accelerating voltage to study the microstructure and morphology of the samples. Prior to the microstructure evaluation, the samples were thermally etched as mentioned in the previous section to delineate grain boundaries for better imaging. The samples were then placed on a pin-type specimen stub with double-sided carbon tape and mounted on the specimen holder before inserted to the FE-SEM chamber. An accelerating voltage of 1 kV was used to provides magnification from 3000 to 20,000 times for microstructure evaluation. The element compositions of the sintered samples were confirmed through Energy Dispersive X-Ray Spectroscopy (EDS) equipped in the FE-SEM.

The FE-SEM micrographs that obtained were utilized in grain size measurement, using line intercept method (ASTM E112-96). Lines were drawn in the micrographs and the number of intercepts between the test line and the grain boundaries were counted. The grain size was calculated by Eqn. 3.8:

$$D = 1.56 \left(\frac{C}{MN} \right) \dots\dots\dots \text{Eqn. 3.8}$$

where D is the grain size, M is the magnification of FE-SEM micrograph, N is the number of intercepts and C is the total length of the test line. The calculation of intercepts is illustrated in Figure 3.7 and average grain size was calculated.

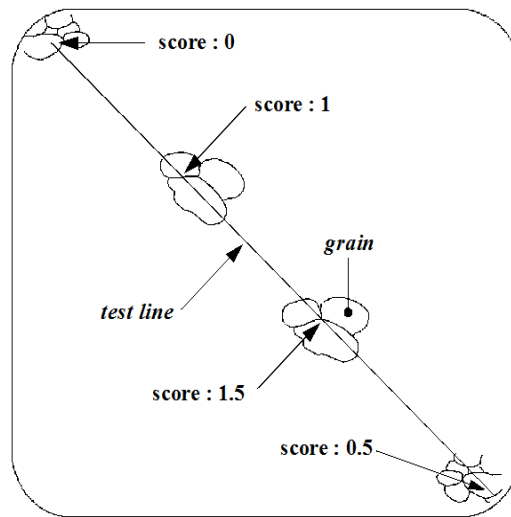


Figure 3.7: Schematic diagram of the number of intercepts at a test line.

3.5.5 Low Temperature Degradation Study

The microwave and conventional sintered samples were aged in an autoclave vessel (Parr instrument, USA). The samples were immersed in 10 ml of distilled water in the vessel and kept in an oven at 180 °C/10 bar. At high temperature, water would change from liquid to vapour (superheated steam). The samples were aged for 1 h, 3 h, 6 h, 24 h, 75 h and 200 h. At each interval, the samples were withdrawn from the vessels for XRD phase analysis. The phase analysis by XRD was necessary to inspect the existence of *t-m* phase transformation at each ageing duration.

3.6 Summary

In brief, the fabrication of insulation housing, preliminary study of microwave processing parameters, experimental methods for sample preparation and characterization techniques were explained. A general experiment procedure and setup were presented for the preliminary study for microwave processing. The detailed preliminary study on the influence of susceptors, heating rates and pre-sintering will be discussed in the next chapter, where the sequential selection of parameters and condition would be deliberated. The experimental methods of sample preparation, powder compaction and sintering were elaborated in detail. Prior to sample characterization, the sintered samples underwent grinding, polishing and thermal etching process. This was followed by different characterization methods for the sintered samples, which includes XRD phase identification, water immersion method for density, Vickers hardness test, FE-SEM analysis and LTD test.

CHAPTER 4: RESULTS AND DISCUSSIONS

4.1 Introduction

This chapter is divided into 3 sections. The first section examines the preliminary study on microwave processing parameters, which covers the influence of susceptors, heating rates and pre-sintering. The second section investigates the effects of CuO addition via microwave sintering with the selected optimum microwave processing parameters. This section discusses the effects of microwave sintering on CuO-doped Y-TZPs which include tetragonal phase stability, densification behaviour, Vickers hardness, fracture toughness, microstructure development and grain size. The third section compares the densification behaviour of the Y-TZPs subjected to microwave and conventional sintering, which also includes the phase stability of Y-TZPs after exposure in the superheated steam environment.

4.2 Preliminary Study: Microwave Processing Parameters

4.2.1 The Influence of Susceptors

In the first configuration, no susceptors were used during microwave sintering of three samples. The samples were placed side by side at the center of the insulator base. A long warm-up time (>15 min) was noted when the samples were initially heated from room temperature to 250 °C. Although the samples could be heated to 500 °C in the first cycle, the samples could not reach 600 °C during heating although the calculated temperature is 600 °C. The actual temperature recorded dropped to 500 °C tremendously in few seconds when the calculated temperature is 600 °C. It is postulated that the disability of Y-TZPs samples to heat up to 600 °C was mainly caused by the low dielectric loss of Y-TZP below 600 °C. The results obtained from this setup is in agreement with the findings found by Zhao et al. (2000), who reported that long warm-up time was required for direct microwave heating Y-TZP before the material begins to couple with microwaves before 250 °C. In the present work, hot spot was also found for the insulator where susceptor

was not used during microwave sintering as illustrated in Figure 4.1. This result were also observed by Charles et al. (2017), who reported that hot spot was developed during direct microwave sintering without susceptors.

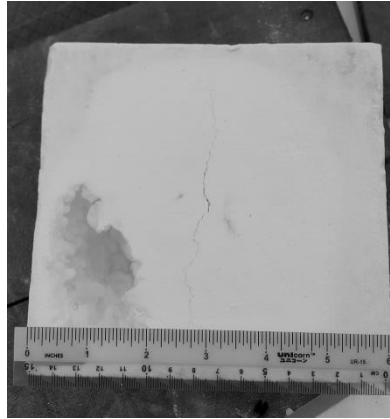


Figure 4.1: Hot spot on insulation base after microwave sintering without susceptors.

From the previous setup, it was apparent that susceptor was necessary to absorb microwave and reached high temperatures during microwave heating, especially at the pre-heating stage below 600 °C. This is to ensure that the green samples reached 600 °C with the assistance of susceptor, to allow self-heating of samples to take place beyond 600 °C, as Y-TZPs have higher dielectric loss when the temperature increased to 600 °C. Silicon carbide (SiC) susceptor rod (diameter of 8 mm and length of 20 mm) was used in the next setup. As shown in Figure 4.2, three samples were surrounded by four susceptors at each corner. However, all the samples were found cracked after microwave sintering as shown in Figure 4.3 (a). This could be caused by the excessive heat boost by the four susceptors. When the susceptor was reduced to three pieces, it was found that the sample near to one susceptor fracture into fragments as shown in Figure 4.3 (b). The present result is in accordance with an earlier findings reported by Sujith et al. (2009), where placing one susceptor at one side of samples will cause sample crack attributed to the low thermal conductivity of zirconia and the initial boost of heating from susceptor, which creates uneven coupling within the sample. This explained why the sample near to the single

susceptor broken into small pieces, while the other neighbouring samples had small cracks.

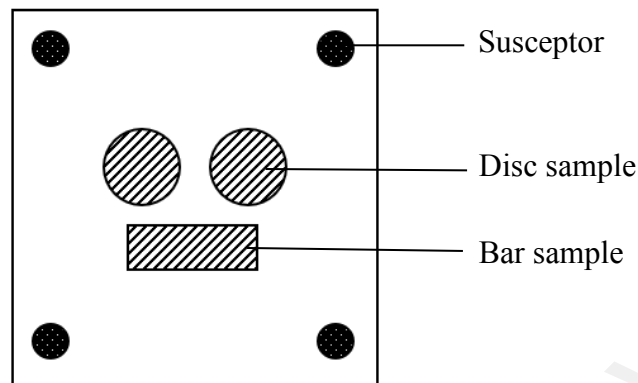


Figure 4.2: Three samples configuration surrounded by four susceptors.



Figure 4.3: Example of samples crack after microwave sintering with (a) four susceptors, (b) three susceptors.

4.2.2 The Influence of Heating Rates

When the green samples increased from three to six samples, the disc samples were stacked up and surrounded by four susceptors as illustrated in Figure 4.4. Four susceptors were used to avoid insufficient heat boost during the pre-heating stage of microwave sintering for six samples. After microwave sintering, all the samples were found crack as shown in Figure 4.5. A sample was found broken into two segments which could be due to the high heating rates of 50 °C/min. Besides, some crack lines were detected for another sample, which could be caused by the excessive quantity of susceptors.

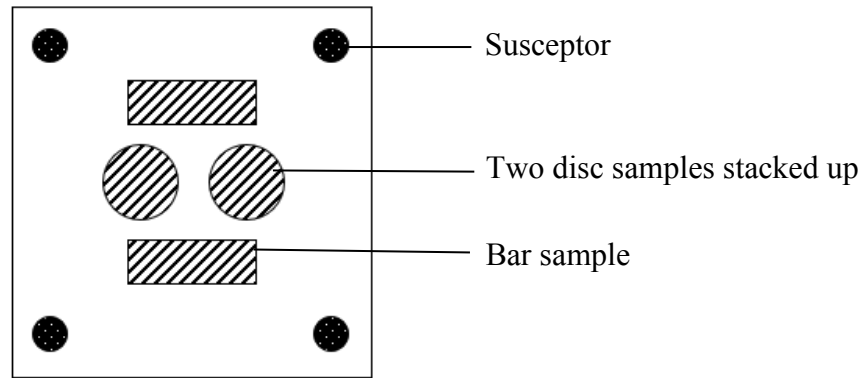


Figure 4.4: Six samples configuration surrounded by four susceptors.

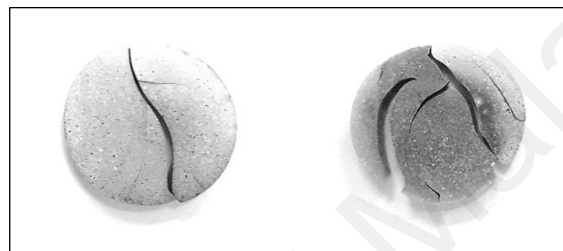


Figure 4.5: Example of samples crack after microwave sintering at 50 °C/min with four susceptors.

A further study was done with the aid of temperature profile recorded from the microwave control panel. According to Figure 4.6, the calculated heating rate of 50 °/min was difficult to be followed by the actual temperature of the samples at below 430 °C and above 800 °C. The great discrepancy of temperatures had suggested that the root cause of sample crack was due to overheating at the high heating rate of 50 °/min. This is in accordance with the findings found by Charmond et al. (2010), where the heating rate of Y-TZP was difficult to regulate in the range up to 1000 °C due to the low dielectric parameters of zirconia. Oghbaei and Mirzaee (2010) also elaborated that sample cracks at high heating rates due to thermal expansion mismatch between surface and center of the sample, owing to the low thermal conductivity of zirconia.

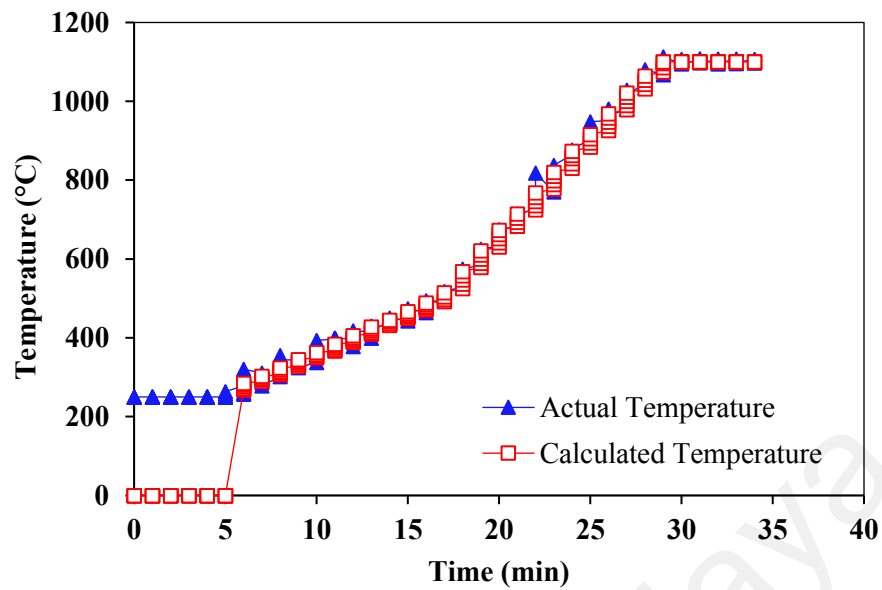


Figure 4.6: Temperature profile for samples during microwave sintering at a heating rate of 50 °C/min.

In a research, Binner et al. (2008) reported that higher heating rates resulted in samples crack, where they suggested that a heating rate of 20 °C/min to be used to ensure volumetric heating using hybrid microwave sintering methods. Borrell et al. (2012) had also explored the microwave effect of 3 mol% Y-TZPs with a heating rate of 30 °C/min, and successfully produced Y-TZP with a homogeneous microstructure than conventional sintering. In the next attempt, the heating rate was revised from 50 °C/min to 30 °C/min, and two susceptors were employed. Heat shield made from alumina fiber material was introduced to avoid overheating boost from the susceptors. Two heat shields with susceptors were placed at the edge of the corners, which faced each other in a diagonal pattern as arranged in Figure 4.7.

Figure 4.8 shows the temperature profile of microwave sintering at a heating rate of 30 °C/min with two susceptors. The result showed that the actual temperature matched well with the calculated temperature when it reached at 430 °C and above. At 200 °C, zirconia (3 mol% Y-TZP) was microwave transparent, where the heating was primarily transferred from the susceptors to the samples (Bhattacharya & Basak, 2016). It was clear

that below 430 °C represents the preheating stage of the samples, where heating was mainly contributed by the susceptors. When the temperature reaches at 600 °C, the Y-TZP started to couple microwave resulting from the rapid increased of dielectric loss (Bhattacharya & Basak, 2016). Although heat shield was introduced during microwave sintering, the samples still suffered from edge crack due to non-uniform heating. This could be caused by the low thermal conductivity of zirconia that produced non-uniform heating (Sujith et al., 2009).

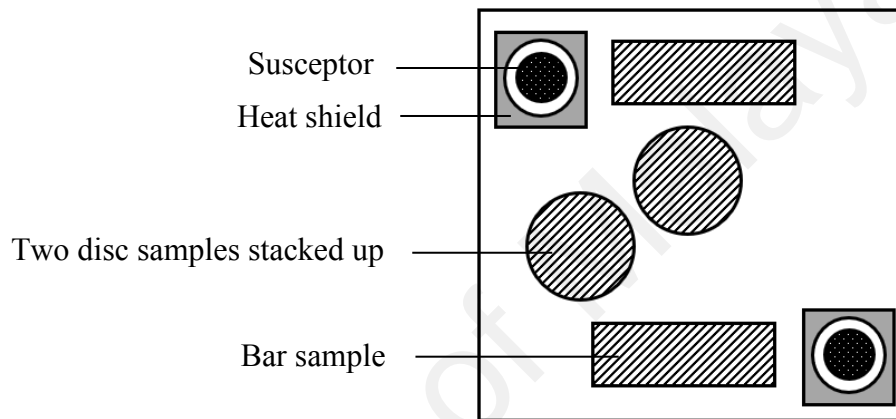


Figure 4.7: Six samples configuration surrounded by two heat shields with susceptors.

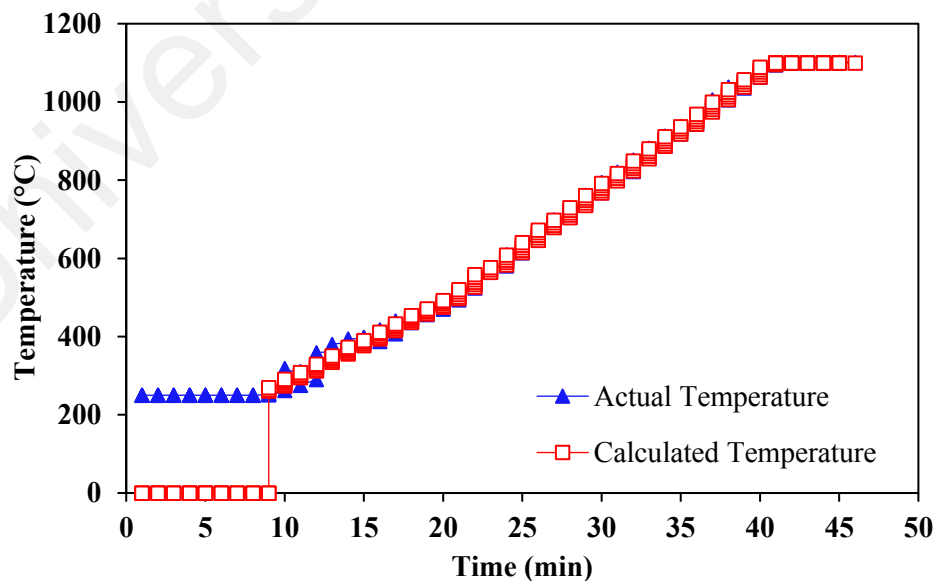


Figure 4.8: Temperature profile for samples during microwave sintering at a heating rate of 30 °C/min.

4.2.3 The Influence of Pre-sintering

Borrell et al. (2013) reported that the pre-sintering stage is essential to avoid development of cracks in samples due to heterogeneous temperature distribution. According to several researchers, the green samples were heated at 600 °C prior to microwave sintering, to provide uniform microwave heating (Borrell et al., 2013; Charmond et al., 2010; Travitzky et al., 2000). In the present work, the green samples were pre-sintered at 600 °C, at a ramp rate of 10 °C/min, with a holding time of 2 hours. The temperature profile of microwave sintering is shown in Figure 4.9 and crack-free samples were produced. The actual temperature followed with the calculated temperature when it reached at 350 °C and above. This clearly shows that pre-sintering contributed on producing homogeneous temperature distribution for green samples, which had lowered the temperatures mismatch of samples as compared with samples without pre-sintering. Pre-sintering was therefore necessary, prior to microwave sintering to acquire crack free samples. Besides, phase stability of both pre-sintered and without pre-sintered samples, were compared in Figure 4.10. It was found that the tetragonal phase was not disrupted regardless of pre-sintering method.

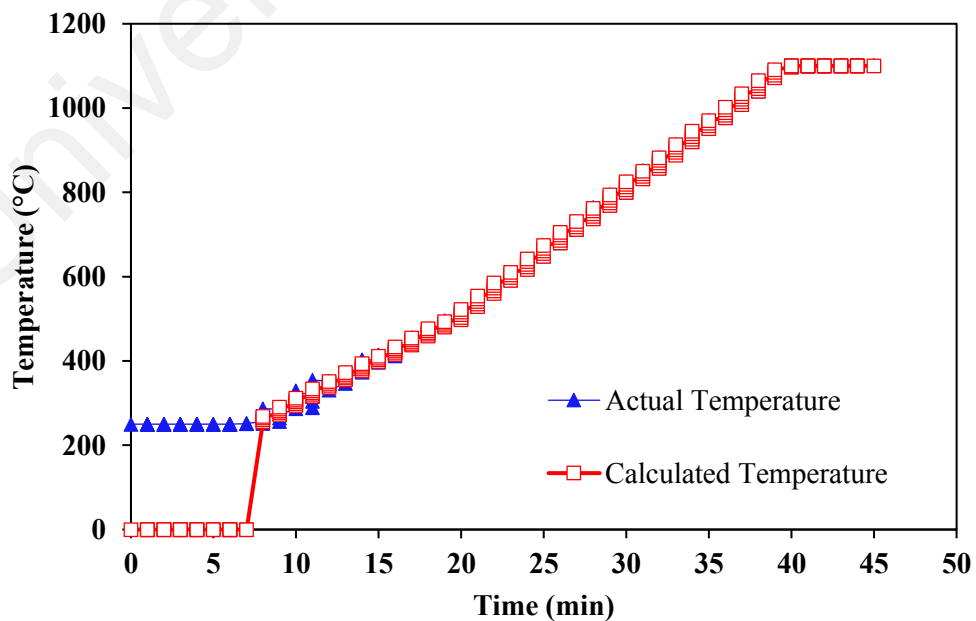


Figure 4.9: Temperature profile for pre-sintered samples during microwave sintering at a heating rate of 30 °C/min.

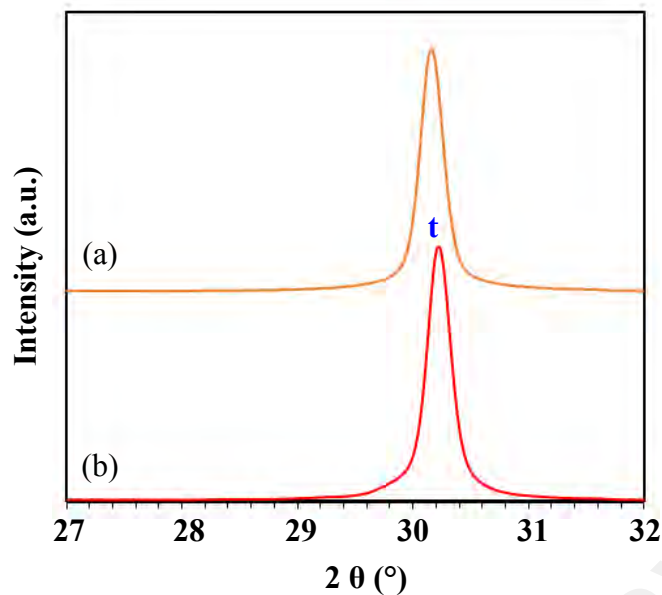


Figure 4.10: Comparison of the XRD traces for undoped Y-TZP when microwave sintered at 1100 °C (a) with pre-sintering and (b) without pre-sintering. Key: t - tetragonal phase.

From the preliminary study, susceptor was found to be essential to prevent hot spot and to obtain crack-free sintered samples. Besides, an adequate heating rate of 30 °C/min was selected to avoid the discrepancy between calculated and actual temperatures due to the low dielectric parameters of zirconia. The heat shield was also introduced to prevent overheating boost from the susceptors to the samples. In addition, pre-sintering prior to microwave sintering contributed to producing homogeneous temperature distribution for samples, resulting in crack-free samples. In the present work, six green samples were placed at the center of the enclosed alumina fiberboard insulator and flanked with two SiC susceptors in the heat shield. Before microwave sintering, these green samples were subjected to pre-sintering at 600 °C, at a ramp rate of 10 °C/min, with a holding time of 2 h in a box furnace. Subsequently, the microwave sintering was operated with a ramp rate of 30 °C/min up to the designated sintering temperatures (1100 °C, 1200 °C, 1250 °C, 1300 °C, 1400 °C), held for 5 min. In the following section, the effect of microwave sintering of CuO-doped Y-TZPs on phase stability, densification, microstructure and mechanical properties will be deliberated by different characterization methods.

4.3 Effect of Microwave Sintering

4.3.1 Tetragonal Phase Stability

Table 4.1 shows the tetragonal and monoclinic phase content of microwave sintered samples of undoped, 0.05 wt%, 0.1 wt%, 0.2 wt%, 0.3 wt%, 0.4 wt%, 0.5 wt% and 1 wt% CuO-doped Y-TZPs as determined from the XRD analysis. The results showed that the addition of CuO up to 0.4 wt% in Y-TZP did not disrupt the tetragonal phase regardless of sintering temperature up to 1400 °C. However, when the CuO content increased to 0.5 wt%, about 21.2% monoclinic phase was detected for samples sintered at 1100 °C but not at higher temperatures as illustrated in Figure 4.11 (a). The addition of 1 wt% CuO was found to be detrimental to the tetragonal stability of the zirconia, where all the samples underwent the phase transformation upon cooling from microwave sintering as shown in Figure 4.11 (b). The monoclinic phase detected was about 50% for the samples sintered from 1100 °C to 1300 °C, before decreased to approximately 35% at 1400 °C.

Table 4.1: Tetragonal and monoclinic phase determined from XRD analysis of microwave sintered samples. The monoclinic phase is given in parenthesis if present.

CuO content (wt%)	Sintering Temperature (°C)				
	1100	1200	1250	1300	1400
0 (undoped)	100	100	100	100	100
0.05	100	100	100	100	100
0.1	100	100	100	100	100
0.2	100	100	100	100	100
0.3	100	100	100	100	100
0.4	100	100	100	100	100
0.5	79.8 (21.2)	100	100	100	100
1	49.3 (50.7)	48.1 (51.9)	51.8 (48.2)	51.6 (48.4)	64.8 (35.2)

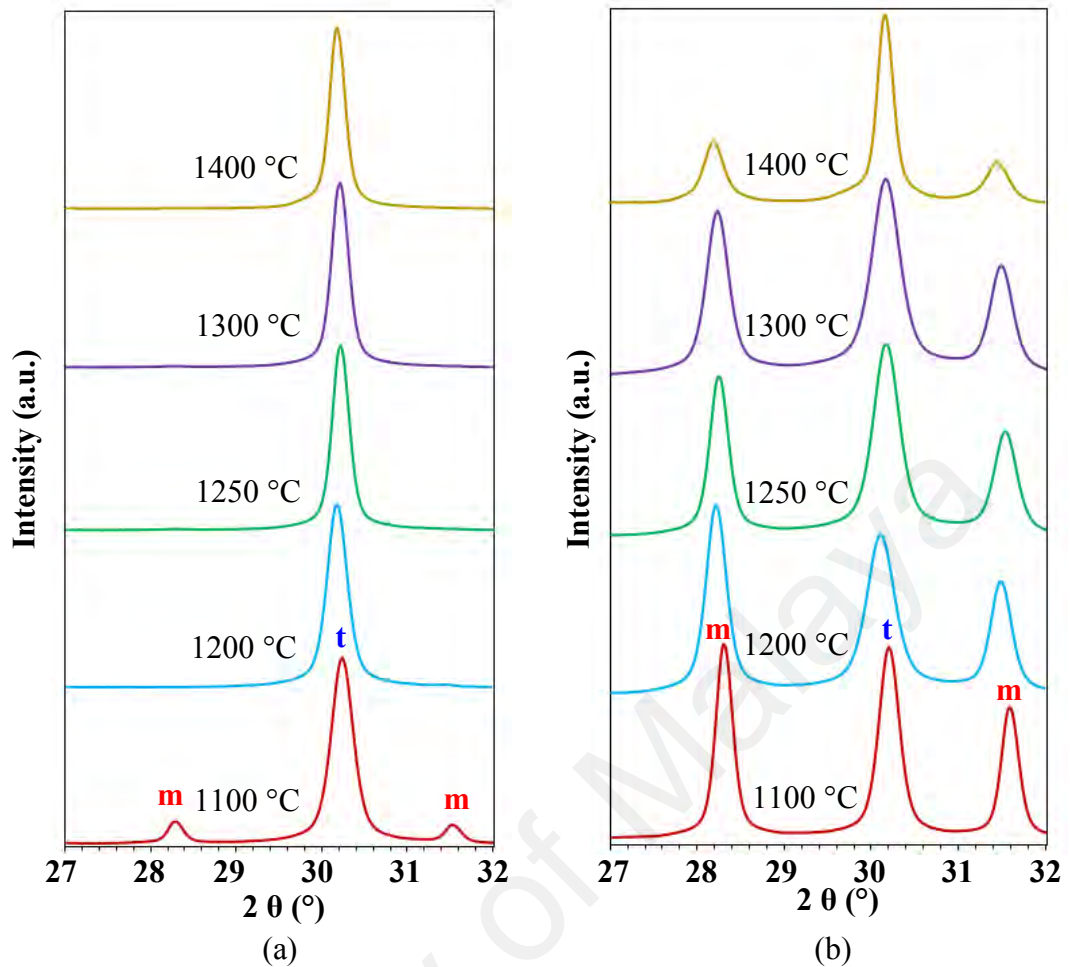


Figure 4.11: XRD traces of microwave sintered samples at different temperatures (a) 0.5 wt% and (b) 1 wt% CuO-doped Y-TZPs. Key: m - monoclinic phase and t - tetragonal phase.

It is unclear at this stage on the monoclinic phase development observed for 0.5 wt% CuO-doped Y-TZP when microwave sintered at 1100 °C. When the sintering temperature increased to 1200 °C, no monoclinic phase was detected up to 1400 °C. In order to exclude the effect of microwave on the phase transformation during sintering, the 0.5 wt% CuO-doped green samples were sintered at various temperatures by the conventional sintering method. The comparison of the XRD traces for both sintering methods performed at 1100 °C is shown in Figure 4.12. Surprisingly, a similar trend on the monoclinic development was also observed for conventional sintered samples, i.e. only monoclinic phase was detected at 1100 °C and not at other sintering temperatures. The measured monoclinic phase content for conventional sintered sample was about 32.7%,

whereas 21.2% was found for microwave sintered Y-TZP. Hence, the results show that the sintering method was not responsible for the spontaneous phase transformation in these samples. This is in agreement with the findings reported by Winnubst et al. (2009), where the authors conventional sintered CuO-doped Y-TZPs at about 1100 °C with a heating rate of 15 °C/min. They reported that the addition of 0.5 wt% CuO and above in Y-TZP matrix resulted in the development of monoclinic phase.

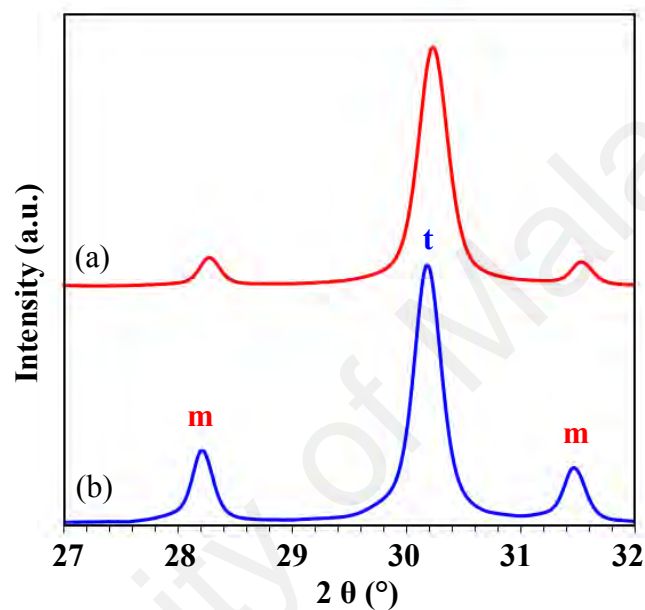


Figure 4.12: Comparison of the XRD traces for 0.5 wt % CuO-doped Y-TZP when sintered at 1100 °C by (a) microwave method and (b) conventional method. Key: m – monoclinic phase and t - tetragonal phase.

In general, the destabilization effect of tetragonal phase could be due to the deficiency of yttria in stabilizing the tetragonal phase. This is envisaged that the interaction between CuO with yttria or zirconia during sintering. Lemaire et al. (1999) and Winnubst et al. (2009) suggested that the reaction between CuO and Y_2O_3 formed $Y_2Cu_2O_5$ phase in the grain boundaries, which was responsible for the yttria depletion and led to destabilization. On the other hand, the retention of tetragonal stability of the lower amount of CuO-doped Y-TZPs was attributed to the formation of a transient liquid phase during sintering, which improved its sinterability. However, the amount of Y_2O_3 was sufficient in stabilizing the tetragonal phase to maintain CuO-doped Y-TZP in metastable form.

4.3.2 Densification Behaviour

The effect of CuO and sintering temperatures on the densification of Y-TZPs are shown in Figure 4.13. The results revealed the beneficial effect of CuO dopants in aiding densification of Y-TZPs. In general, the addition of CuO up to 0.4 wt% in Y-TZPs exhibited higher relative density than undoped Y-TZPs regardless of sintering temperatures. Apart from the 1 wt% CuO-doped Y-TZP, all samples recorded a relative density above 93.5% when the sintering temperatures reached above 1200 °C. Similar densification behaviour was observed in other study where the relative density above 92% was recorded for undoped and CuO-doped samples (except for 1 wt% CuO-doped sample) after conventional sintering beyond 1250 °C (Bowen et al., 1998; Ramesh et al., 1999; Ran et al., 2006).

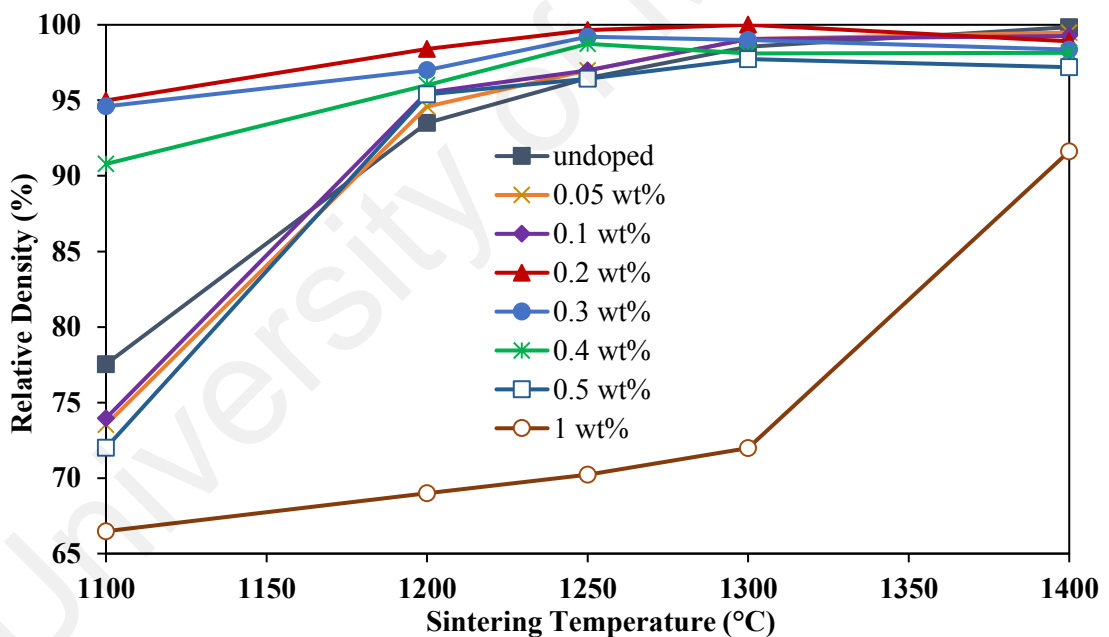


Figure 4.13: The effect of CuO and microwave sintering temperature on the relative density of Y-TZPs.

The additions of 0.2, 0.3 and 0.4 wt% CuO were beneficial in promoting sintering of Y-TZP when sintered at lower temperatures, below 1300 °C. In contrast, the undoped Y-TZP exhibited a low relative density of 77.5%, if compared to 95% for the 0.2 wt% CuO-doped Y-TZP when sintered at 1100 °C. This observation correlated with the results

reported by Ting et al. (2017), when conventional sintering MnO₂ doped-YTZPs at 1100 °C. The authors found that the addition of 0.5 wt% MnO₂ resulted in a sintered body having a higher relative density of approximately 70% when compared to 55% for the undoped Y-TZP. In the present work, a high relative density of 98.4% was attained for 0.2 wt% CuO-doped Y-TZP when sintered at 1200 °C, before reaching the maximum dense of 100% at 1300 °C. This is a remarkable performance since undoped sample could only attain 98.5% at 1300 °C and 99.8 % at 1400 °C. In the case of 0.05 wt% and 0.1 wt% CuO doped Y-TZPs, there was a substantial increase in relative density when the sintering temperature increased from 1100 °C to 1200 °C. Minimal pores were removed from the microstructure from 1100 °C to 1200 °C, which had contributed to the increment of relative density as shown in Figure 4.14.

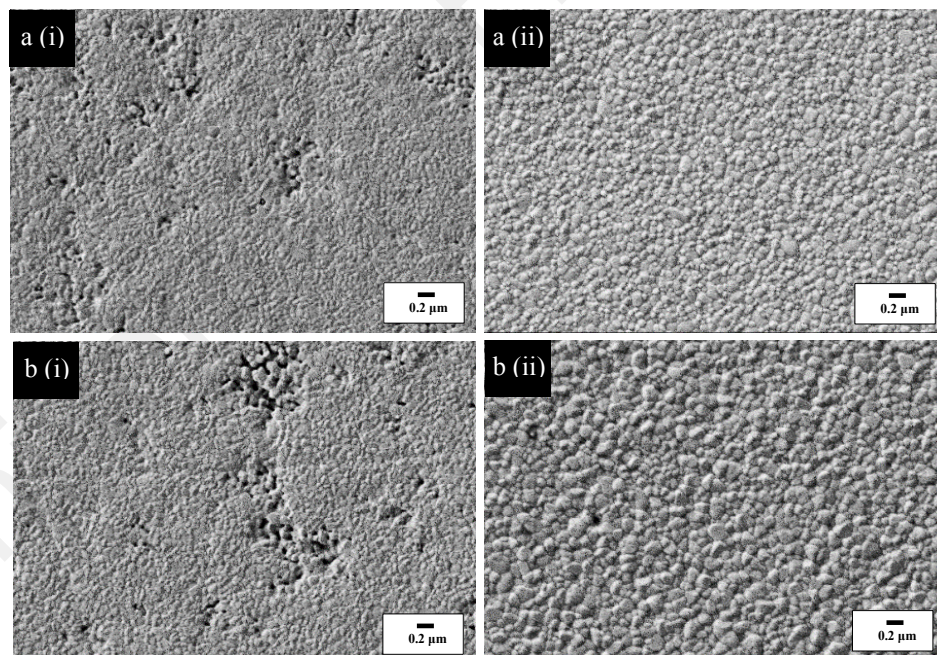


Figure 4.14: FE-SEM micrographs of different content of CuO-doped Y-TZPs (a) 0.05 wt% and (b) 0.1 wt% microwave sintered at (i) 1100 °C and (ii) 1200 °C respectively.

In the case of the 1 wt% CuO-doped Y-TZP, a lower relative density below 75% was recorded when sintered between 1100 and 1300 °C. This could be due to the relatively high monoclinic phase present (about 48% to 52%) as given in Table 4.1. Besides, it could

be attributed to the ill-formed microstructure consists of pore-like voids observed after sintering as shown in Figure 4.15. However, sintering at 1400 °C resulted in an increase in the relative density to about 92%, which could be attributed to the reduction of monoclinic phase content and the formation of a denser microstructure as shown in Figure 4.15 (e). In addition, the low density of the 0.5 wt% CuO doped Y-TZP at 1100 °C could be attributed to the presence of monoclinic phase at about 21%.

4.3.3 Microstructure Development and Grain Size

Figure 4.16 shows the effect of grain size at different CuO dopant content up to 0.5 wt% at various microwave sintering temperatures. In general, the grain size of Y-TZPs was found to increase with the increasing of CuO content from 0.3 wt% to 0.5 wt% and sintering temperatures. It was also found that the addition of small amounts of CuO up to 0.2 wt% did not dramatically affected the grain size of the Y-TZPs, which was similar to the undoped Y-TZPs. At 1100 °C, the grain size for undoped and CuO-doped samples (≤ 0.2 wt%) were small, i.e. about 0.1 μm as shown in Figure 4.17. This is in accordance with the findings reported by other authors who examined the tetragonal grain size of Y-TZPs with the addition of minute amounts such as alumina, manganese oxide, graphene oxide and silica. They reported that the tetragonal grain size was almost similar to the undoped when sintered at the same temperatures (≤ 1450 °C) (Kanellopoulos & Gill, 2002; Nogiwa-Valdez et al., 2013; Ramesh et al., 2016; Ramesh et al., 2008; Ramesh et al., 2012; Samodurova et al., 2015; Zhang et al., 2015).

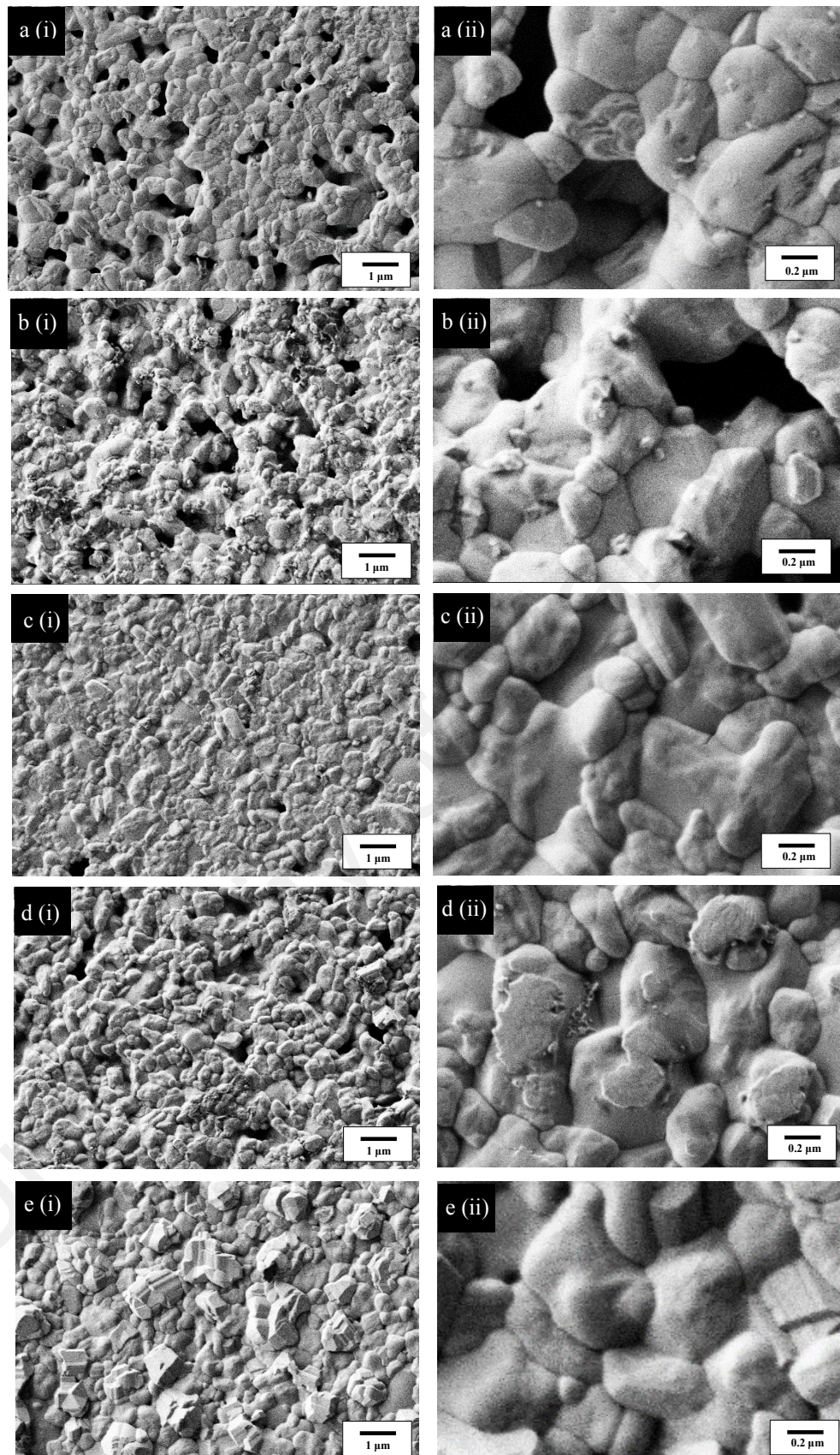


Figure 4.15: FE-SEM micrographs of 1 wt% CuO-doped Y-TZPs microwave sintered at (a) 1100 °C, (b) 1200 °C, (c) 1250 °C, (d) 1300 °C and (e) 1400 °C. Figure (ii) in each case represents the microstructure taken at higher magnification.

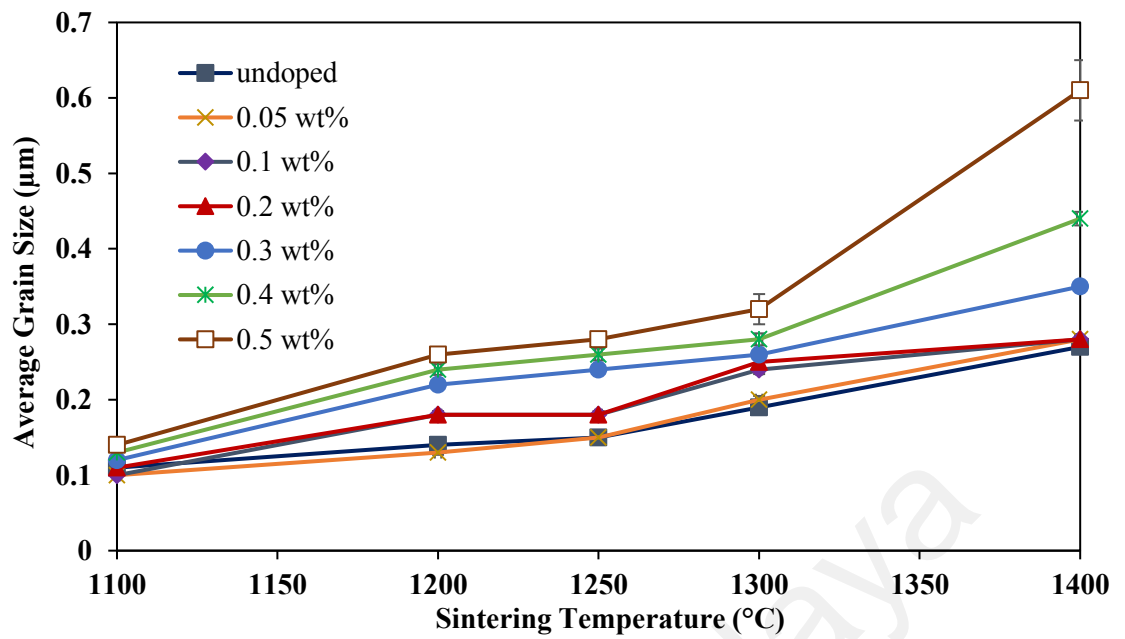


Figure 4.17: The effect of microwave sintering and CuO doping on the average grain size of Y-TZPs.

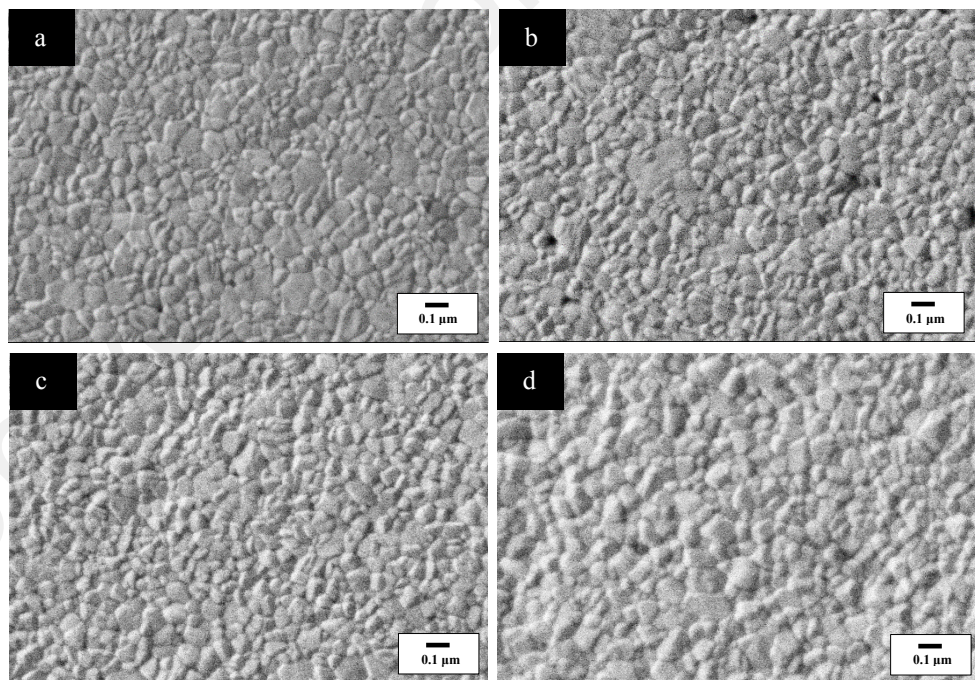


Figure 4.16: FE-SEM micrographs of Y-TZPs containing low amounts of CuO that microwave sintered at 1100 °C (a) undoped, (b) 0.05 wt%, (c) 0.1 wt% and (d) 0.2 wt%.

In the present work, a small change in the grain size was observed for CuO-doped samples (≤ 0.2 wt%) when sintered below 1250 °C. These samples exhibited grain size less than 0.20 μm . However, sintering at 1300 °C enhanced the grain size of 0.2 wt% CuO-doped Y-TZP to 0.25 μm , A slightly larger grain size of 0.28 μm was recorded when the sintering temperature reached at 1400 °C. The evolution of the microstructure of 0.2 wt% CuO-doped Y-TZP is illustrated in Figure 4.18.

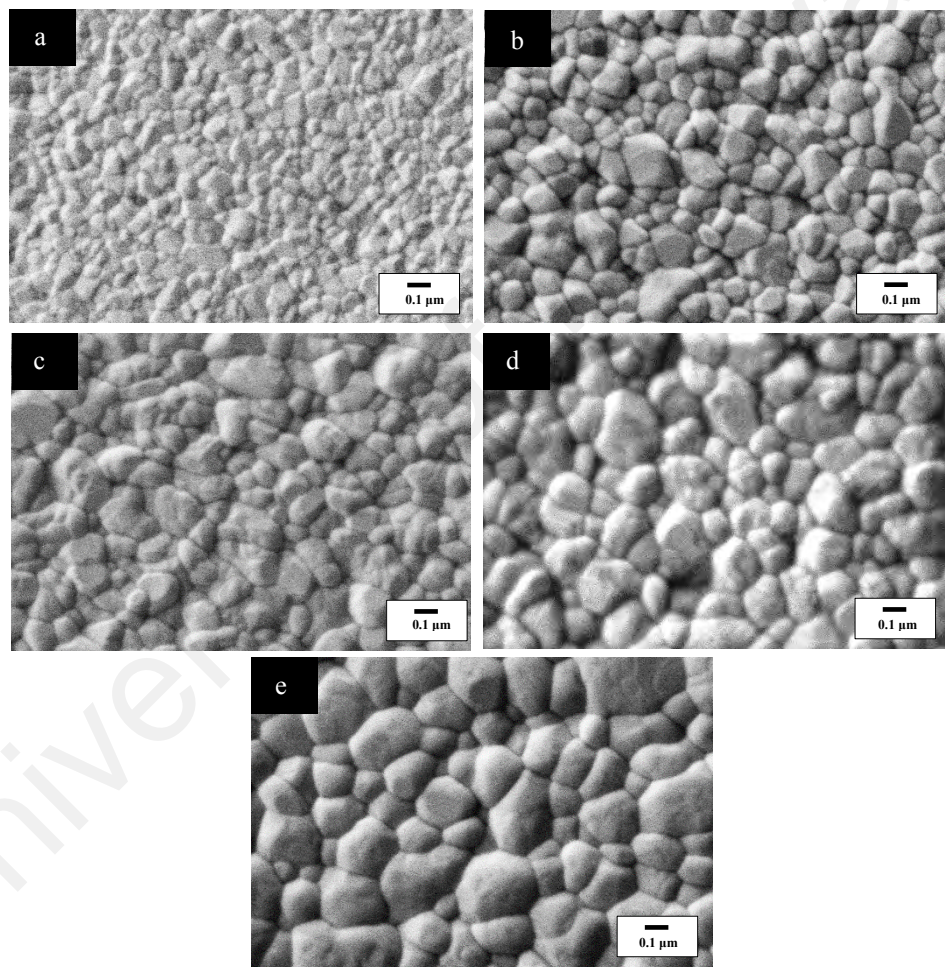


Figure 4.18: FE-SEM micrographs of 0.2 wt% CuO-doped Y-TZPs at different microwave sintering temperatures (a) 1100 °C, (b) 1200 °C, (c) 1250 °C, (d) 1300 °C and (e) 1400 °C

The sintered microstructure of Y-TZPs at 1400 °C is depicted in Figure 4.19. The microstructure and grain size of the samples containing CuO up to 0.2 wt% were generally similar (0.27-0.28 μm) as the undoped Y-TZP. A fine microstructure comprising of equiaxed grains was observed for these samples. In contrast, exaggerated grain growth occurred for 0.5 wt% and 1 wt% CuO-doped Y-TZPs. At 1400 °C, the average grain size was found to increase significantly to 0.61 μm and 0.69 μm respectively as shown in Figure 4.19 (e) and (f).

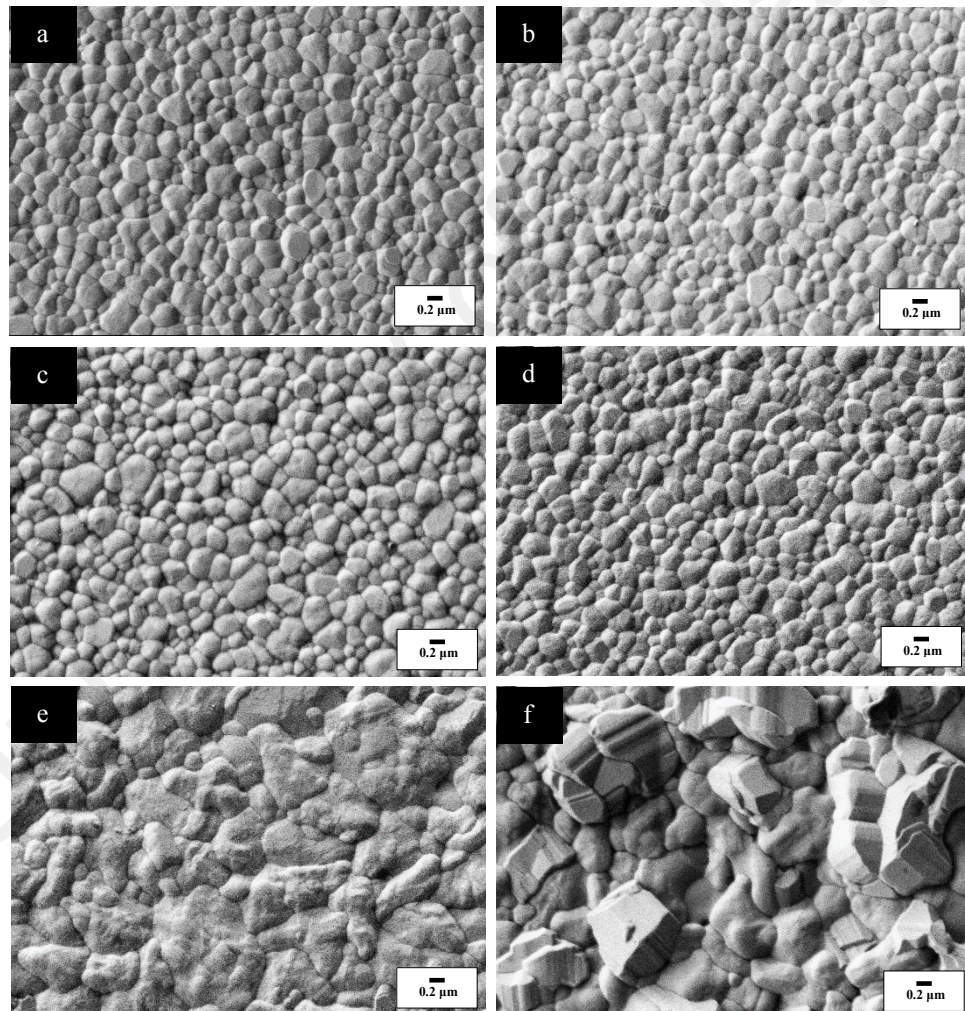


Figure 4.19: FE-SEM micrographs of microwave sintered samples of different amounts of CuO that microwave sintered at 1400 °C (a) undoped, (b) 0.05 wt%, (c) 0.1 wt%, (d) 0.2 wt%, (e) 0.5 wt% and (f) 1 wt%.

4.3.4 Vickers Hardness and Fracture Toughness

The effect of CuO and sintering temperatures on the Vickers hardness of Y-TZPs is shown in Figure 4.20. There is a good correlation observed between Vickers hardness and relative density of Y-TZPs with increasing temperatures. In general, all Y-TZPs (except for the 1 wt% CuO) showed a steep increase in the hardness as the temperature increased from 1100 °C to 1250 °C. At 1100 °C, these samples yielded Vickers hardness values between 3 GPa to 6 GPa, while 1 wt% CuO-doped sample had a low hardness of about 2 GPa. Specifically, a relatively high Vickers hardness above 5 GPa was obtained for 0.2 wt% to 0.4 wt% CuO-doped Y-TZPs, when compared with 4.2 GPa measured for the undoped Y-TZP.

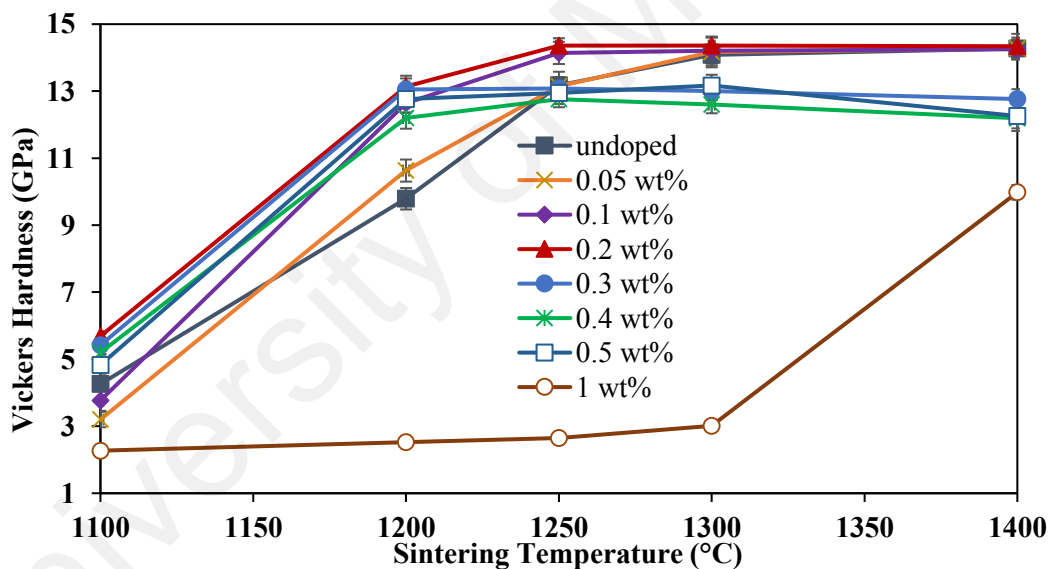


Figure 4.20: The effect of CuO addition on the Vickers hardness of Y-TZPs microwave sintered at different temperatures.

There is a significant enhancement in hardness for all the CuO-doped Y-TZPs (≤ 0.5 wt%) if compared to the undoped Y-TZP when sintered at 1200 °C. High hardness between 10 GPa to 13 GPa was achieved by CuO-doped samples, whereas undoped Y-TZP yielded a low hardness of about 9 GPa. It was also noted that the addition of 0.2 wt% CuO showed a remarkable high Vickers hardness of 13 GPa at 1200 °C and reached a

high value of 14.4 GPa at 1250 °C. The hardness remained almost constant with further increased in temperature up to 1400 °C. On the other hand, the undoped Y-TZP could only attained similar hardness of 14 GPa when sintered at 1400 °C.

Higher addition of CuO beyond 0.2 wt%, however experienced a decreased in hardness, particularly beyond 1250 °C. The result is in good agreement with that reported by Lawson et al. (1995), where they found that higher CuO concentration above 0.2 wt% (up to 0.35 wt%) resulted in a reduction in density and hardness of the ceramic. In the present work, the 1 wt% CuO-doped sample exhibited a low hardness of about 2 GPa to 3 GPa when microwave sintered between 1100 °C and 1300 °C. Although the sample was sintered to 1400 °C, a low Vickers hardness of about 10 GPa was obtained. This is relatively lower than all the CuO-doped samples that microwave sintered at 1200 °C. The low hardness obtained for 1 wt% CuO-doped Y-TZP is in accordance with the findings reported by Ramesh et al. (1999), where 1 wt% CuO-doped Y-TZP yielded low hardness of 9 GPa at 1400 °C. In brief, the Vickers hardness trend of CuO-doped Y-TZPs is corresponding with the density trend as shown in Figure 4.13.

The variation in fracture toughness of the microwave sintered CuO-doped Y-TZPs at different temperatures is shown in Figure 4.21. For dopant content up to 0.5 wt%, fracture toughness increases with increasing temperatures and peaked at either 1250 °C or 1300 °C, followed by a decrease with further sintering. It was evident that the fracture toughness of the Y-TZP showed some improvement with the addition of up to 0.5 wt% CuO. In the case of 0.2 wt% CuO-doped Y-TZP, the fracture toughness showed a remarkable improvement throughout the sintering temperature employed. The sample recorded a maximum fracture toughness of 7.8 MPa.m^{1/2} at 1250 °C. In contrast, the undoped ceramic could only achieved a maximum of 6.8 MPa.m^{1/2} at 1300 °C. As expected, based on the densification trend and phase analysis, the addition of 1 wt% CuO

showed a low fracture toughness between 2 MPa.m^{1/2} to 3 MPa.m^{1/2} up to 1300 °C, before reaching at about 4.6 MPa.m^{1/2} at 1400 °C.

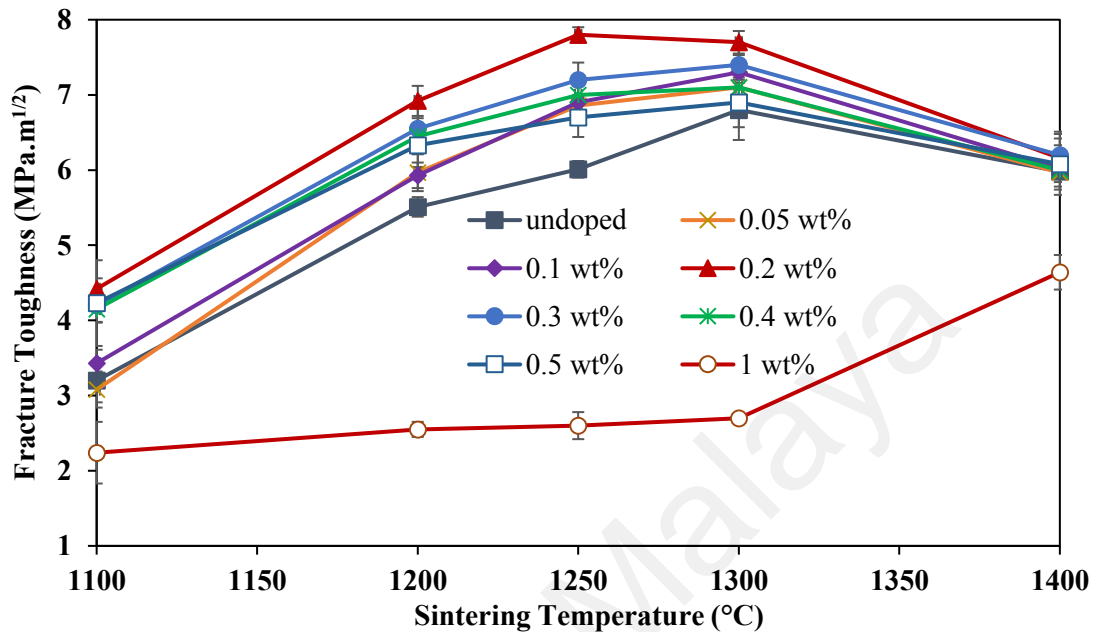


Figure 4.21: The effect of CuO addition on the fracture toughness of Y-TZPs microwave sintered at different temperatures.

This observation has shed some light on the effect of low amounts of CuO in terms of enhancing the transformation toughening effect of Y-TZP. The enhancement in toughness of the CuO-doped samples could not be associated with the grain size effect since the 0.2 wt% CuO-doped sample had almost similar grain size as the undoped Y-TZP as discussed earlier. Thus, it is envisaged that small amounts of CuO addition (≤ 0.5 wt%) could have formed a transient liquid phase during sintering (Hwang, 1990; Ramesh et al., 2011). Minute amounts of yttria could have been drawn out from the zirconia matrix, however the remaining Y₂O₃ would be sufficient to stabilize the tetragonal phase since no monoclinic phase was detected after sintering. The resulting tetragonal grains of this CuO-doped Y-TZP would be in the metastable state if compared to those of the undoped Y-TZP. This explained the higher toughness of the CuO-doped samples (≤ 0.5 wt%), where the transformation toughening effect would have activated readily during Vickers indentation test. However, the toughness of 1 wt% CuO-doped Y-TZPs was

much lower than the undoped samples, where a larger amount of Y_2O_3 would have been depleted from the zirconia matrix. This has been shown to be detrimental, where high monoclinic phase content was developed upon sintering. The detailed schematic diagram is shown in Figure 4.22.

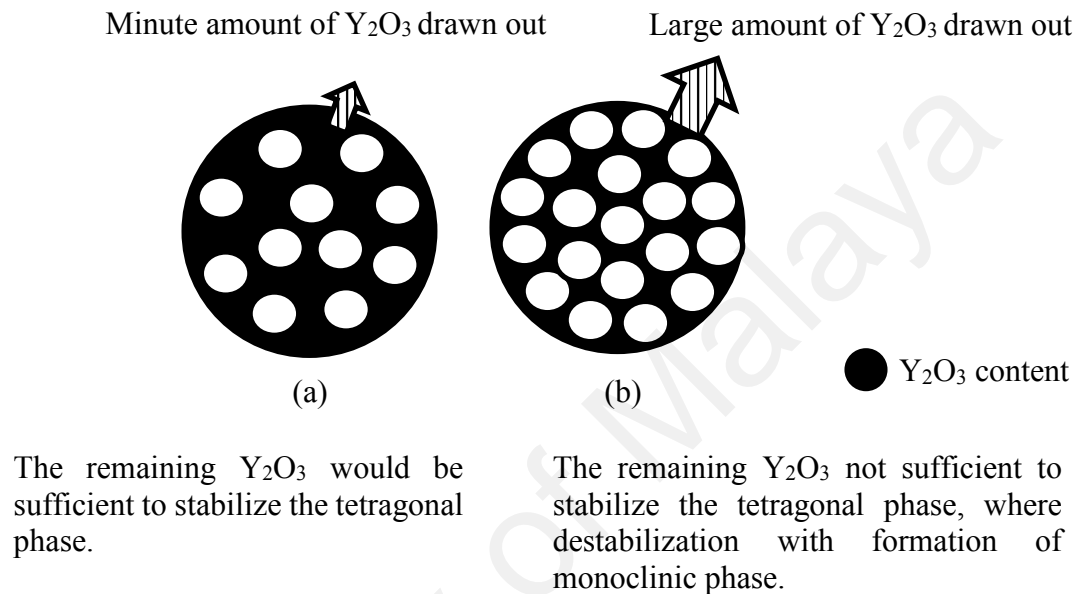


Figure 4.22: Schematic diagram on the stabilization and yttria content of CuO-doped Y-TZPs (a) with content ≤ 0.5 wt% (b) 1.0 wt%.

Figure 4.23 shows the EDS spectrums of CuO-doped Y-TZPs microwave sintered at 1100 °C. Since low CuO content could not be detected due to detection limit, the appearance of Cu could only be recorded for 0.5 wt% and 1 wt% CuO-doped Y-TZPs. The reference peaks for CuO-doped Y-TZPs samples with the respective energy (keV) are oxygen O $K\alpha$ (0.525), yttrium Y $L\alpha$ (1.922), zirconium Zr $L\alpha$ (2.042), and copper Cu $L\alpha$ (0.93). The detection of carbon (C $K\alpha$ 0.277) would be discovered due to carbon contamination in the chamber. In the present work, the EDS spectrum showed a reduction of yttrium concentration with the increase of CuO content in Y-TZPs. Besides, higher amount of oxygen was detected for 0.5 wt% and 1 wt% CuO-doped Y-TZP samples

which could signify the reaction between yttria and CuO. It is envisaged that the yttria could have drawn out and reacted with CuO at 1100 °C and led to destabilization, which had been discussed earlier.

In summary, the 0.2 wt% CuO-doped Y-TZPs achieved the highest density, Vickers hardness and fracture toughness among all the undoped and CuO-doped samples regardless of sintering temperatures via microwave sintering methods. Besides, the tetragonal stability of Y-TZP matrix was not disrupted with the addition of 0.2 wt% CuO. Therefore, the 0.2 wt% CuO-doped Y-TZP was believed to be in the metastable state as compared to undoped Y-TZP. In addition, a full density (relative density of 100%) was achieved by 0.2 wt% CuO-doped sample when microwave sintered at 1300 °C, with a remarkable Vickers hardness of 14.4 GPa and fracture toughness of 7.7 MPa.m^{1/2}. In contrast, undoped Y-TZP could only achieved comparable performance of 99.8% dense, Vickers hardness of 14.3 GPa and fracture toughness of about 6 MPa.m^{1/2} when microwave sintered at 1400 °C. In the next section, the densification behaviour of conventional sintering undoped Y-TZP and 0.2 wt% CuO-doped Y-TZP will be discussed.

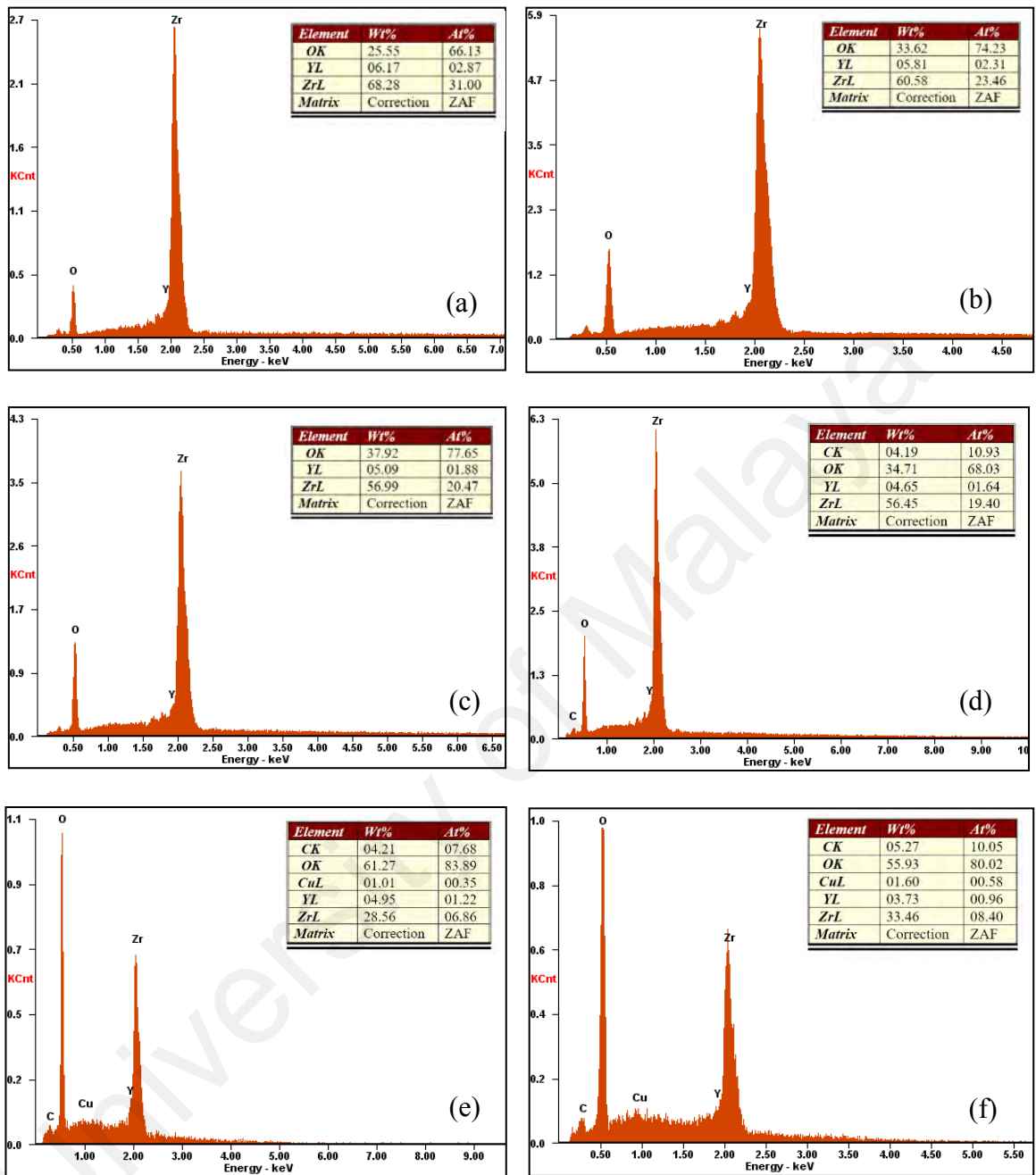


Figure 4.23: EDS Spectrum of microwave sintered Y-TZPs of different amounts of CuO that microwave sintered at 1100 °C (a) undoped, (b) 0.05 wt%, (d) 0.1 wt%, (d) 0.2 wt%, (e) 0.5 wt% and (f) 1 wt%.

4.4 Comparison between Conventional Sintering and Microwave Sintering

4.4.1 Densification Behaviour

The densification behaviour of the 0.2 wt% CuO and undoped Y-TZP was examined by conventional sintering method and compared with that obtained via microwave sintering method, as presented in Figure 4.24. As mentioned earlier for the microwave sintering, a relative density of 77.5% and 93.5% were obtained for the undoped samples when microwave sintered at 1100 °C and 1200 °C, respectively. These densities were remarkably high if compared to that reported by Mazaheri et al. (2008), who found that conventional sintered Y-TZP exhibited a low density of about 50% at 1100 °C, whereas a high temperature of 1350 °C was necessary to attain a relative density of more than 90%. According to several researchers, conventional sintering would require a high temperature of at least 1350 °C or higher to achieve a high density of 99% (Kumar et al., 2010; Palmeira et al., 2016; Rayón et al., 2013; Zhang et al., 2014).

In the present work, the beneficial effect of the microwave sintering in enhancing the densification of undoped Y-TZP has been revealed, particularly when sintered below 1300 °C. As shown in Figure 4.23, a relative density of 77.5% was recorded for the microwave sintered undoped Y-TZP at 1100 °C, whereas a higher sintering temperature of 1200 °C was required for conventional method to achieve an equivalent relative density. Likewise, microwave sintered undoped samples could reached a relative density of 93.5% at 1200 °C, whereas a higher temperature of 1250 °C was needed to accomplish similar performance by the conventional sintering method. The present results correlate with the results reported by Presenda et al. (2015), where samples that MW sintered at 1300 °C showed similar density with the conventional sintered samples at 1200 °C. In the present work, the effect of microwave sintering on densification of the undoped ceramic was not significant when sintered at 1300 °C and above. Both, the conventional and microwave sintered undoped samples attained 98.5% dense when sintered at 1300 °C,

before reaching 99.8% at 1400 °C. Similar observations were also reported by several researchers who compared the effect of microwave sintering and conventional sintering methods on the densification of Y-TZP at 1300 °C and above (Goldstein et al., 1999; Mazaheri et al., 2008; Zhao et al., 2000). This suggested that higher density could be achieved using microwave sintering techniques at relatively lower sintering temperatures with shorter sintering time below 1300 °C, whereas the effect of microwave sintering was not apparent at higher sintering temperature at 1300 °C and above.

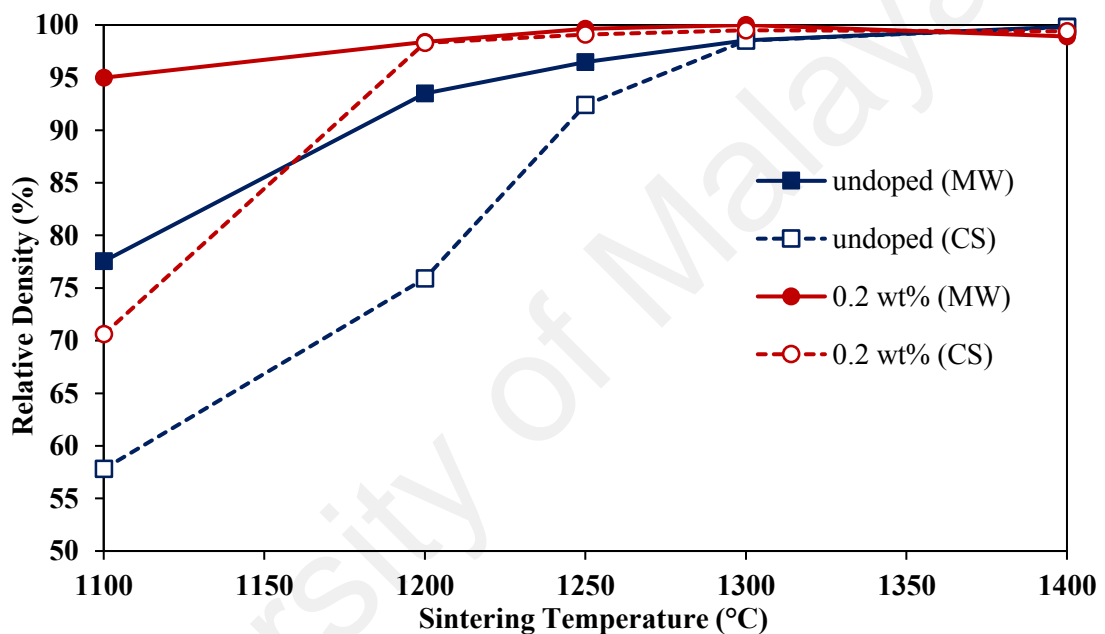


Figure 4.24: The effect of conventional sintering (CS) and microwave sintering (MW) on the relative density of the undoped and 0.2 wt% CuO-doped Y-TZPs.

In the case of 0.2 wt% CuO-doped Y-TZP, a different pattern was observed where similar densification of above 98% was recorded for samples sintered ≥ 1200 °C, regardless of sintering methods. This observation clearly shows that the density of Y-TZPs could be enhanced with the aid of 0.2 wt% CuO without microwave-assisted heating. Nevertheless, a significant enhancement in densification was evident for sample sintered at 1100 °C, i.e. the relative density was observed to increase from 70.6% (conventional sintering method) to 95% (microwave sintering method). This result is encouraging and suggested that CuO could have played a role to increase the overall

dielectric loss of the Y-TZP matrix at lower temperatures such as at 1100 °C, thus resulting in effective volumetric heating (Upadhyaya et al., 2001).

In brief, it could be observed that the effect of microwave sintering on 0.2 wt% CuO doped Y-TZPs is almost similar with conventional sintering when the samples reached the critical temperatures (≥ 1200 °C), which gave a high density beyond 98 %. This shows that the addition of 0.2 wt% CuO was beneficial without microwave-assisted heating beyond 1200 °C. However, microwave sintering is also a good alternative to increase densification of undoped Y-TZP at low temperatures, i.e. below 1300 °C.

4.4.2 Vickers Hardness and Fracture Toughness

Figure 4.25 presented the Vickers hardness of the undoped and 0.2 wt% CuO-doped Y-TZPs, which were sintered at different temperatures via microwave and conventional sintering methods. The microwave sintered undoped ceramic exhibited enhanced Vickers hardness at low temperature regime especially below 1300 °C, if compared to conventional sintered undoped samples. For instance, microwave sintered Y-TZPs recorded a Vickers hardness of about 9.8 GPa at 1200 °C, while a similar hardness could only be achieved at a higher sintering temperature of 1250 °C via conventional sintering method. At 1300 °C, microwave sintered undoped samples achieved a hardness of about 14 GPa, whereas conventional sintered samples yielded lower hardness of 13.5 GPa. These results coincided with the hardness reported by Presenda et al. (2015), where microwave sintered Y-TZP exhibited a greater hardness of about 14 GPa, as opposed to sample that was conventional sintered at 1300 °C (13 GPa).

In the present work, sintering at 1400 °C was necessary for undoped Y-TZP to attain high Vickers hardness of 14.3 GPa, regardless of sintering techniques employed. This is in agreement with Goldstein et al. (1999), where similar hardness of approximately 14.4 GPa and relative density of about 99% were obtained for 3 mol% Y-TZP when

sintered at 1350 °C for both conventional and microwave sintering methods. Likewise, several researchers had also reported similar hardness obtained via microwave and conventional sintering at the same temperatures, as summarized in Table 4.2 (Goldstein et al., 1999; Kumar et al., 2010; Sujith et al., 2009; Zhao et al., 2000). In a recent study, a higher Vickers hardness was obtained with microwave sintered at 1300 °C as compared with conventional sintered at 1400 °C (Presenda et al., 2017).

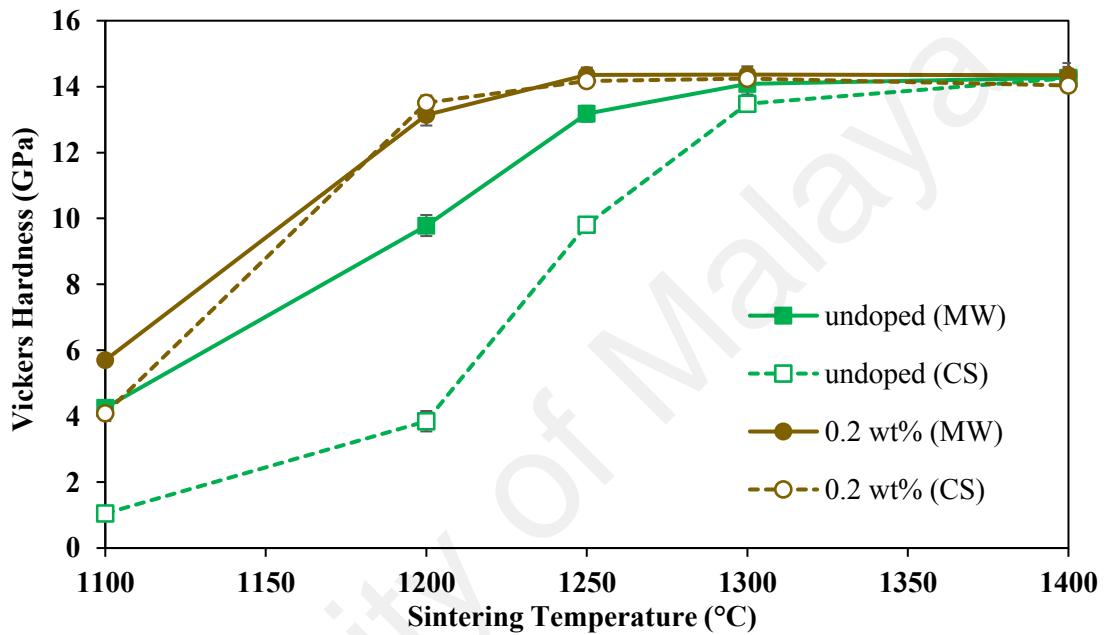


Figure 4.25: The effect of conventional sintering (CS) and microwave sintering (MW) on the Vickers hardness of the undoped and 0.2 wt% CuO-doped Y-TZPs.

In the case of 0.2 wt% CuO-doped Y-TZPs, the Vickers hardness exhibited a similar trend with the density trend. Both conventional and microwave sintered 0.2 wt% CuO-doped Y-TZPs attained similar Vickers hardness throughout the sintering regime, particularly at above 1200 °C. This is in good agreement with the results reported by Ai et al. (2015), where they found that Al₂O₃-doped Y-TZP yielded a similar hardness of approximately 12 GPa when conventional or microwave sintered at 1500 °C. In this work, sintering at 1250 °C and above could obtain high hardness of above 14 GPa, regardless of sintering techniques. At 1250 °C and 1300 °C, microwave sintered 0.2 wt% CuO-doped Y-TZPs achieved an optimum hardness of 14.4 GPa. In brief, the addition of 0.2

wt% CuO enhanced the hardness of Y-TZP without the needs for microwave sintering. In contrast, the microwave heating was necessary to achieve higher Vickers hardness for undoped Y-TZPs.

Table 4.2: Summary of Vickers hardness of Y-TZP ceramics sintered at different temperatures.

Reference	Sintering Method	Sintering Temperature (°C)	Vickers Hardness (GPa)
(Goldstein et al., 1999)	Conventional	1350	14.4
	Microwave	1350	14.5
(Zhao et al., 2000)	Conventional	1450	12.4
	Microwave	1450	12.4
(Sujith et al., 2009)	Conventional	1500	13.5
	Microwave	1460	13.5
(Kumar et al., 2010).	Conventional	1400	11-12
	Microwave	1400	11-12
(Presenda et al., 2017)	Conventional	1400	13.9
	Microwave	1300	14.7

Figure 4.26 shows the fracture toughness of undoped and 0.2 wt% CuO-doped Y-TZPs at different sintering temperatures. In general, the fracture toughness values were recorded between 5 MPa.m^{1/2} to 8 MPa.m^{1/2} when sintered between 1250 °C and 1400 °C. The 0.2 wt% CuO-doped Y-TZPs exhibited higher fracture toughness values if compared with undoped Y-TZPs, regardless of sintering method. There was some improvement in fracture toughness for 0.2 wt% CuO-doped Y-TZPs due to the metastable state as compared to undoped ceramic as discussed earlier.

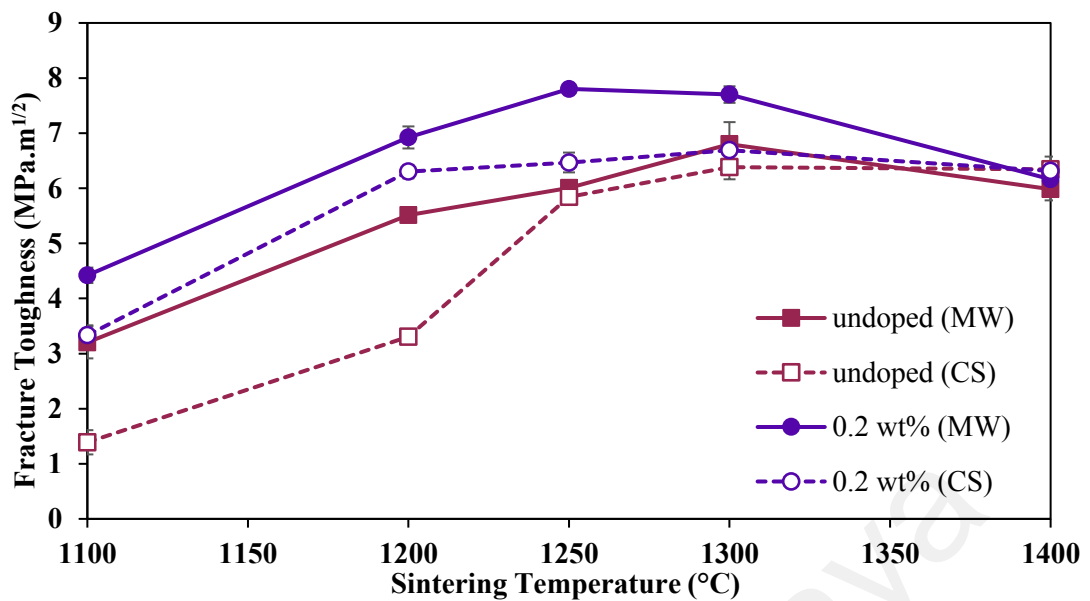


Figure 4.26: The effect of conventional sintering (CS) and microwave sintering (MW) on the Fracture toughness of the undoped and 0.2 wt% CuO-doped Y-TZPs.

4.4.3 Microstructure and Grain Size

Figure 4.27 illustrates the FE-SEM micrographs of conventional and microwave sintered undoped Y-TZPs at different sintering temperatures. It was apparent that conventional sintered undoped samples at 1100 °C was insufficient to eliminate residual porosity, whereas microwave sintered sample at the equivalent temperature showed denser microstructure. There was no substantial difference in the grain size between conventional and microwave sintered samples at above 1200 °C. A grain size of about 0.2 μm was recorded for the undoped Y-TZPs when sintered at 1300 °C, before increased to about 0.26 μm at 1400 °C. This is in accordance with the findings reported by Reidy et al. (2011) who found that 3 mol% Y-TZP samples sintered at 1300 °C with a heating rate of about 16 °C/min. They reported a similar grain size of about 0.2 μm for conventional and microwave sintering method. The similarities of grain size were also observed by Mazaheri et al. (2008), with conventional and microwave sintering Y-TZPs at 1500 °C with a heating rate of 5 °C/min. In this work, the addition of 0.2 wt% CuO in Y-TZP matrix showed similar equiaxed microstructure throughout the sintering

temperatures as depicted in Figure 4.28. Likewise, there was no significant difference in the grain size for both sintering methods.

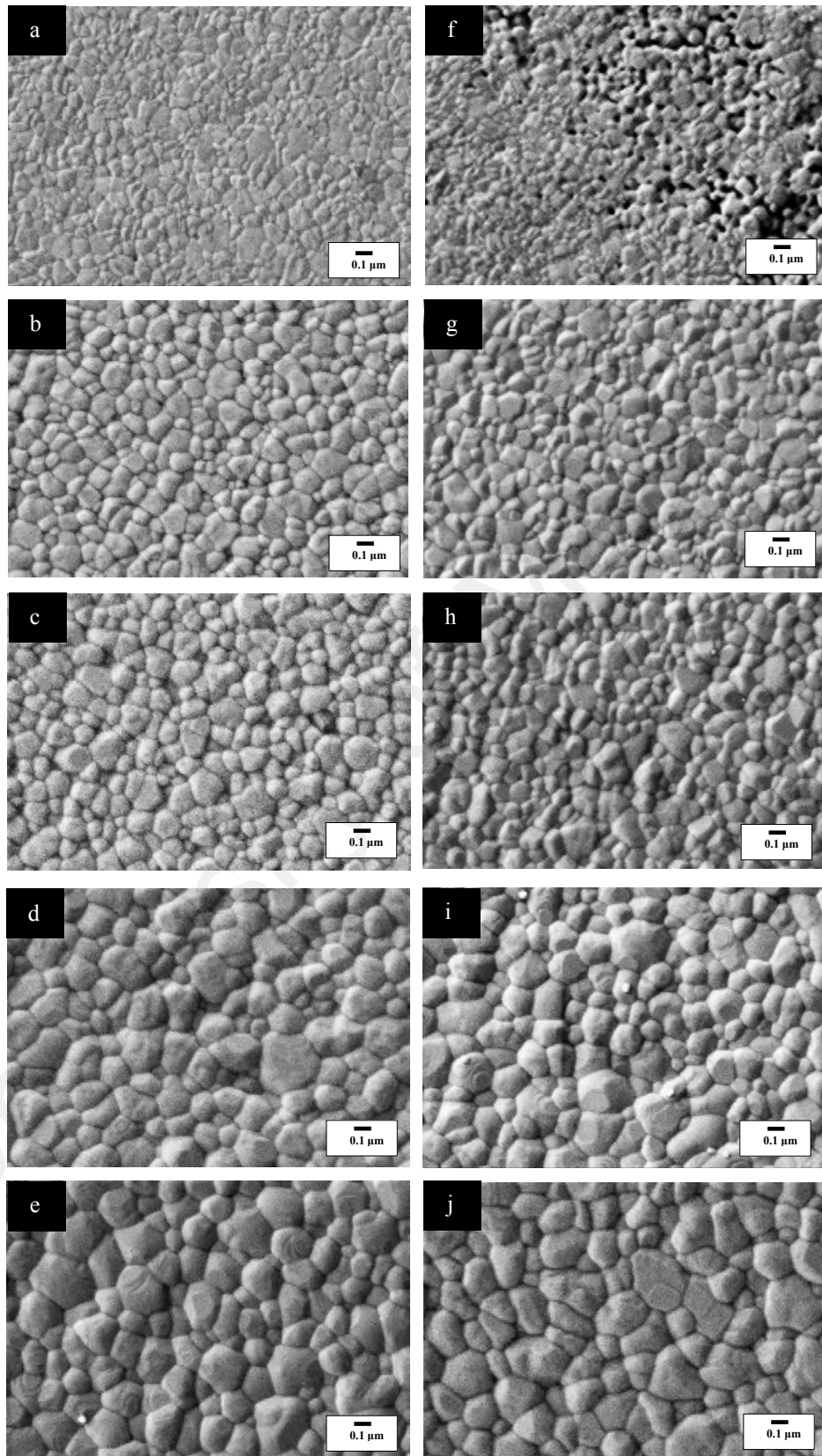


Figure 4.27: FE-SEM micrographs of undoped Y-TZPs sintered via: microwave sintering (a) 1100 °C, (a) 1200 °C, (c) 1250 °C, (d) 1300 °C, (e) 1400 °C and conventional sintering (f) 1100 °C, (g) 1200 °C, (h) 1250 °C, (i) 1300 °C, (j) 1400 °C.

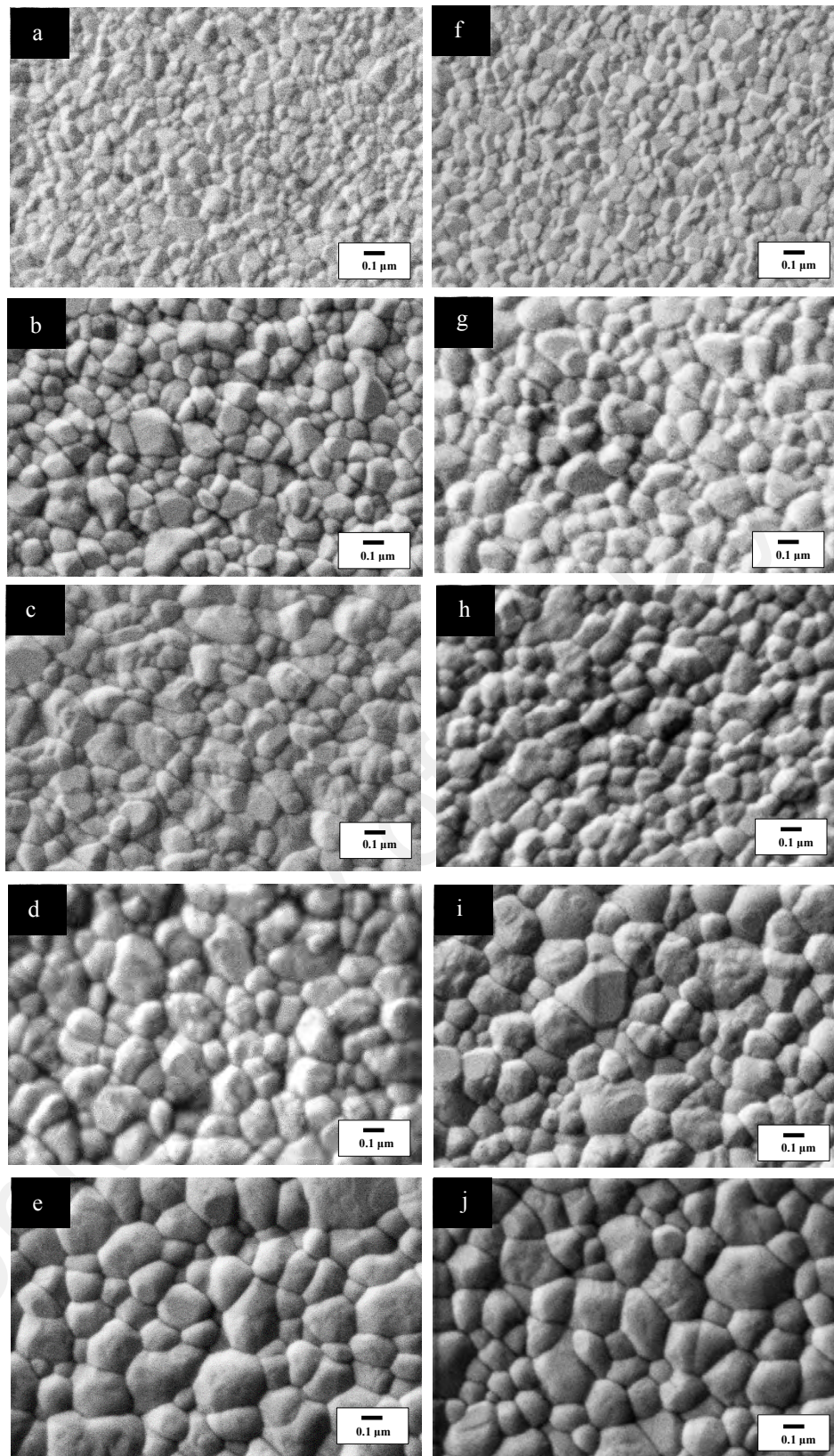


Figure 4.28: FE-SEM micrographs of 0.2 wt% CuO-doped Y-TZPs sintered via: microwave sintering (a) 1100 °C, (a) 1200 °C, (c) 1250 °C, (d) 1300 °C, (e) 1400 °C and conventional sintering (f) 1100 °C, (g) 1200 °C, (h) 1250 °C, (i) 1300 °C, (j) 1400 °C.

Figure 4.29 shows a comparison in grain size between conventional and microwave sintered samples at different temperatures. The use of microwave sintering for undoped and 0.2 wt% CuO-doped Y-TZPs resulted in a similar grain size as compared to conventional samples. Besides, the addition of small amounts of CuO up to 0.2 wt% did not dramatically affected the grain size of the Y-TZPs, as mentioned in the previous section. A summary of grain size reported by several authors is presented in Table 4.3 based on different heating conditions. The present observations concurred with the results of Reidy et al. (2011) who found that microwave sintered Y-TZPs exhibited a grain size of 200 nm, which is similar with conventional sintered samples (192 nm), with the exact same heating profile at 1300 °C.

However, the present results were not in agreement with the findings of several researchers, who observed the reduction of grain size using microwave sintering techniques. For further clarification, several authors had microwave sintered samples at different heating rates. For instance, Charmond et al. (2010) reported a finer grain size of 0.13-0.18 μm via microwave sintering 2 mol% Y-TZPs at a heating rate of 250 °C/min, as opposed to 0.22 μm recorded by microwave sintering methods at a lower heating rate. Mazaheri et al. (2008) also identified that microwave sintered 8 mol% yttria stabilized zirconia with a heating rate of 50 °C/min yielded a smaller grain size of 0.9 μm . In contrast, a heating rate of 5 °C/min would induce larger grain size exceeded 2 μm regardless of the sintering methods employed. Based on the literature, it was observed that high heating rates difference between conventional and microwave (~10 times difference) could suppress grain growth and resulted in finer microstructure during microwave sintering.

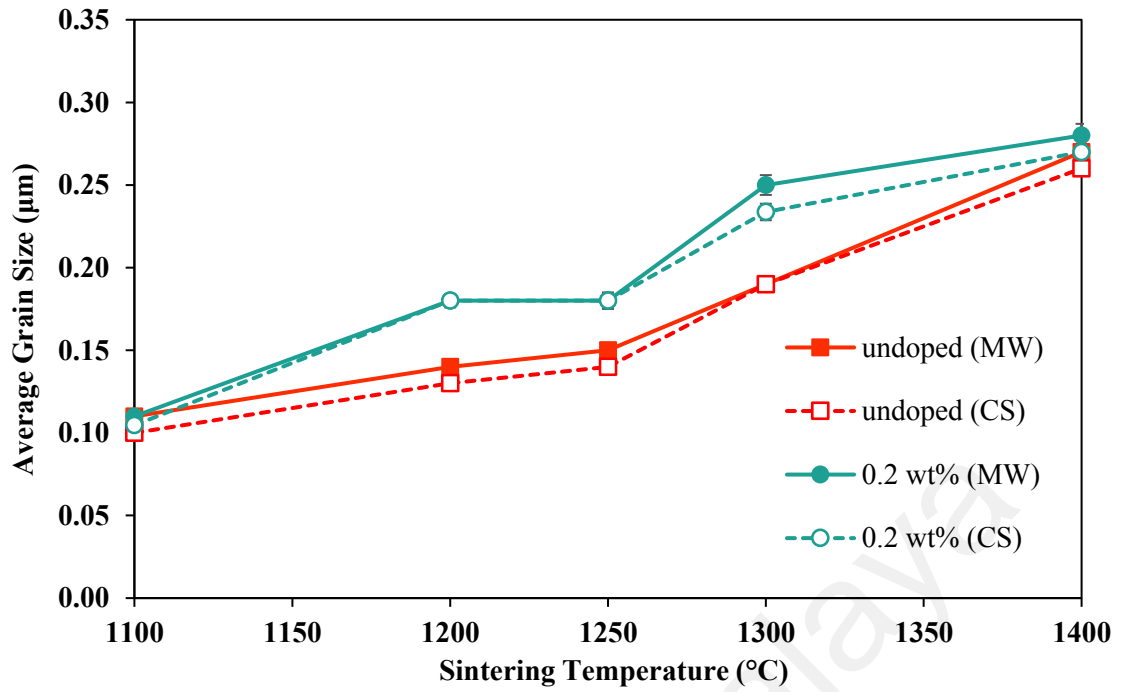


Figure 4.29: Effect of conventional and microwave sintering on the grain size of undoped and 0.2 wt% CuO-doped Y-TZPs at different sintering temperatures.

Table 4.3: Summary of grain size for conventional and microwave sintered Y-TZPs at different sintering temperatures and heating rate.

Reference	Samples	Sintering Method	Sintering Temperature (°C)	Heating Rate (°C/min)	Grain Size (µm)
(Reidy et al., 2011)	3Y-TZP	Conventional	1300	16	0.19
		Microwave	1300	16	0.20
(Presenda et al., 2015)	3Y-TZP	Conventional	1300	10	0.20
		Microwave	1300	100	0.19
(Charmond et al., 2010)	2Y-TZP	Conventional	1360	25	0.22
		Microwave	1340	25	0.21-0.23
		Microwave	1225	250	0.13-0.18
(Kumar et al., 2010)	3Y-TZP	Conventional	1400	10	0.21
		Microwave	1400	100	0.17
(Borrell et al., 2013)	3Y-TZP	Conventional	1400	5	0.27
		Microwave	1400	25	0.22

The grain size as a function of relative density is shown in Figure 4.30. It was observed that the conventional sintered samples generally exhibited larger grain size than microwave sintered samples until the relative density reached about 96%. Thereafter, grain growth predominated densification regardless of sintering method. In contrast, microwave sintered samples generally had finer grain size but higher density due to the higher heating rate of microwave heating. However, the results showed that sintering temperature was the key parameter governing grain growth for densities above 96%. These results are in good agreement with that reported by Borrell et al. (2013), where the authors suggested that high heating rates of microwave had postponed the grain boundary activation energy. They explained that the absorbed energy during microwave heating had contributed to densification rather than grain growth.

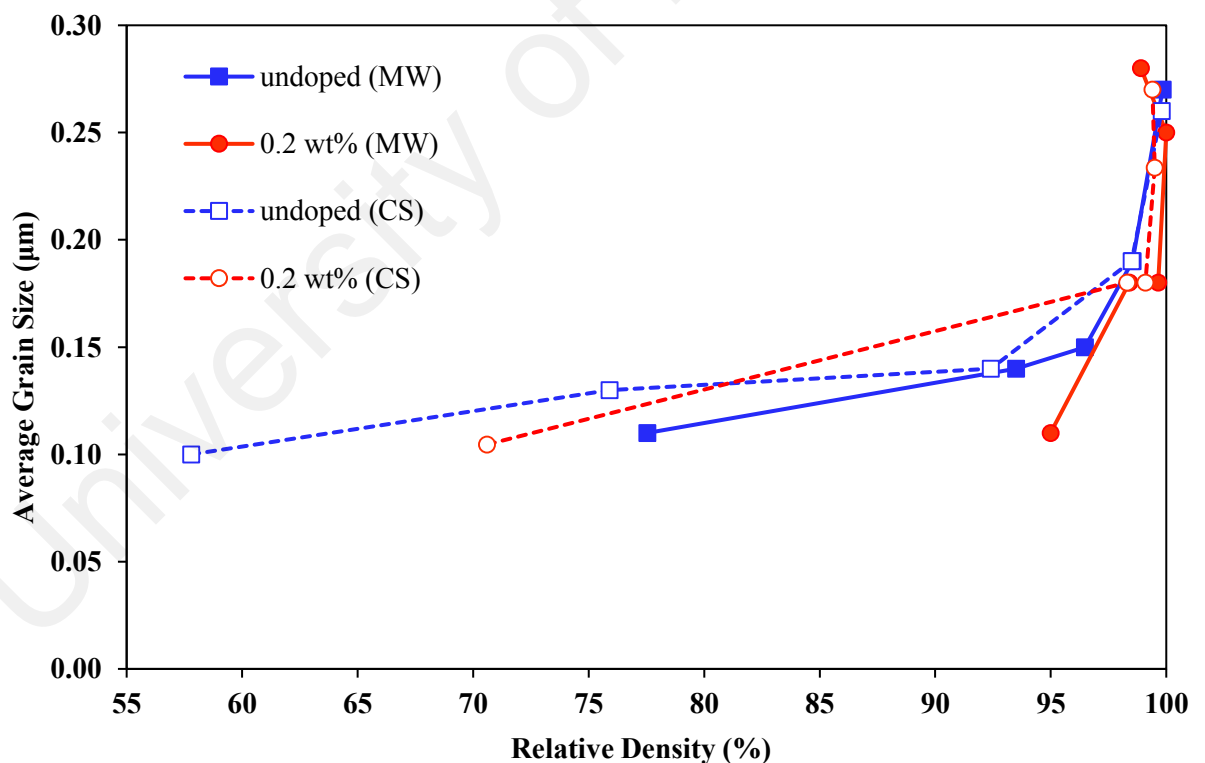


Figure 4.30: Effect of conventional and microwave sintering on the grain size and density of undoped and 0.2 wt% CuO-doped Y-TZPs.

It is believed that this behaviour was due to the difference sintering mechanism for densification. Conventional sintering transferred heat via traditional heat transfer mode

of conduction where the surface was heated earlier than the core of the samples, which consumed longer time and delayed the activation of densification mechanism. Conversely, microwave heating utilized electromagnetic field to induce molecular interactions within the sample which resulted in volumetric heating of the entire body of the samples. Several researchers had also elaborated that microwave sintering accelerated the lattice diffusion/volume diffusion, rather than grain boundary and surface diffusion, which contributed on the densification instead of grain coarsening during the preliminary stage of sintering (Demirskyi et al., 2013; Nightingale et al., 1996). This had also elucidated the earlier densification observed in the previous section, where microwave sintered undoped samples contributed to higher density as compared to the conventional sintered samples, especially below 1300 °C.

The use of Y-TZPs in implant surgery applications must meet the requirement for of ISO 13356 and ASTM standard F1873, where the chemical composition if Y-TZP must be ≥ 99 wt%, bulk density ≥ 6.00 g/cm³, grain size ≤ 0.6 μ m, Vickers hardness > 11.77 GPa (Haraguchi et al., 2001). Also, according to ISO 6872 standards, fracture toughness must be ≥ 5.0 MPa.m^{1/2} for dental ceramics for restoration and prostheses application (Miragaya et al., 2017). In the current research, the 0.2 wt% CuO-doped Y-TZPs which sintered via microwave or conventional sintering methods above 1200 °C had met the requirements for dental and surgical applications.

4.4.4 Low Temperature Degradation

Grain size is an essential parameter of phase transformation, where grains smaller than a critical size did not undergo phase transformation due to lack of transformation nuclei (Rauchs et al., 2002). In the present research, hydrothermal ageing was done at 180 °C/10 bar up to 200 h for undoped and 0.2 wt% CuO doped Y-TZPs, for conventional and microwave sintered samples. There was no monoclinic phase detected for both undoped

and 0.2 wt% CuO-doped Y-TZPs after ageing for 200 h, regardless of sintering methods, with sintering temperature up to 1400 °C. Figure 4.31 and Figure 4.32 show the XRD traces of undoped and 0.2 wt% CuO-doped Y-TZPs respectively, where tetragonal phase was the only phase detected when sintered at 1400 °C via conventional or microwave method. Besides, no sign of surface spalling or crack was found for all samples as shown in Figure 4.33.

The LTD resistance of undoped and 0.2 wt% CuO-doped Y-TZPs is envisaged to be owing to the small grain size obtained, which the size is lower than 0.28 µm. Therefore, it can be deduced that grain size smaller than 0.28 µm did not undergo phase transformation after ageing. In a study, Denry et al. (2010) reported that small grain size of 3 mol% Y-TZP (0.23 µm) led to negligible amount of monoclinic phase (1%) after ageing in steam at 134 °C/2 bar for 10 h, while larger grain size (0.32 µm) led to 1.7% of monoclinic phase. They also found that samples were susceptible to ageing with monoclinic phase more than 10% when the grain size increased to 0.61 µm. Ruiz and Readey (1996) had also reported that when the grain size reached about 1 µm, the 3Y-TZP was susceptible to *t-m* transformation. With the supported literature, the grain size is therefore suggested as the key factor in determining the LTD behaviour of zirconia. In the present work, undoped and 0.2 wt% CuO-doped Y-TZPs with the grain size of 0.28 µm or below was LTD resistance after exposure at 180 °C/10 bar up to 200 h.

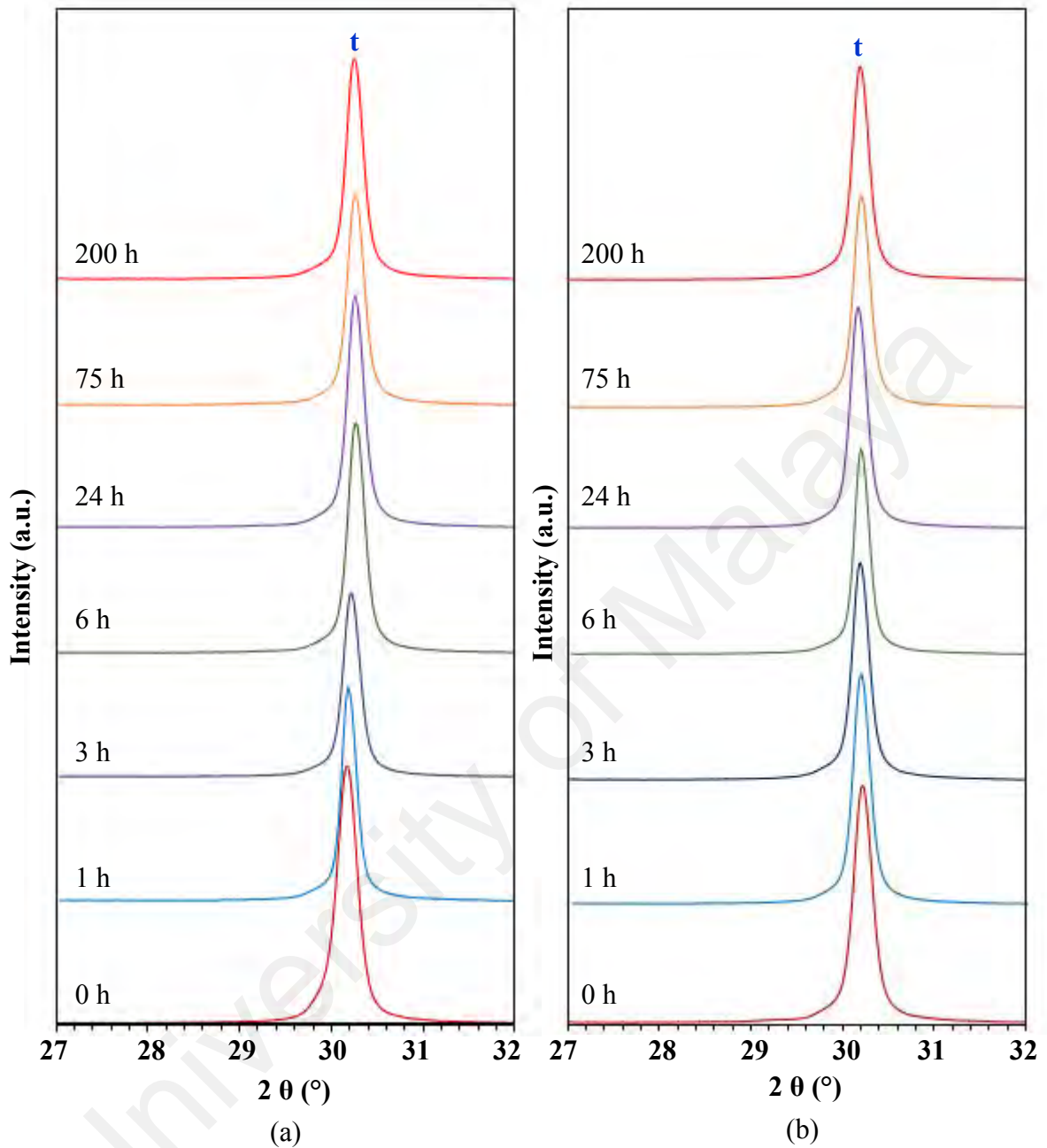


Figure 4.31: XRD traces of undoped Y-TZPs sintered at 1400 °C via (a) conventional sintering, (b) microwave sintering, after exposure in superheated steam at 180 °C/10 bar up to 200 h. Key: t-tetragonal phase.

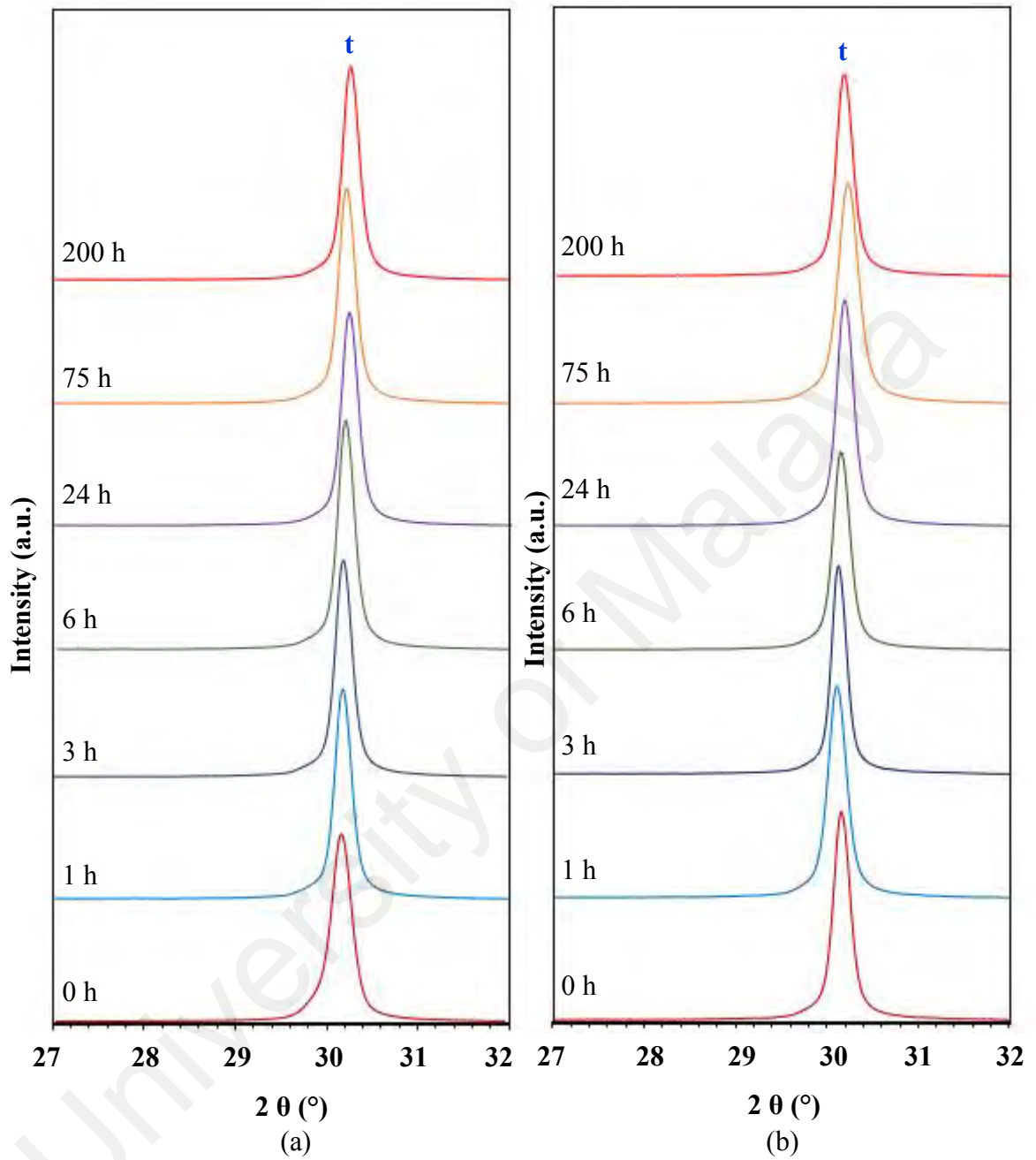
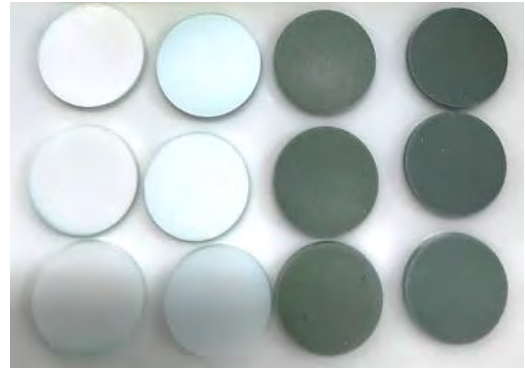


Figure 4.32: XRD traces of 0.2 wt% CuO-doped Y-TZPs sintered at 1400 °C via (a) conventional sintering, (b) microwave sintering, after exposure in superheated steam at 180 °C/10 bar up to 200 h. Key: t-tetragonal phase.



(a)



(b)

Figure 4.33: Surface observation of several samples (a) before ageing and (b) after ageing for 200 h, where the white samples are undoped Y-TZPs and dark grey samples are 0.2 wt% CuO-doped Y-TZPs.

University of Malaya

CHAPTER 5: CONCLUSIONS AND FUTURE WORK

5.1 Conclusions

In conclusion, all four objectives had been achieved. According to the first objective, the optimum microwave sintering parameters had been optimized with pre-sintering of green samples at 600 °C at 10 °C/min for 2 hours prior to microwave sintering to produce crack-free sintered samples. Microwave sintering of CuO-doped Y-TZPs could be successfully conducted at a heating rate of 30 °C/min with the assistance of two susceptors enclosed in an alumina fiberboard housing. In the case of the second objective, low amounts of CuO up to 0.4 wt% was beneficial in enhancing densification of Y-TZPs. In particular, the 0.2 wt% CuO-doped Y-TZP achieved a relative density of $\geq 99.8\%$ at 1250 °C and 1300 °C, as compared with undoped sample at 1300°C (98.5%). The 0.2 wt% CuO-doped Y-TZP showed a remarkable high Vickers hardness (>14 GPa) and high fracture toughness (> 6.5 MPa.m^{1/2}) when sintered above 1200 °C. In contrast, 1 wt% CuO-doped Y-TZP yielded the lowest density, Vickers hardness and fracture toughness among all the samples, which could be attributed to the high monoclinic phase present and ill-formed microstructure from FE-SEM micrographs. For the third objective, it was revealed that the addition of 0.2 wt% CuO was most effective as a sintering aid for Y-TZP especially in the case for conventional sintering at temperatures above 1200 °C, where the samples exhibited almost identical density and Vickers hardness when sintered by microwave method. However, for sintering $\geq 1250^\circ\text{C}$, the samples attained a high density of 99% and Vickers hardness of more than 14 GPa, regardless of sintering methods used. For the final objective, it was found that, regardless of sintering methods, there was no monoclinic phase detected for both undoped and 0.2 wt% CuO-doped Y-TZP after exposure to superheated steam at 180 °C/10 bar up to 200 h. The improved hydrothermal ageing resistance of the Y-TZPs was attributed mainly to the small grain size of sintered body, below 0.28 μm .

5.2 Future Work

The following are some suggestions for future extension of work:

1. A transmission electron microscopy (TEM) study could be done on the CuO-doped Y-TZP to understand the effect of CuO on the densification of zirconia.
2. Other sintering methods such as spark plasma sintering could be employed to evaluate the mechanical properties and low temperature degradation behaviour of CuO-doped Y-TZPs.
3. The incorporation of other sintering additives such as iron oxide in Y-TZPs could be considered for microwave sintering to improve the dielectric properties of the ceramic and promote sintering.

University of Malaysia

REFERENCES

- Abd El-Ghany, O. S., & Sherief, A. H. (2016). Zirconia based ceramics, some clinical and biological aspects: Review. *Future Dental Journal*, 2(2), 55-64.
- Ai, D., & Kang, S. (2004). Synthesis of 3Y-ZrO₂ nano-powders via a W/O emulsion. *Ceramics International*, 30(4), 619-623.
- Ai, Y., Xie, X., He, W., Liang, B., & Fan, Y. (2015). Microstructure and properties of Al₂O₃(n)/ZrO₂ dental ceramics prepared by two-step microwave sintering. *Materials & Design*, 65, 1021-1027.
- Almazdi, A. A., Khajah, H. M., Monaco Jr, E. A., & Kim, H. (2012). Applying microwave technology to sintering dental zirconia. *The Journal of Prosthetic Dentistry*, 108(5), 304-309.
- Ban, S., Sato, H., Suehiro, Y., Nakanishi, H., & Nawa, M. (2008). Biaxial flexure strength and low temperature degradation of Ce-TZP/Al₂O₃ nanocomposite and Y-TZP as dental restoratives. *Journal of Biomedical Materials Research Part B: Applied Biomaterials*, 87B(2), 492-498.
- Basu, B., Lee, J., & Kim, D. (2004). Development of Nanocrystalline Wear-Resistant Y-TZP Ceramics. *Journal of the American Ceramic Society*, 87(9), 1771-1774.
- Bhattacharya, M., & Basak, T. (2016). A review on the susceptor assisted microwave processing of materials. *Energy*, 97, 306-338.
- Binner, J., Annapoorani, K., Paul, A., Santacruz, I., & Vaidhyanathan, B. (2008). Dense nanostructured zirconia by two stage conventional/hybrid microwave sintering. *Journal of the European Ceramic Society*, 28(5), 973-977.
- Binner, J., Vaidhyanathan, B., Paul, A., Annapoorani, K., & Raghupathy, B. (2011). Compositional Effects in Nanostructured Yttria Partially Stabilized Zirconia. *International Journal of Applied Ceramic Technology*, 8(4), 766-782.
- Borchers, L., Stiesch, M., Bach, F., Buhl, J., Hübsch, C., Kellner, T.,... (2010). Influence of hydrothermal and mechanical conditions on the strength of zirconia. *Acta Biomaterialia*, 6(12), 4547-4552.
- Borrell, A., Salvador, M. D., Peñaranda-Foix, F. L., & Cátala-Civera, J. M. (2013). Microwave Sintering of Zirconia Materials: Mechanical and Microstructural Properties. *International Journal of Applied Ceramic Technology*, 10(2), 313-320.
- Borrell, A., Salvador, M. D., Rayón, E., & Peñaranda-Foix, F. L. (2012). Improvement of microstructural properties of 3Y-TZP materials by conventional and non-conventional sintering techniques. *Ceramics International*, 38(1), 39-43.
- Bowen, C., Ramesh, S., Gill, C., & Lawson, S. (1998). Impedance spectroscopy of CuO-doped Y-TZP ceramics. *Journal of Materials Science*, 33(21), 5103-5110.

- Bravo-Leon, A., Morikawa, Y., Kawahara, M., & Mayo, M. J. (2002). Fracture toughness of nanocrystalline tetragonal zirconia with low yttria content. *Acta Materialia*, 50(18), 4555-4562.
- Camposilvan, E., Leone, R., Gremillard, L., Sorrentino, R., Zarone, F., Ferrari, M.,... (2018). Aging resistance, mechanical properties and translucency of different yttria-stabilized zirconia ceramics for monolithic dental crown applications. *Dental Materials*, 34(6), 879-890.
- Cattani-Lorente, M., Scherrer, S. S., Ammann, P., Jobin, M., & Wiskott, H. W. A. (2011). Low temperature degradation of a Y-TZP dental ceramic. *Acta Biomaterialia*, 7(2), 858-865.
- Chandrasekaran, S., Ramanathan, S., & Basak, T. (2012). Microwave material processing—a review. *AIChE Journal*, 58(2), 330-363.
- Charles, M., Tony, Z., & A., O. E. (2017). Fully coupled electromagnetic-thermal-mechanical comparative simulation of direct vs hybrid microwave sintering of 3Y-ZrO₂. *Journal of the American Ceramic Society*, 100(6), 2439-2450.
- Charmond, S., Carry, C. P., & Bouvard, D. (2010). Densification and microstructure evolution of Y-Tetragonal Zirconia Polycrystal powder during direct and hybrid microwave sintering in a single-mode cavity. *Journal of the European Ceramic Society*, 30(6), 1211-1221.
- Chen, I. W., & Wang, X. H. (2000). Sintering dense nanocrystalline ceramics without final-stage grain growth. *Nature*, 404(6774), 168-171.
- Chen, S., & Lu, H. (1989). Low-temperature ageing map for 3mol% Y₂O₃-ZrO₂. *Journal of Materials Science*, 24(2), 453-456.
- Chevalier, J. (2006). What future for zirconia as a biomaterial? *Biomaterials*, 27(4), 535-543.
- Chevalier, J., Deville, S., Munch, E., Jullian, R., & Lair, F. (2004). Critical effect of cubic phase on aging in 3 mol% yttria-stabilized zirconia ceramics for hip replacement prosthesis. *Biomaterials*, 25(24), 5539-5545.
- Chevalier, J., & Gremillard, L. (2009). Ceramics for medical applications: A picture for the next 20 years. *Journal of the European Ceramic Society*, 29(7), 1245-1255.
- Chevalier, J., Gremillard, L., Virkar, A. V., & Clarke, D. R. (2009). The Tetragonal-Monoclinic Transformation in Zirconia: Lessons Learned and Future Trends. *Journal of the American Ceramic Society*, 92(9), 1901-1920.
- Chowdhury, S., Vohra, Y. K., Lemons, J. E., Ueno, M., & Ikeda, J. (2007). Accelerating aging of zirconia femoral head implants: Change of surface structure and mechanical properties. *Journal of Biomedical Materials Research Part B: Applied Biomaterials*, 81B(2), 486-492.

- Ćorić, D., Majić Renjo, M., & Ćurković, L. (2017). Vickers indentation fracture toughness of Y-TZP dental ceramics. *International Journal of Refractory Metals and Hard Materials*, 64, 14-19.
- Cotes, C., Arata, A., Melo, R. M., Bottino, M. A., Machado, J. P. B., & Souza, R. O. A. (2014). Effects of aging procedures on the topographic surface, structural stability, and mechanical strength of a ZrO₂-based dental ceramic. *Dental Materials*, 30(12), e396-e404.
- Cutler, R. A., Reynolds, J. R., & Jones, A. (1992). Sintering and Characterization of Polycrystalline Monoclinic, Tetragonal, and Cubic Zirconia. *Journal of the American Ceramic Society*, 75(8), 2173-2183.
- Das, S., Mukhopadhyay, A. K., Datta, S., & Basu, D. (2008). Prospects of microwave processing: An overview. *Bulletin of Materials Science*, 31(7), 943–956.
- Demirskiyi, D., Agrawal, D., & Ragulya, A. (2013). Comparisons of grain size-density trajectory during microwave and conventional sintering of titanium nitride. *Journal of Alloys and Compounds*, 581, 498-501.
- Denry, I., & Kelly, J. R. (2008). State of the art of zirconia for dental applications. *Dental Materials*, 24(3), 299-307.
- Denry, I. L., Peacock, J. J., & Holloway, J. A. (2010). Effect of heat treatment after accelerated aging on phase transformation in 3Y-TZP. *Journal of Biomedical Materials Research Part B: Applied Biomaterials*, 93B(1), 236-243.
- Deville, S., Chevalier, J., Fantozzi, G., Bartolomé, J. F., Requena, J. n., Moya, J. S.,... (2003). Low-temperature ageing of zirconia-toughened alumina ceramics and its implication in biomedical implants. *Journal of the European Ceramic Society*, 23(15), 2975-2982.
- Deville, S., Gremillard, L., Chevalier, J., & Fantozzi, G. (2005). A critical comparison of methods for the determination of the aging sensitivity in biomedical grade yttria-stabilized zirconia. *Journal of Biomedical Materials Research Part B: Applied Biomaterials*, 72B(2), 239-245.
- Evan, P., Yuval, C., Amikam, B., Tayo, O., David, G., Jeff, C.,... (2001). Temperature Measurements during Microwave Processing: The Significance of Thermocouple Effects. *Journal of the American Ceramic Society*, 84(9), 1981-1986.
- Flinn, B. D., deGroot, D. A., Mancl, L. A., & Raigrodski, A. J. (2012). Accelerated aging characteristics of three yttria-stabilized tetragonal zirconia polycrystalline dental materials. *The Journal of Prosthetic Dentistry*, 108(4), 223-230.
- Flinn, B. D., Raigrodski, A. J., Singh, A., & Mancl, L. A. (2014). Effect of hydrothermal degradation on three types of zirconias for dental application. *The Journal of Prosthetic Dentistry*, 112(6), 1377-1384.
- Ghatee, M., & Irvine, J. T. S. (2010). Investigation of electrical and mechanical properties of tetragonal/cubic zirconia composite electrolytes prepared through stabilizer coating method. *International Journal of Hydrogen Energy*, 35(17), 9427-9433.

- Goldstein, A., Travitzky, N., Singurindy, A., & Kravchik, M. (1999). Direct microwave sintering of yttria-stabilized zirconia at 2.45 GHz. *Journal of the European Ceramic Society*, 19(12), 2067-2072.
- Gremillard, L., Chevalier, J., Epicier, T., & Fantozzi, G. (2002). Improving the Durability of a Biomedical-Grade Zirconia Ceramic by the Addition of Silica. *Journal of the American Ceramic Society*, 85(2), 401-407.
- Gremillard, L., Martin, L., Zych, L., Crosnier, E., Chevalier, J., Charbouillot, A.,... (2013). Combining ageing and wear to assess the durability of zirconia-based ceramic heads for total hip arthroplasty. *Acta Biomaterialia*, 9(7), 7545-7555.
- Hallmann, L., Ulmer, P., Reusser, E., Louvel, M., & Hämmerle, C. H. F. (2012). Effect of dopants and sintering temperature on microstructure and low temperature degradation of dental Y-TZP-zirconia. *Journal of the European Ceramic Society*, 32(16), 4091-4104.
- Harada, K., Shinya, A., Gomi, H., Hatano, Y., Shinya, A., & Raigrodski, A. J. (2016). Effect of accelerated aging on the fracture toughness of zirconias. *The Journal of Prosthetic Dentistry*, 115(2), 215-223.
- Haraguchi, K., Sugano, N., Nishii, T., Miki, H., Oka, K., & Yoshikawa, H. (2001). Phase transformation of a zirconia ceramic head after total hip arthroplasty. *The Journal of Bone and Joint Surgery*, 83-B(7), 996-1000.
- Holz, L., Macias, J., Vitorino, N., Fernandes, A. J. S., Costa, F. M., & Almeida, M. M. (2018). Effect of Fe₂O₃ doping on colour and mechanical properties of Y-TZP ceramics. *Ceramics International*.
- Hwang, C. M. J. C., I.W. (1990). Effect of a liquid phase on superplasticity of 2-mol%-Y₂O₃-stabilized tetragonal zirconia polycrystals. *Journal of the American Ceramic Society*, 73(6), 1626-1632.
- Inokoshi, M., Zhang, F., De Munck, J., Minakuchi, S., Naert, I., Vleugels, J.,... (2014). Influence of sintering conditions on low-temperature degradation of dental zirconia. *Dental Materials*, 30(6), 669-678.
- Janney, M. A., Calhoun, C. L., & Kimrey, H. D. (1992). Microwave Sintering of Solid Oxide Fuel Cell Materials: I, Zirconia-8 mol% Yttria. *Journal of the American Ceramic Society*, 75(2), 341-346.
- Kalousek, R., Spousta, J., Zlámal, J., Dub, P., Šikola, T., Shen, Z.,... (2017). Rapid heating of zirconia nanoparticle-powder compacts by infrared radiation heat transfer. *Journal of the European Ceramic Society*, 37(3), 1067-1072.
- Kanellopoulos, P., & Gill, C. (2002). Hydrothermal ageing of yttria-stabilised zirconia, sintered at 1300°C–1325°C: the effects of copper oxide doping and sintering time variations. *Journal of Materials Science*, 37(23), 5075-5082.
- Kawai, Y., Motohiro, U., Wang, Y., Kono, S., Ohnuki, S., & Watari, F. (2011). Phase transformation of zirconia ceramics by hydrothermal degradation. *Dental Materials Journal*, 30(3), 286-292.

- Kelly, J. R., & Denry, I. (2008). Stabilized zirconia as a structural ceramic: An overview. *Dental Materials*, 24(3), 289-298.
- Kelvin Chew, W. J., Bang, L. T., Ramesh, S., & Teng, W. D. (2015). Mechanical Properties and Hydrothermal Ageing Behaviour of Flyash-doped Y-TZP Ceramic. *International Journal of the Institute of Materials Malaysia*, 2(2), 292-299.
- Keuper, M., Berthold, C., & Nickel, K. G. (2014). Long-time aging in 3 mol.% yttria-stabilized tetragonal zirconia polycrystals at human body temperature. *Acta Biomaterialia*, 10(2), 951-959.
- Khan, M. M., Ramesh, S., Bang, L. T., Wong, Y. H., Ubenthiran, S., Tan, C. Y.,... (2014). Effect of Copper Oxide and Manganese Oxide on Properties and Low Temperature Degradation of Sintered Y-TZP Ceramic. *Journal of Materials Engineering and Performance*, 23(12), 4328-4335.
- Khaskhoussi, A., Calabrese, L., Bouaziz, J., & Proverbio, E. (2017). Effect of TiO₂ addition on microstructure of zirconia/alumina sintered ceramics. *Ceramics International*, 43(13), 10392-10402.
- Kim, H., Han, J., Yang, J., Lee, J., & Kim, S. (2009). The effect of low temperature aging on the mechanical property & phase stability of Y-TZP ceramics. *Journal of Advanced Prosthodontics*, 1(3), 113-117.
- Kosmač, T., Oblak, Č., & Marion, L. (2008). The effects of dental grinding and sandblasting on ageing and fatigue behavior of dental zirconia (Y-TZP) ceramics. *Journal of the European Ceramic Society*, 28(5), 1085-1090.
- Kumar, B. V. M., Kim, W.-S., Hong, S.-H., Bae, H.-T., & Lim, D.-S. (2010). Effect of grain size on wear behavior in Y-TZP ceramics. *Materials Science and Engineering: A*, 527(3), 474-479.
- Lange, F. F. (1982). Transformation toughening Part 1 Size effects associated with the thermodynamics of constrained transformations. *Journal of Materials Science*, 17(1), 225-234.
- Lange, F. F., Dunlop, G. L., & Davis, B. I. (1986). Degradation During Aging of Transformation-Toughened ZrO₂-Y₂O₃ Materials at 250°C. *Journal of the American Ceramic Society*, 69(3), 237-240.
- Langer, J., Hoffmann, M. J., & Guillon, O. (2011). Electric Field-Assisted Sintering in Comparison with the Hot Pressing of Yttria-Stabilized Zirconia. *Journal of the American Ceramic Society*, 94(1), 24-31.
- Lawson, S. (1995). Environmental degradation of zirconia ceramics. *Journal of the European Ceramic Society*, 15(6), 485-502.
- Lawson, S., Gill, C., & Dransfield, G. P. (1995). The effects of copper and iron oxide additions on the sintering and properties of Y-TZP. *Journal of Materials Science*, 30(12), 3057-3060.

- Lawson, S., Gill, C., & Dransfield, G. P. (1995). Hydrothermal and Corrosive Degradation of Y-TZP Ceramics. *Key Engineering Materials*, 113, 207-214.
- Lee, J. G., Jeon, O. S., Ryu, K. H., Park, M. G., Min, S. H., Hyun, S. H.,... (2015). Effects of 8mol% yttria-stabilized zirconia with copper oxide on solid oxide fuel cell performance. *Ceramics International*, 41(6), 7982-7988.
- Lemaire, L., Scholz, S. M., Bowen, P., Dutta, J., Hofmeister, H., & Hofmann, H. (1999). Effect of CuO additives on the reversibility of zirconia crystalline phase transitions. *Journal of Materials Science*, 34(9), 2207-2215.
- Li, J., & Watanabe, R. (1998). Phase Transformation in Y₂O₃-Partially-Stabilized ZrO₂ Polycrystals of Various Grain Sizes during Low-Temperature Aging in Water. *Journal of the American Ceramic Society*, 81(10), 2687-2691.
- Lorenzo, C., Flores, J. A., Gómez, D., Muñoz, A., Domínguez, A., Xue, D.,... (2002). Mechanical behaviour of yttria tetragonal zirconia polycrystalline nanoceramics: dependence on the glassy phase content. *Journal of the European Ceramic Society*, 22(14–15), 2603-2607.
- Lucas, T. J., Lawson, N. C., Janowski, G. M., & Burgess, J. O. (2015). Effect of grain size on the monoclinic transformation, hardness, roughness, and modulus of aged partially stabilized zirconia. *Dental Materials*, 31(12), 1487-1492.
- Lucas, T. J., Lawson, N. C., Janowski, G. M., & Burgess, J. O. (2015). Phase transformation of dental zirconia following artificial aging. *Journal of Biomedical Materials Research Part B: Applied Biomaterials*, 103(7), 1519-1523.
- Lughi, V., & Sergo, V. (2010). Low temperature degradation -aging- of zirconia: A critical review of the relevant aspects in dentistry. *Dental Materials*, 26(8), 807-820.
- Manicone, P. F., Rossi Iommetti, P., & Raffaelli, L. (2007). An overview of zirconia ceramics: Basic properties and clinical applications. *Journal of Dentistry*, 35(11), 819-826.
- Masaki, T. (1986). Mechanical properties of Y-PSZ after aging at low temperature. *International Journal of High Technology Ceramics*, 2(2), 85-98.
- Matsui, K., Nakamura, K., Kumamoto, A., Yoshida, H., & Ikuhara, Y. (2016). Low-temperature degradation in yttria-stabilized tetragonal zirconia polycrystal doped with small amounts of alumina: Effect of grain-boundary energy. *Journal of the European Ceramic Society*, 36(1), 155-162.
- Mazaheri, M., Simchi, A., & Golestani-Fard, F. (2008). Densification and grain growth of nanocrystalline 3Y-TZP during two-step sintering. *Journal of the European Ceramic Society*, 28(15), 2933-2939.
- Mazaheri, M., Zahedi, A. M., & Hejazi, M. M. (2008). Processing of nanocrystalline 8 mol% yttria-stabilized zirconia by conventional, microwave-assisted and two-step sintering. *Materials Science and Engineering: A*, 492(1–2), 261-267.

- Miragaya, L. M., Guimaraes, R. B., Souza, R., Santos Botelho, G. D., Antunes Guimaraes, J. G., & da Silva, E. M. (2017). Effect of intra-oral aging on t→m phase transformation, microstructure, and mechanical properties of Y-TZP dental ceramics. *Journal of the Mechanical Behavior of Biomedical Materials*, 72, 14-21.
- Mishra, R. R., & Sharma, A. K. (2016). Microwave–material interaction phenomena: Heating mechanisms, challenges and opportunities in material processing. *Composites Part A: Applied Science and Manufacturing*, 81, 78-97.
- Monaco, C., Prete, F., Leonelli, C., Esposito, L., & Tucci, A. (2015). Microstructural study of microwave sintered zirconia for dental applications. *Ceramics International*, 41(1, Part B), 1255-1261.
- Muñoz-Saldaña, J., Balmori-Ramírez, H., Jaramillo-Vigueras, D., Iga, T., & Schneider, G. A. (2003). Mechanical properties and low-temperature aging of tetragonal zirconia polycrystals processed by hot isostatic pressing. *Journal of Materials Research*, 18(10), 2415-2426.
- Murugan, R., & Ramakrishna, S. (2005). Development of nanocomposites for bone grafting. *Composites Science and Technology*, 65(15), 2385-2406.
- Nakamura, T., Usami, H., Ohnishi, H., Takeuchi, M., Nishida, H., Sekino, T.,... (2011). The effect of adding silica to zirconia to counteract zirconia's tendency to degrade at low temperatures. *Dental Materials Journal*, 30(3), 330-335.
- Nath, S., Sinha, N., & Basu, B. (2008). Microstructure, mechanical and tribological properties of microwave sintered calcia-doped zirconia for biomedical applications. *Ceramics International*, 34(6), 1509-1520.
- Nightingale, S. A., Dunne, D. P., & Worner, H. K. (1996). Sintering and grain growth of 3 mol% yttria zirconia in a microwave field. *Journal of Materials Science*, 31(19), 5039-5043.
- Nogiwa-Valdez, A. A., Rainforth, W. M., Zeng, P., & Ross, I. M. (2013). Deceleration of hydrothermal degradation of 3Y-TZP by alumina and lanthana co-doping. *Acta Biomaterialia*, 9(4), 6226-6235.
- Oghbaei, M., & Mirzaee, O. (2010). Microwave versus conventional sintering: A review of fundamentals, advantages and applications. *Journal of Alloys and Compounds*, 494(1–2), 175-189.
- Palmeira, A. A., Bondioli, M. J., Strecker, K., & Santos, C. d. (2016). Densification and grain growth of nano- and micro-sized Y-TZP powders. *Ceramics International*, 42(2, Part A), 2662-2669.
- Paul, A., Vaidhyanathan, B., & Binner, J. G. P. (2011). Hydrothermal Aging Behavior of Nanocrystalline Y-TZP Ceramics. *Journal of the American Ceramic Society*, 94(7), 2146-2152.

- Paula, V. G., Lorenzoni, F. C., Bonfante, E. A., Silva, N. R. F. A., Thompson, V. P., & Bonfante, G. (2015). Slow cooling protocol improves fatigue life of zirconia crowns. *Dental Materials*, *31*(2), 77-87.
- Pereira, G. K. R., Venturini, A. B., Silvestri, T., Dapieve, K. S., Montagner, A. F., Soares, F. Z. M.,... (2016). Low-temperature degradation of Y-TZP ceramics: A systematic review and meta-analysis. *Journal of the Mechanical Behavior of Biomedical Materials*, *55*, 151-163.
- Pian, X., Fan, B., Chen, H., Zhao, B., Zhang, X., & Zhang, R. (2014). Preparation of m-ZrO₂ compacts by microwave sintering. *Ceramics International*, *40*(7, Part B), 10483-10488.
- Piconi, C., Burger, W., Richter, H. G., Cittadini, A., Maccauro, G., Covacci, V.,... (1998). Y-TZP ceramics for artificial joint replacements. *Biomaterials*, *19*(16), 1489-1494.
- Piconi, C., & Maccauro, G. (1999). Review Zirconia as a Ceramic Biomaterial. *Biomaterials*, *20*, 1-25.
- Piyapanna, P., Ailbhe, M., Anne, Y., & C., K. J. (2009). Flexural strength, fatigue life, and stress-induced phase transformation study of Y-TZP dental ceramic. *Journal of Biomedical Materials Research Part B: Applied Biomaterials*, *88B*(2), 366-377.
- Presenda, Á., Salvador, M. D., Moreno, R., & Borrell, A. (2015). Hydrothermal Degradation Behavior of Y-TZP Ceramics Sintered by Nonconventional Microwave Technology. *Journal of the American Ceramic Society*, *98*(12), 3680-3689.
- Presenda, Á., Salvador, M. D., Penaranda-Foix, F. L., Catalá-Civera, J. M., Pallone, E., Ferreira, J.,... (2017). Effects of microwave sintering in aging resistance of zirconia-based ceramics. *Chemical Engineering and Processing: Process Intensification*, *122*, 404-412.
- Presenda, Á., Salvador, M. D., Peñaranda, F. L., Moreno, R., & Borrell, A. (2015). Effect of microwave sintering on microstructure and mechanical properties in Y-TZP materials used for dental applications. *Ceramics International*, *41*(5, Part B), 7125-7132.
- Presenda, Á., Salvador, M. D., Vleugels, J., Moreno, R., & Borrell, A. (2017). Fretting fatigue wear behavior of Y-TZP dental ceramics processed by non-conventional microwave sintering. *Journal of the American Ceramic Society*, *100*(5), 1842-1852.
- Ramesh, S., Amiriyani, M., Meenaloshini, S., Tolouei, R., Hamdi, M., Pruboloksono, J.,... (2011). Densification behaviour and properties of manganese oxide doped Y-TZP ceramics. *Ceramics International*, *37*(8), 3583-3590.
- Ramesh, S., & Gill, C. (2001). Environmental degradation of CuO-doped Y-TZP ceramics. *Ceramics International*, *27*(6), 705-711.

- Ramesh, S., Gill, C., & Lawson, S. (1999). The effect of copper oxide on sintering, microstructure, mechanical properties and hydrothermal ageing of coated 2.5Y-TZP ceramics. *Journal of Materials Science*, 34(22), 5457-5467.
- Ramesh, S., Khan, M. M., Alexander Chee, H. C., Wong, Y. H., Ganesan, P., Kutty, M. G.,... (2016). Sintering behaviour and properties of graphene oxide-doped Y-TZP ceramics. *Ceramics International*, 42(15), 17620-17625.
- Ramesh, S., Meenaloshini, S., Tan, C. Y., Chew, W. J. K., & Teng, W. D. (2008). Effect of manganese oxide on the sintered properties and low temperature degradation of Y-TZP ceramics. *Ceramics International*, 34(7), 1603-1608.
- Ramesh, S., Purbolaksono, J., Hamdi, M., Sopyan, I., Tolouei, R., Amiriyani, M.,... (2012). Low-Temperature Degradation (LTD) Behaviour of CuO-Doped Tetragonal Zirconia Ceramic. *Ceramics - Silikat*, 56(1), 15-19.
- Ran, S., Winnubst, L., Blank, D. H. A., Pasaribu, H. R., Sloetjes, J.-W., & Schipper, D. J. (2007). Effect of Microstructure on the Tribological and Mechanical Properties of CuO-Doped 3Y-TZP Ceramics. *Journal of the American Ceramic Society*, 90(9), 2747-2752.
- Ran, S., Winnubst, L., Wiratha, W., & Blank, D. H. A. (2006). Sintering Behavior of 0.8 mol%-CuO-Doped 3Y-TZP Ceramics. *Journal of the American Ceramic Society*, 89(1), 151-155.
- Rauchs, G., Fett, T., & Munz, D. (2002). R-curve behaviour of 9Ce-TZP zirconia ceramics. *Engineering Fracture Mechanics*, 69(3), 389-401.
- Rayón, E., Moreno, R., Alcázar, C., Salvador, M. D., Manjón, F. J., Jiménez-Piqué, E.,... (2013). Enhanced Hydrothermal Resistance of Y-TZP Ceramics Through Colloidal Processing. *Journal of the American Ceramic Society*, 96(4), 1070-1076.
- Reidy, C. J., Fleming, T. J., Hampshire, S., & Towler, M. R. (2011). Comparison of Microwave and Conventionally Sintered Yttria - Doped Zirconia Ceramics. *International Journal of Applied Ceramic Technology*, 8(6), 1475-1485.
- Roy, M. E., Whiteside, L. A., Katerberg, B. J., & Steiger, J. A. (2007). Phase transformation, roughness, and microhardness of artificially aged yttria- and magnesia-stabilized zirconia femoral heads. *Journal of Biomedical Materials Research Part A*, 83A(4), 1096-1102.
- Ruiz, L., & Readey, M. J. (1996). Effect of Heat Treatment on Grain Size, Phase Assemblage, and Mechanical Properties of 3 mol% Y-TZP. *Journal of the American Ceramic Society*, 79(9), 2331-2340.
- Rybakov, K. I., Olevsky, E. A., Krikun, E. V., & Green, D. J. (2013). Microwave Sintering: Fundamentals and Modeling. *Journal of the American Ceramic Society*, 96(4), 1003-1020.

- Samodurova, A., Kocjan, A., Swain, M. V., & Kosmač, T. (2015). The combined effect of alumina and silica co-doping on the ageing resistance of 3Y-TZP bioceramics. *Acta Biomaterialia*, *11*, 477-487.
- Samodurova, A., Vengust, D., Kocjan, A., & Kosmač, T. (2015). The sintering-temperature-related microstructure and phase assemblage of alumina-doped and alumina-silica-co-doped 3-mol%-yttria-stabilized tetragonal zirconia. *Scripta Materialia*, *105*, 50-53.
- Sevilla, P., Sandino, C., Arciniegas, M., Martínez-Gomis, J., Peraire, M., & Gil, F. J. (2010). Evaluating mechanical properties and degradation of YTZP dental implants. *Materials Science and Engineering: C*, *30*(1), 14-19.
- Shetty, D. K., & Wright, I. G. (1986). On estimating fracture toughness of cemented carbides from Palmqvist crack sizes. *Journal of Materials Science Letters*, *5*(3), 365-368.
- Shukla, S., & Seal, S. (2005). Mechanisms of room temperature metastable tetragonal phase stabilisation in zirconia. *International Materials Reviews*, *50*(1), 45-64.
- Singh, R. (1999). Review of Ageing Behaviour of Yttria-Tetragonal Zirconia Polycrystals (Y-TZP): Part 3, Ageing Inhibition. *Journal of Industrial Technology*, *8*(2), 1-18.
- Sivakumar, S., Ramesh, S., Chin, K. L., Tan, C. Y., & Teng, W. D. (2011). Effect of Sintering Profiles on the Properties and Ageing Resistance of Y-TZP Ceramic. *International Journal of Automotive and Mechanical Engineering*, *4*, 406-413.
- Smirnov, A., Kurland, H.-D., Grabow, J., Müller, F. A., & Bartolomé, J. F. (2015). Microstructure, mechanical properties and low temperature degradation resistance of 2Y-TZP ceramic materials derived from nanopowders prepared by laser vaporization. *Journal of the European Ceramic Society*, *35*(9), 2685-2691.
- Soon, G., Pingguan-Murphy, B., Lai, K. W., & Akbar, S. A. (2016). Review of zirconia-based bioceramic: Surface modification and cellular response. *Ceramics International*, *42*(11), 12543-12555.
- Sujith, A. V., Amar Kumar, N., & Sharan, N. (2009). Microwave Sintering of Zirconia and Alumina. *International Journal of Recent Trends in Engineering*, *1*(3), 320-323.
- Sutharsini, U., Ramesh, S., Wong, Y. H., Misran, H., Yusuf, F., Tan, C. Y.,... (2014). Effect of sintering holding time on low-temperature degradation of yttria stabilised zirconia ceramics. *Materials Research Innovations*, *18*(sup6), S6-408-S406-411.
- Sutharsini, U., Thanishaichelvan, M., Ting, C. H., Ramesh, S., Tan, C. Y., Chandran, H.,... (2017). Effect of two-step sintering on the hydrothermal ageing resistance of tetragonal zirconia polycrystals. *Ceramics International*, *43*(10), 7594-7599.
- Swab, J. J. (1991). Low temperature degradation of Y-TZP materials. *Journal of Materials Science*, *26*(24), 6706-6714.

- Takigawa, Y., Shibano, T., Kanzawa, Y., & Higashi, K. (2009). Effect of Small Amount of Insoluble Dopant on Tetragonal to Monoclinic Phase Transformation in Tetragonal Zirconia Polycrystal. *Materials Transactions*, 50(5), 1091-1095.
- Tan, H. C., Gill, C., & Lawson, S. (1996). The Effect of Sintering Additives on the Hydrothermal and Corrosive Degradation of Y-TZP. *Key Engineering Materials*, 113, 199-206.
- Tanaka, K., Tamura, J., Kawanabe, K., Nawa, M., Uchida, M., Kokubo, T.,... (2003). Phase stability after aging and its influence on pin-on-disk wear properties of Ce-TZP/Al₂O₃ nanocomposite and conventional Y-TZP. *Journal of Biomedical Materials Research Part A*, 67A(1), 200-207.
- Ting, C. H., Ramesh, S., Tan, C. Y., Zainal, A. N. I., Teng, W. D., Urries, I.,... (2017). Low-temperature sintering and prolonged holding time on the densification and properties of zirconia ceramic. *Journal of Ceramic Processing Research*, 18(8), 569-574.
- Tong, H., Tanaka, C. B., Kaizer, M. R., & Zhang, Y. (2016). Characterization of three commercial Y-TZP ceramics produced for their High-Translucency, High-Strength and High-Surface Area. *Ceramics International*, 42(1, Part B), 1077-1085.
- Toraya, H., Yoshimura, M., & Somiya, S. (1984). Calibration curve for quantitative analysis of the monoclinic-tetragonal ZrO₂ system by X-ray diffraction. *Journal of American Ceramic Society*, 67(6), C-119-121.
- Tran, T. H., & Nguyen, V. T. (2014). Copper Oxide Nanomaterials Prepared by Solution Methods, Some Properties, and Potential Applications: A Brief Review. *International Scholarly Research Notices*, 2014.
- Travitzky, N. A., Goldstein, A., Avsian, O., & Singurindi, A. (2000). Microwave sintering and mechanical properties of Y-TZP/20 wt.% Al₂O₃ composites. *Materials Science and Engineering: A*, 286(2), 225-229.
- Tredici, I. G., Sebastiani, M., Massimi, F., Bemporad, E., Resmini, A., Merlati, G.,... (2016). Low temperature degradation resistant nanostructured yttria-stabilized zirconia for dental applications. *Ceramics International*, 42(7), 8190-8197.
- Upadhyaya, D. D., Ghosh, A., Dey, G. K., Prasad, R., & Suri, A. K. (2001). Microwave sintering of zirconia ceramics. *Journal of Materials Science*, 36(19), 4707-4710.
- Vasylykiv, O., Sakka, Y., & Skorokhod, V. V. (2003). Low-Temperature Processing and Mechanical Properties of Zirconia and Zirconia–Alumina Nanoceramics. *Journal of the American Ceramic Society*, 86(2), 299-304.
- Wang, J., Binner, J., Vaidyanathan, B., Joomun, N., Kilner, J., Dimitrakis, G.,... (2006). Evidence for the Microwave Effect During Hybrid Sintering. *Journal of the American Ceramic Society*, 89(6), 1977-1984.

- Wei, C., & Gremillard, L. (2018). Towards the prediction of hydrothermal ageing of 3Y-TZP bioceramics from processing parameters. *Acta Materialia*, 144(Supplement C), 245-256.
- Winnubst, L., Ran, S., Speets, E. A., & Blank, D. H. A. (2009). Analysis of reactions during sintering of CuO-doped 3Y-TZP nano-powder composites. *Journal of the European Ceramic Society*, 29(12), 2549-2557.
- Wu, Z., Li, N., Jian, C., Zhao, W., & Yan, J. (2013). Low temperature degradation of Al₂O₃-doped 3Y-TZP sintered at various temperatures. *Ceramics International*, 39(6), 7199-7204.
- Xu, G., Olorunyolemi, T., Carmel, Y., Lloyd, I. K., & Wilson, O. C. (2003). Design and Construction of Insulation Configuration for Ultra-High-Temperature Microwave Processing of Ceramics. *Journal of the American Ceramic Society*, 86(12), 2082-2086.
- Yan, X., Zhengyi, F., Vaclav, P., Karel, M., & Zhijian, S. (2014). Preparation of Transparent 3Y-TZP Nanoceramics with No Low-Temperature Degradation. *Journal of the American Ceramic Society*, 97(5), 1402-1406.
- Yang, H., & Ji, Y. (2016). Low-temperature Degradation of Zirconia-based All-ceramic Crowns Materials: A Mini Review and Outlook. *Journal of Materials Science and Technology*, 32(7), 593-596.
- Zembic, A., Bosch, A., Jung, R. E., Hammerle, C. H., & Sailer, I. (2013). Five-year results of a randomized controlled clinical trial comparing zirconia and titanium abutments supporting single-implant crowns in canine and posterior regions. *Clinical Oral Implants Research*, 24(4), 384-390.
- Zhang, B., & Li, L. (2017). Microstructure and microwave dielectric properties of CuO-modified CoWO₄ ceramics. *Journal of Materials Science: Materials in Electronics*, 28(4), 3523-3529.
- Zhang, F., Vanmeensel, K., Batuk, M., Hadermann, J., Inokoshi, M., Van Meerbeek, B.,... (2015). Highly-translucent, strong and aging-resistant 3Y-TZP ceramics for dental restoration by grain boundary segregation. *Acta Biomaterialia*, 16, 215-222.
- Zhang, F., Vanmeensel, K., Inokoshi, M., Batuk, M., Hadermann, J., Van Meerbeek, B.,... (2014). 3Y-TZP ceramics with improved hydrothermal degradation resistance and fracture toughness. *Journal of the European Ceramic Society*, 34(10), 2453-2463.
- Zhang, F., Vanmeensel, K., Inokoshi, M., Batuk, M., Hadermann, J., Van Meerbeek, B.,... (2015). Critical influence of alumina content on the low temperature degradation of 2–3 mol% yttria-stabilized TZP for dental restorations. *Journal of the European Ceramic Society*, 35(2), 741-750.
- Zhang, Y. (2014). Making yttria-stabilized tetragonal zirconia translucent. *Dental Materials*, 30(10), 1195-1203.

- Zhang, Y., & Zhang, J. (2014). First Principles Study of Structural and Thermodynamic Properties of Zirconia. *Materials Today: Proceedings*, 1(1), 44-54.
- Zhao, C., Vleugels, J., Groffils, C., Luypaert, P. J., & Van Der Biest, O. (2000). Hybrid sintering with a tubular susceptor in a cylindrical single-mode microwave furnace. *Acta Materialia*, 48(14), 3795-3801.
- Zhu, W., Fujiwara, A., Nishiike, N., Marin, E., Sugano, N., & Pezzotti, G. (2018). Transition metals increase hydrothermal stability of yttria-tetragonal zirconia polycrystals (3Y-TZP). *Journal of the European Ceramic Society*, 38(10), 3573-3577.
- Žymelka, D., Saunier, S., Goeriot, D., & Molimard, J. (2013). Densification and thermal gradient evolution of alumina during microwave sintering at 2.45GHz. *Ceramics International*, 39(3), 3269-3277.

University of Malaysia

LIST OF PUBLICATIONS AND PAPERS PRESENTED

1. Ramesh, S., Sara Lee, K. Y., Tan, C. Y., Wong, Y. H., Johnson Alengaram, U., Tarlochan, F., Ramesh, S., Teng, W. D., Sutharsini, U., Sarhan, Ahmed A. D. (2018). Effect of microwave sintering on the properties of copper oxide doped Y-TZP ceramics. *Ceramics International*, 44 (16), 19639-19645.
<https://doi.org/10.1016/j.ceramint.2018.07.215>
2. Ramesh, S., Sara Lee, K. Y., Tan, C. Y. (2018). A review on the hydrothermal ageing behaviour of Y-TZP ceramics. *Ceramics International*, 44 (17), 20620-20634. <https://doi.org/10.1016/j.ceramint.2018.08.216>

University of Malaya